REGULATION OF CFTR ENDOCYTOSIS BY THE VASOACTIVE INTESTINAL PEPTIDE: ROLE OF PKCε

by

Walaa A. Alshafie

Submitted in partial fulfilment of the requirements
for the degree of Master of Science

at

Dalhousie University
Halifax, Nova Scotia
December 2013

DEDICATION

In the name of God, The most merciful, the most compassionate
"Say: My Lord increase me in knowledge"

I like to dedicate this work for one great scientist and person

Dr Susan Suarez

who showed me how a succeeful scientist could be at the research level as well as

at the personal level. She was and will continue to be a source of inspiration for me

for the years to come.

My parents for all what they had done and continue doing for me

My husband Mahmoud and my kids Omar and Menna for their smiles, love and support.

My friends Anita Watkins, Cheryl Barbach and Mayuka Yasui for their consistant support and love.

Walaa

Table of Contents

LIST OF TABLES

List of Figures

Abstract

The Vasoactive Intestinal Peptide (VIP) is an agonist of the CFTR chloride channel in the human airways. In the genetic disease Cystic Fibrosis, where CFTR is defective or absent from the apical membrane of epithelial cells, VIP innervations are lost. Our group has demonstrated that VIP increases CFTR membrane stability through PKCε. However, the mechanism remained to be determined. Here we found that VIP stimulation increases the interaction of NHERF1 and P-ERMs with CFTR through PKCε phosphorylation. Moreover a reduction of the interaction between intracellular CFTR and the Golgi associated protein, CAL was observed following VIP stimulation. Silencing either ERMs or NHERF1 with siRNA prevented the VIP ability to increase CFTR surface expression and function, confirming that NHERF1 and P-ERMs are necessary for VIP regulation of the sustained activity of membrane CFTR. This study shows the cellular mechanism by which prolonged VIP stimulation of airway epithelial cells regulates CFTR-dependent secretions.

List of Abbreviations Used

(α)	Alpha
(ε)	Epsilon
(μ)	Micro
β2AR	Beta 2 Adrenergic Receptors
ΔF508-CFTR	Deletion mutation where phenylalanine amino acid at position 508 is missing
ABC	ATP-Binding Cassette
ACh	Acetyle Choline
AP2	Adaptor Protein 2
AKAP	A kinase Anchoring Protein
ATP	Adenosine Triphosphate
ASL	Airway Surface Liquid
BSA	Bovine Serum Albumin
bp	Base Pair
BHK	Baby Hamster Kidney
Ca^{++}	Calcium Ion
CaCC	Calcium Activated Chloride Channel
cAMP	3'-5'-Cyclic Adinosine Monophosphate
CF	Cystic Fibrosis
CFTR	Cystic Fibrosis Transmembrane Conductance Regulator
COPD	Chronic Obstructive Pulmonary Disease
CNG	Cyclic Nucleotide-Gated cation channel
Cdc2	Cyclin Dependent Kinase 2
DAG	Diacyle Glycerol
ddH_2O	Double Distilled Water
DIC	Differential Interface Contrast
DIOS	Distal intestinal obstrauction Syndrome
EBP50	ERM-binding Phosphoprotein 50

ENaC	Epithelial Sodium Channel
ER	Endoplasmic Reticulum
ERQC	Endoplasmic Reticulum Quality Control
GPCR	G-Protein Coupled Receptors
GRK6A	GPCR Regulatry Kinase A6
h	Hour
ICAM	Intercellular Adhesion Molecule
IP	Immunopreciption
IP3	Inositol-1, 4, 5,-triphosphate
kDa	Kilodalton
KO	Knock-Out
LMS	Laser Scanning Microscope
MAST205	Microtubule-Associated Serine/Threonine kinase with Molecular Mass of 205 kDa
Min	Minute
mRNA	Messenger RNA
MRP4	Multi Drug Resistance protein 4
NBD1	Nucleotide Binding Domain 1
NBD2	Nucleotide Binding Domain 2
NEP	Neural Endo-Peptidase
NHERF1	Sodium Hydrogen / Exchange Regulatory Factor 1
N/K ATPase	Sodium/Potassium ATPase
NKCC1	Sodium Potassium Chloride Co-transporter
O/N	Overnight
PAC1	PACAP Receptor 1
PACAP	Pitutary Adenyl Cyclase Activating Peptide
PBS	Phosphate Buffered Saline
PCL	Periciliary Liquid
PDGF-R	Platelet-derived growth factor receptor
PFA	Paraformaldhyde
PIP2	Phosphoinositol-4-5-biphoshate

PKA	Protein Kinase A
PKC	Protein Kinase C
PHM	Peptide with N-terminal histidine and C-terminal methionine amide
PHI	Peptide with N-terminal histidine and C-terminal isoleucine amide
PLC	Phospholipase C
PMA	Phorbol 12-Myristate 13-Acetate, Phorbol Ester
PCD	Primary Ciliary Dyskinesia
RACK1	Receptor for Active C Kinase 1
RD	Regulatory Domain
RER	Rough Endoplasmic Reticulum
RIPA	Radio Immuno Precipitation Assay
RT	Room Temperature
RT-PCR	Reverse Transcription Polymerase Chain Reaction
TBS	Tris Buffered Saline
TCA	Trichloroacetic Acid
TJ	Tight Junction
Tm	Annealing Temperature
TMD1	Transmembrane Spanning Domain 1
TMD2	Transmembrane Spanning Domain 2
VIP	Vasoactive Intestinal Peptide
VIP-KO	VIP Kock-Out
VPAC1	VIP Receptor 1
VPAC2	VIP Recptor 2
WT	Wild Type

Acknowledgments

I like to sincerely thank my supervisor Dr. Valerie Chappe for her consistence guidance and support through out the study. I am gratful for the time she spent with me, definetly, she helped shape up my scientific thinking. I am indebted to her for her mentorship and through training that will continue to serve as my foundation for scientific ventures.

I also like to thank my supervisory committee members Dr. Younes Anini, Dr. Xianping Dong and Dr. Robert Rose for the critical feedbacks and valuable advices.

I am gratful to our lab manager Fredric Chappe for his through supervision and patience and to mansong Li for all her technical support. I like to thank Stephen Whitefield for providing me with the training for the confocal and flouresecnce microscopes and Pat Colp for training me on the histology microtome.

Thanks for Cystic Fibrosis Canada for funding my project.

Last but not least, I like to thank the Department of Physiology and Biophysic, Dalhousie University and Canada for kindely hosting me.

Chapter 1: Introduction

I Cystic Fibrosis

Loss of CFTR (Cystic Fibrosis Transmembrane Conductance Regulator) protein membrane localization and / or function, resulting from gene mutations, leads to Cystic Fibrosis (CF), the most common lethal recessive genetic disease in Caucasians, with an estimated one in every 3,500 newborns affected every year (Canadian Cystic Fibrosis Foundation: www.cysticfibrosis.ca). A characteristic feature in CF is plugging and occlusion of secretory gland ducts with thick mucus in many organs including the airways, pancreas, intestine and epididymis leading to a wide range of disease pathologies (Turcios, 2005). This includes obstructive lung disease, pancreatic insufficiency and eventual fibrosis, meconium ileum in newborns, Distal Intestinal Obstruction Syndrome (DIOS) and male infertility. A high level of NaCl in sweat gland secretions is considered diagnostic for CF. Perhaps the most serious feature in CF is the pulmonary disease from which almost all the mortality results (Turcios, 2005). In the airways, bacterial infection starts soon after birth, and later on, bacteria alter their patterns of infection to produce mucoid coating. The bacterial mucoid phenotype, which is characteristic to the CF lung, is associated with accelerated decline of pulmonary function and eventually leads to lung failure and death. How mutations in CFTR results in the development of chronic infection and inflammation is still uncertain with many hypotheses under scrutiny.

Although there is no cure yet for CF, symptomatic treatments helped extend the life of CF patients to their mid-forties. Generally, the gastrointestinal symptoms are controlled by existing therapies while the respiratory disease is not well controlled. There is great hope on research to develop effective treatment strategies to control CF respiratory disease and help CF patients live healthier and longer lives.

1. ΔF508: The Most Common CF Mutation

More than 1,900 mutations have been identified (Canadian Cystic Fibrosis Foundation: www.cysticfibrosis.ca) resulting in CF disease with varying range of severity. These mutations are grouped into five classes according to the effect they produce. Class I mutations include mutations that prevent the protein production often by generating premature stop codons that lead to mRNA degradation. Class II mutations result in reduced or absence of CFTR protein from the apical plasma membrane. Class III mutants affect channel regulation leading to impaired channel opening. Class IV mutants exhibit reduced ion conduction. Class V mutants cause significant reduction in mRNA and/or protein levels.

The class II ΔF508-CFTR is the most common CF mutation found in nearly 91.5% of CF patients (www.cysticfibrosis.ca) results from deletion of phenylalanine residue at position 508. This mutation results in translational and post-translational defects leading to improper folding of the protein (Welsh *et al*., 1993; Lukacs & Verkman, 2012). The improperly folded ΔF508-CFTR is recognized by the Endoplasmic Reticulum Quality Control machinery (ERQC) and targeted for proteosomal degradation. The majority of ΔF508-CFTR cannot reach the cell surface, resulting in absence of functional CFTR proteins at the apical membrane of epithelial cells (Cheng *et al*., 1990; Kartner *et al*., 1992; Kälin *et al*., 1999; Penque *et al*., 2000). Other defects that characterize ΔF508-CFTR are reduced gating properties (Dalemans *et al*., 1991; Cai *et al*., 2011) and surface instability (Heda *et al*., 2001). The very few ΔF508-CFTR proteins that are able to escape the ERQC and traffic to the cell membrane are metabolically unstable and quickly removed by the peripheral quality control machinery (Okiyoneda *et al*., 2010) resulting in shorter surface half-life (Heda *et al*., 2001) compared to the wild type (WT) CFTR. Huge research efforts to repair ΔF508-CFTR are directed toward rescuing of its trafficking and restoring its surface stability, trying to take advantage of the small functional properties that ΔF508-CFTR retains.

II The Airway Physiology

1. The Airway Epithelium

The respiratory epithelium constitutes the first line of defense against external environmental insults. It consists primarily of ciliated, serous and mucus (goblet) cells that function together in an effort to keep the airway sterile. The primary task of the airways epithelium is mucus clearance from the lung to the mouth by the help of coordinated ciliary beating as well as local regulation of the volume and composition of the mucus layer covering the respiratory epithelium.

Ciliated epithelial cells are predominant within the airway epithelium. The classic ciliated cell is covered by up to 300 cilia and posses numerous mitochondria beneath the apical surface to provide the energy needed for the ciliary movement (Knight & Holgate, 2003). Mucus cells contain many mucin granules that secrete their content on the top of the epithelium layer to play an important role in trapping pathogens and other particles. The fine regulation of mucin secretion is crucial in determining the right visco-elasticity of the mucus which is essential for efficient mucociliary clearance. The increased rate of mucin secretion due to inhalation of irritants like tobacco smoke or during mucus cell hyperplasia and metaplasia that is seen in chronic airway inflammatory diseases demonstrate the importance of mucin in protecting the airway against any insult. Serous cells are another cell type described primarily in the tracheobronchial epithelium of the airways but not in the bronchiolar or alveolar epithelium. Unlike Rodents, in humans, airway serous cells are primarily localized to the submucosal gland secretory acini and their existence in the surface epithelium is rare (Basbaum *et al*., 1990). Serous cells secrete liquid and proteins which serve many purposes to protect the airway surface. Serous cells therefore exhibit typical features of protein secreting cells with basally oriented nuclei, a perinuclear rough endoplasmic reticulum (ER), a well-developed Golgi apparatus and apically protein packed secretory granules (Basbaum *et al*., 1990). Proteins produced by serous cells play defensive roles against infectious agents including lysozyme, lactoferrin, secretary immunoglobulin, peroxidase and protease inhibitors (Basbaum *et al*., 1990). Proline rich proteins secreted by serous cells might interact with mucins to influence surface mucus viscosity. Liquid secretion by serous cells plays many

roles serving the airway defense mechanism such as sustaining the volume and consistency of the mucus layer covering the respiratory epithelium. The liquid secretion properties of serous cells influence their structural organization with the existence of many ions channels and transporters both on their apical and basolateral membranes.

2. The Airway Innate Defense Mechanism

2.1 Mucociliary Clearance

Mucociliary clearance is the innate or house-keeping defense mechanism of the airways that protects against air-borne pathogens and other irritants. Disturbed mucociliary clearance is a shared feature in many chronic respiratory diseases that display recurrent infection (Mall, 2008). In the human airway, the mucociliary clearance is the function of the surface epithelial layer and the submucosal glands secretions. The success of the respiratory mucociliary clearance depends on a delicate physiological balance of several factors mainly the Airway Surface Liquid (ASL), a mucus blanket covering the surface epithelium, and the cilia function. The mechanism of mucociliary clearance includes: 1- trapping inhaled particles and pathogens in the upper most viscous mucus layer, 2- lysis and killing of pathogens by dissolved antibacterial substances secreted by serous cells, 3- coordinated and rhythmic ciliary beating to generate propulsive force for mucus clearance to be coughed out or swallowed.

Successful mucociliary clearance depends on the ASL composition / volume and cilia activity. Thus any disease condition that affects any of these components compromises the mucociliary clearance leading to the development of recurrent infections. Primary ciliary dyskinesia (PCD) is a genetic condition characterized by chronic airway infection caused by impaired mucociliary clearance due to cilia defects. Cystic Fibrosis is characterized by chronic airway infection and eventual lung failure represents another example of mucociliary clearance defect resulting from improper ASL composition due to the disturbance of ions and fluid secretion secondary to genetically mutated ion channel.

Certainly, the use of genetically engineered Mouse models with deficiency of one element of the mucociliary clearance emphasized the importance of each individual element and / or the concerted action between them for the efficient bacterial clearance from the airways. Disturbance in the ion transport balance either in CF mouse model where the CFTR gene is deleted or in transgenic mice with airway specific over-expression of the sodium channel ENaC resulted in features of ASL depletion and failure in the mucociliary clearance *in vivo* (Mall, 2008). Data from these models emphasized that the ASL volume is a vital determinant of the success of the mucociliary clearance mechanism. Mouse models with over-expression of IL-13 and various other Th2 cell-derived cytokines, exhibit asthma features (Mall, 2008). However, the absence of mucus plugging in the presence of goblet cells metaplasia and mucin hyper-secretion indicated that the overproduction of mucus alone is not the rate limiting factor for mucociliary clearance (Mall, 2008). The development of mouse models with airway specific deletion of genes involved in the ciliogenesis or ciliary structure might provide better understanding for the role of cilia in the mucociliary clearance mechanism.

2.2 The Airways Surface Liquid (ASL)

The ASL consists of two layers (figure 1.1): 1- A low viscosity periciliary liquid layer (PCL) (~7 μm) surrounding the cilia that lubricates the airway surface and facilitates ciliary beating for an efficient mucus clearance from the lungs; 2- A more viscous Gel layer (Gel) on the top of the PCL where its high viscosity property is the function of secreted mucins and that is needed to trap inhaled microorganisms and debris (Hollenhorst *et al*., 2011).

Both the surface epithelial secretory cells and its associated submucosal glands are believed to contribute to the ASL formation and maintenance. However, the relative contribution of the submucosal glands versus the surface epithelium in the ASL secretion and their respective roles in diseases like Cystic Fibrosis remain controversial due to the difficulty to differentiate glandular from superficial secretions (Chambers *et al*., 2007).

In humans, submucosal glands are numerous in the proximal airway (trachea and bronchi) with approximately 1 gland / mm^2 and they seem to be the major source (~ 95%) for surface liquid / mucus secretions needed to keep the airway sterile (Quinton, 1979; Ballard & Inglis, 2004; Ballard & Spadafora, 2007;). One study showed no significant difference in the airway's response to stimulation by a fluid secretagouge after removal of the surface epithelium compared to the intact tissue (Trout *et al*., 2001). In another study, comparing tracheal xenograft epithelium with and without glands, the authors found that the absence of gland secretions resulted in depletion of the ASL and compromised the mucociliary clearance efficiency (Dajani *et al*., 2005). These studies provided evidences that submucosal glands are a major source of ASL in the human proximal airway.

2.3 Regulation of the ASL Composition and Volume

Since the height and correct hydration of the ASL are very important factors for successful mucociliary clearance, it must be regulated. Studies have shown that normal airway epithelia are capable of regulating the ASL and this regulation is lost in CF airways (Tarran *et al*., 2005). Evidence are accumulating that the ion transport mechanism and therefore the fluid secretion / absorption are the determinant of the ASL height. The net ion transport is a function of the concerted activity of several ion channels and transporters both on the basolateral and apical membranes of epithelial cells as well as the acinar serous cells of the submucosal glands. Cl^-, Na^+ and K^+ are the primary ions involved in ASL composition (figure 1.1).

The fine balance between ions absorption (Na^+) and secretion (Cl^-) determines the net fluid secretion and, therefore, the ASL height on top of epithelial cells. Ions composition of the ASL creates the osmotic driving force for the water to flow passively through both paracellular and trans-cellular pathways to yield an isotonic secretory product (Frizzell & Hanrahan, 2012). In human airways, the trans-cellular pathway consists of apical AQP5 and basolateral AQP3 and AQP4 water channels (Kreda *et al*., 2001).

Chloride transport: Active Cl^- secretion has been shown to drive fluid secretion necessary for maintaining the ASL volume. Chloride entry across the basolateral membrane of secretory epithelial cells is mediated primarily by the $Na^+/K^+/2Cl^-$ co-transporter (NKCC). Reduced intracellular Cl^- concentration and volume changes trigger the signaling cascade that lead to the activation of the NKCC. Inhibition of Cl^- secretion by bumetanide (NKCC inhibitor) caused a decrease in ASL height that was similar to that seen in CF airways where the CFTR chloride channel is defective (Tarran *et al*, 2006; Trout, *et al*., 2003). Chloride exit at the apical membrane is mediated mainly by CFTR and Calcium-Activated Cl^- Channels (CaCC). Whereas CFTR is the predominant pathway for chloride secretion in response to cAMP elevating agonists, CaCC is activated in response to increased intracellular Ca^{++} to micromolar concentrations (as in case of muscarinic stimulation). Active Cl^- transport establishes an electrochemical driving force (lumen-negative) for sodium secretion via the paracellular pathway to provide the osmotic driving force needed for fluid to flow passively. The disturbed Cl^- transport due to mutated CFTR chloride channel in CF results in low liquid secretion providing evidence that water secretion is secondary to Cl^- transport. Further evidence came from studies showing that inhibiting Cl^- secretion by applying the inhibitor bumetanide to isolated porcine lungs resulted in reduced liquid secretion with accumulation of thick mucus on the airway surface, depletion of periciliary fluid and ciliary collapse (Trout *et al*., 2003).

Sodium transport: The sodium channel ENaC has been characterized in human airway epithelium primarily for its contribution to apical Na^+ absorption to regulate the ASL. The secretion of Na^+ from the cells by the basolateral Na^+/K^+ ATPase provides the driving force for apical Na^+ absorption by the ENaC (Hollenhorst *et al*., 2011) Thus, the Na^+/K^+ ATPase together with ENaC mediate the trans-epithelial Na^+ reabsorption.

Evidence exist for the coordinated action between the chloride channel CFTR and the sodium channel ENaC. In normal human airways, agonists which raise cAMP to activate CFTR-dependent Cl^- secretion also inactivate ENaC (Chambers *et al*., 2007) and this regulation is lost in CF airways. Direct and indirect interactions of CFTR and ENaC

have also been described to suggest a direct regulatory function of CFTR on ENaC (Kunzelmann *et al*., 1997; Ji *et al*., 2000).

The concerted action between CFTR and ENaC was also evidenced in a mouse model transgenically overexpressing the β-subunit of ENaC in an attempt to shift the balance of salt and water movement away from Cl^- secretion and towards Na^+ absorption. The imbalance between absorption and secretion in this mouse model produced the predicted depletion of the ASL volume, inflammation and goblet cell hyperplasia which are characteristic of CF lung disease (Mall *et al*., 2004). This model provided strong evidence that the fine balance between ions absorption and secretion is a determinant of the net fluid secretion and, therefore, the ASL height on epithelial surface. Therefore, the disturbance of this balance could produce airway surface dehydration and favor the inflammation and infection that is typical of CF lung disease.

Potassium transport: K^+ accumulation in the cells is the function of the basolateral membrane Na^+/K^+ pump (ATPase), the primary energy using process to establish the electrochemical gradient for active anions secretion. Several basolateral K^+ channels are also activated to recycle potassium brought into the cell by the Na^+/K^+ ATPase. These K^+ channels are important for regulating the membrane potential and for maintaining the electrochemical gradient for apical Cl^- secretion (Mall *et al*., 2000). By re-polarizing the membrane toward the K^+ equilibrium potential, potassium channels establish the electrical driving force for chloride to exit epithelial cells across the apical membrane. The requirement for basolateral K^+ conductance activation was evidenced by the impact of blocking this pathway with the general potassium channel blocker barium. Barium inhibits anion secretion by depolarizing the membrane potentials toward electrochemical equilibrium for Cl^- at the apical membrane thereby blocking Cl^- secretion (Mall *et al*., 2000).

Figure 1.1 Schematic Diagram of Ciliated Airway Epithelial Cells Representing Ions and Water Transport. On the apical side, the airway epithelium is covered by the airway surface liquid (ASL) that consists of PCL surrounding the cilia and gel layer on the top. The composition of the PCL is regulated by ion transport processes, mainly apical Na^+ reabsorption and Cl^- secretion, with H_2O following passively along the osmotic gradient. Trans-epithelial Na^+ reabsorption is mediated by the concerted activity of apical epithelial Na^+ channels (ENaC) and the basolateral Na^+/K^+ ATPase. The apical Cl^- secretion is mainly mediated by CFTR channels and to a lesser extent by $Ca2^+$-dependent Cl^- channels (CaCC). The chloride gradient for secretion is maintained by the basolateral $Na^+/K^+/2Cl^-$ cotransporter (NKCC). K^+ is brought into the cell through the NKCC and removed by various K^+ channels. Figured adapted from Hollenhorst *et al*., J. of Biomed. and Biotech., 2011, doi:10.1155/2011/174306.

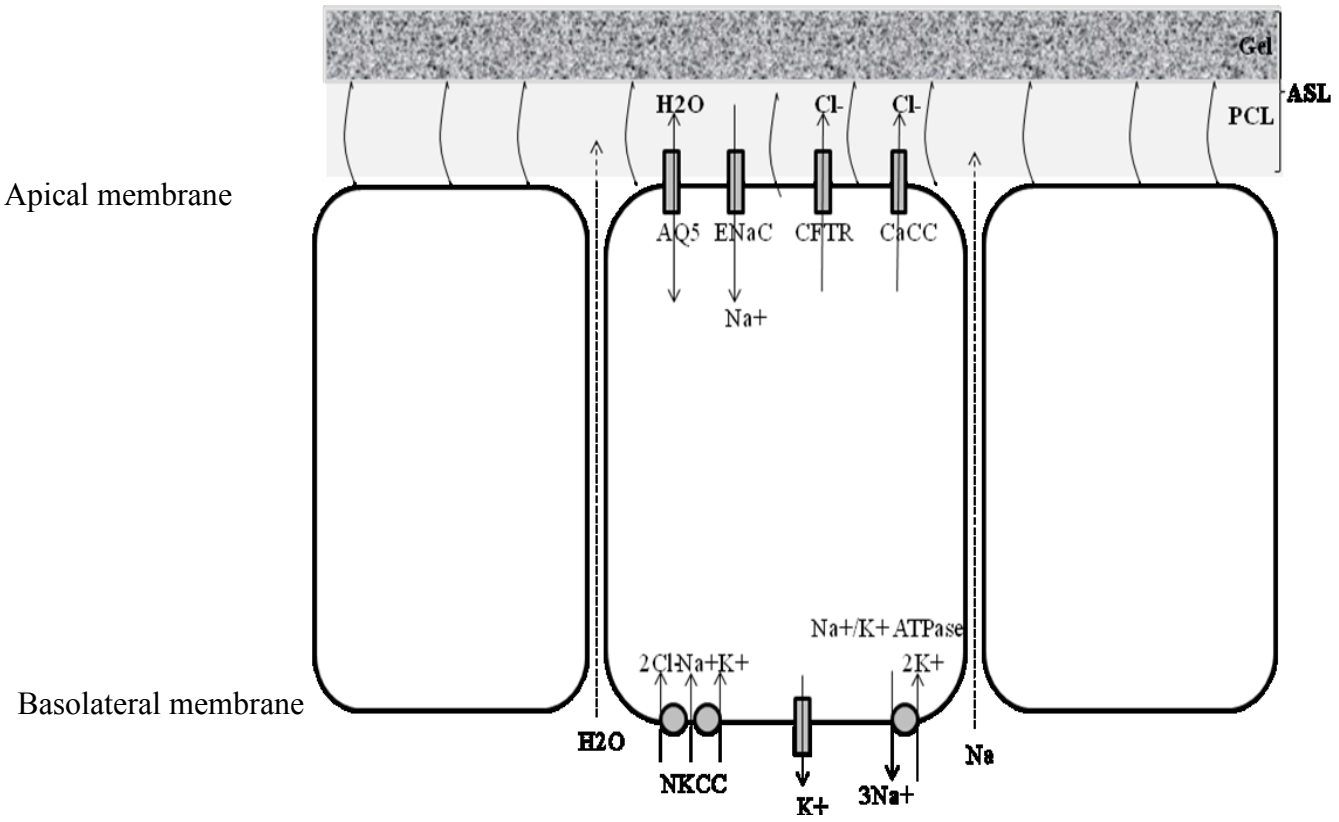

3. The Role of Submucosal Gland Secretions in Innate Defense Mechanism

Many studies have demonstrated the importance of the tracheobronchial submucosal gland secretions in the airway innate defense mechanism (Quinton, 1979; Trout *et al*., 2001; Ballard & Inglis, 2004; Dajani *et al*., 2005; Ballard & Spadafora, 2007). The role of the airway submucosal glands in the mucocilary clearance relies on the secretion of ions, fluid and antibacterial substances including lysozyme, lactoferrin, collectins, and β-defensins by its serous cells and mucin (carbohydrate-rich glycoproteins) by its mucus cells. The submucosal gland secretions (antimicrobial-rich mucus) is composed of ~95 % water, 0.5–1 % mucins, ~ 1 % NaCl, and ~0.5 – 1 % proteins (Antunes & Cohen, 2007).This unique composition makes it hard for bacteria to invade the healthy mucus layer covering the airway.

Mucins not only give the mucus its visco-elasticity needed for microbial trapping but also contain carbohydrate side chains that serve as binding sites for pathogens. Antibacterial substances secreted by the submucosal gland serous cells play an important role in killing and lysis of pathogens. The importance of submucosal glands antibacterial secretions was demonstrated in a study comparing tracheal xenograft airways with and without glands (Dajani *et al*., 2005). The authors found that airways containing glands were much more resistant to infections than those that lacked glands. Also, the amount of lysozyme in secretions from tracheas with glands was higher than in those having only epithelia. Water present in secretions from submucosal glands is important to 1- provide a vehicle for mucin and antibacterial substances in the gland's lumen, 2- sustain the volume of the periciliary fluid layer (PCL) surrounding the cilia needed to support ciliary beating 3- hydrate the mucus layer on top of the PCL to the osmolarity required for trapping pathogens.

4. Neural Control of Submucosal Gland Secretions

Submucosal glands ability to secrete fluid is neurally controlled through both central and local mechanisms. Vagal stimulation of the glands produces copious fluid secretion (Ueki *et al*., 1980; Davis *et al*., 1982). Direct application of acetyl choline (ACh) or muscarinic receptor agonists to excised porcine trachea or bronchi mimicked

the vagal stimulation (Quinton, 1979; Trout *et al*., 2001). The mechanism of muscarinic receptors (M3 muscarinic receptors) stimulation of the glandular secretions relies on the increase in intracellular Ca^{++} and PKC activation (Ballard & Spadafora, 2007). Adrenergic stimulation has been shown to exert minimal effect on human gland fluid secretion compared to its effect in other species (Ballard & Inglis, 2004).

Submucosal gland secretions can also be induced by local neuropeptides. Both human and porcine secretions can be induced by VIP or cAMP-elevating agonists (Joo *et al*., 2002; Ballard *et al*., 2006), however, this stimulation produces lower amount of fluid than the muscarinic stimulation. Also, substance P stimulation of the glands has been shown to produce copious gland fluid secretion (Trout *et al*., 2001; Phillips *et al*., 2003). Autocrine and paracrine control might also play a role in regulating submucosal fluid secretions. Extracellular nucleotides such as ATP, UTP and adenosine (Yamaya *et al*., 1996) as well as platelets activating factors (Steiger *et al*., 1987) were shown to induce gland secretions.

4.1 Regulation of Basal Glandular Secretions by VIP

The control of routine submucosal secretions that supports the ASL height and composition is believed to be intrinsic to the lung because transplanted lung can survive many years without central innervation. *In vitro*, application of low quantities of VIP and ACh to human and porcine submucosal glands produced significant mucus secretion via strong synergistic interactions. This synergy is lost in glands from CF tissues (Choi *et al*., 2007). The synergistic model supports the theory of an endogenous gland regulation responsible for maintaining the routine tone of fluid secretion needed to sustain mucociliary clearance (Wine, 2007). In this theory, routine fluid secretion of the glands is mediated primarily by VIP through the activation of CFTR-dependent ions secretion, while the ACh-dependent component of the fluid secretion is mediated by the activation of calcium activated potassium channel to increase the driving force of chloride secretion through CFTR. It has been shown that low quantities of ACh are released as a result of the low vagal tone of breathing. Evidence came from early studies describing submucosal glands to receive rhythmic excitatory input during breathing derived from airway vagal

preganglionic neurons that fire during the inspiratory phase of breathing and this drive increases in intensity during high rates of breathing (Widdicombe, 1966; Baker, 1986).

4.2 The Emergency Airway Reflex as a Function of Vagal Stimulation

A better characterized pathway for stimulated submucosal gland secretions is the central vagal defense reflex: the emergency airway defense reflex (Wine, 2007). This reflex guards the airway from strong or acute insults e.g. acute inhalation of harmful substances. It is characterized by copious secretions that result from two mechanisms. One includes induction of glandular fluid secretion through direct activation of muscarinic receptors by large quantities of ACh release that raise intracellular calcium and mediate fluid secretion through active chloride transport through the apical CaCC. The other mechanism is the contraction of smooth muscle cells surrounding submucosal glands which results in squeezing the content of the glandular lumen to the surface epithelium. This copious secretion is part of a series of events including epiglottis closure, cough, rapid shallow breathing, airway constriction, apnea, and increased blood flow. Interestingly, in CF lung this reflex is still functional, however, it fails to protect against lung damage.

To summarize, the airway submucosal glands help protect the airways against any insult in two different ways. First, the basal secretions of low quantities of antimicrobial rich mucus under the control of local intrinsic airway neurons (VIP) protects against low level of pathogens coming with normal breathing (innate defense). Second, the production of copious amount of the antimicrobial rich mucus under the control of central vagal stimulation protects against acute, potentially life-threatening inhalation of larger amounts of harmful substances (emergency reflex) (Wine, 2007).

4.3 Importance of Submucosal Gland Secretions in CF

The early observation of thick viscous mucus plugging the airways especially in the submucosal gland lumen and duct (hallmark of CF disease) (Zuelzer & Newton, 1949), the common feature of hyperplasia and metaplasia of CF submucosal glands and the observation of higher viscosity glandular secretions in CF patients (Jayaraman *et al*.,

2001; Salinas *et al*., 2005) all confirm the involvement of the submucosal glands in the pathogenesis of CF. Initially it was thought that the cause behind these symptoms was mucus overproduction only. Later the attention was shifted to epithelial ion transport physiology when Quinton (1983) showed that the problem in CF arose from low fluid secretion due to disturbed ions secretion (Quinton, 1983). This was soon confirmed after the cloning of the CFTR gene (Riordan *et al*., 1989; Rommens *et al*., 1989) and reinforced by the understanding of the role of CFTR, a cAMP-activated anion channel, in fluid secretion. Immunocytochemical studies that localized CFTR primarily to submucosal serous cells brought the attention back to submucosal glands as once more to be the center of CF pathophysiology. Further evidence to the disturbed ions / fluid secretions in CF submucosal glands came from studies with inhibitors for Cl^- and $HCO3^-$ secretions (Inglis *et al*., 1997; Trout *et al*., 1998; Trout *et al*., 2003). These studies reported that the secreted mucus was thick and poorly hydrated, and the gland ducts became clogged with thick mucus similar to that observed in CF airway glands. The use of 5-nitro-2-(3-phenylpropylamino) benzoic acid (NPPB), an anion channel blocker that is known to inhibit CFTR, also was shown to reduce mucociliary transport in porcine tracheas (Ballard *et al*., 2002), as a support to the involvement of CFTR in fluid secretion capacity of submucosal glands and its inhibition could reproduce features of CF airway pathology. Additionally, hypo-secretion of the submucosal glands in CFTR-deficient pigs confirmed the role of defective submucosal gland CFTR-dependent secretions in CF pathology (Joo *et al*., 2010).

5. Impact of Impaired Ion / Fluid Secretions on Mucociliary Clearance in CF

Failure in fluid production second to disturbed ion transport in Cystic Fibrosis results in mucociliary clearance failure with consequences of recurrent chronic infections. Researchers recently have proposed that the initiating event in CF lung disease is the rapid depletion of the ASL due to Cl^- hypo-secretion coupled to hyper-absorption of Na^+, due to the loss of the regulatory function of CFTR on the Na channel ENaC (Boucher, 2007). Despite the reduced glandular fluid capacity, the glands however, continue to secrete mucins and macromolecules which accumulate in the ducts as a viscous material.

Together, dehydrated surface mucus and disturbed clearance favors bacterial colonization, inflammation, fibrosis and eventually lung failure.

The imbalance between absorption and secretion produces a depletion of airway surface liquid (ASL) volume which induces neutrophilic inflammation and goblet cells hyperplasia characteristic of CF lung disease with death due to mucus obstruction in ~50% of ENaC overepxressing transgenic animals (Mall *et al*., 2004). Another *in vivo* study provided evidence for the role of disturbed ions secretion on the disturbed mucociliary clearance with the use of VIP-KO mice, where CFTR-dependent chloride secretion is lost. VIP-KO mice develop CF-like lung pathology with inflammation and goblet cells metaplasia suggesting that CFTR-dependent ions secretion is necessary for the innate lung defense (Chappe and Said, 2012).

III The Cystic Fibrosis Transmembrane Conductance Regulator (CFTR) Chloride Channel

1. Structure and Domains Organization

Since the cloning of the gene encoding the CFTR protein (or ABCC7) in 1989 (Riordan *et al*., 1989), affluence of information on the genetics, tissue distribution and function of CFTR are accumulating. CFTR is a multi-domain integral membrane glycoprotein which belongs to the ATP-binding cassette transporter super family of proteins. CFTR is localized at the apical plasma membrane of epithelial cells of multiple tissues, including digestive, respiratory, reproductive and most exocrine glands. At the apical membrane of epithelial cells, CFTR functions as a bidirectional ion channel responsible for electrolytes and fluid secretion. CFTR consists of 6 domains: two membrane spanning domains that each crosses the membrane with six α-helixes and form the pore of the channel (TMD1 and TMD2), two nucleotide binding domains which cooperate to bind and hydrolyze ATP for the channel gating (NBD1 and NBD2), and a regulatory (R) domain, that regulates the channel function by phosphorylation (figure 1.2). The N- and the C- termini of CFTR are located inside the cytoplasm and mediate the interactions between CFTR and a wide variety of binding proteins that regulate CFTR trafficking, surface expression and functional interactions between CFTR and other transporters, receptors and ion channels (Zhang *et al*., 2012). CFTR gating is regulated by ATP binding and hydrolysis; however, CFTR is considered an atypical ABC transporter by the presence of a unique R-domain, rich in consensus sites for phosphorylation by kinases A and C. Phosphorylation by PKA is necessary for the activation of CFTR gating while PKC phosphorylation produces negligible gating activation on its own but largely increases the responsiveness of the channel to PKA phosphorylation (Jia *et al*., 1997; Liedtke *et al*., 2001; Chappe *et al*., 2003;). Another effect for PKA and PKC phosphorylation of the R-domain includes the modulation of CFTR trafficking and membrane density (Ameen *et al*., 2003; Chappe *et al*., 2008).

Figure 1.2 Diagram of CFTR Domains

The 1,480 amino acids of CFTR are organized in 6 domains. The two Trans-Membrane Domains (TMD1 and TMD2) are forming the channel pore. Each TMD crosses the membrane with 6 alpha helixes. The two Nucleotide Binding Domains (NBD1 and NBD2) are intra-cytoplasmically located and catalyze ATP binding and hydrolysis. The Regulatory Domain (RD) contains many phosphorylation sites for PKA and PKC (P). Figure kindly provided by Fredric and Valerie Chappe.

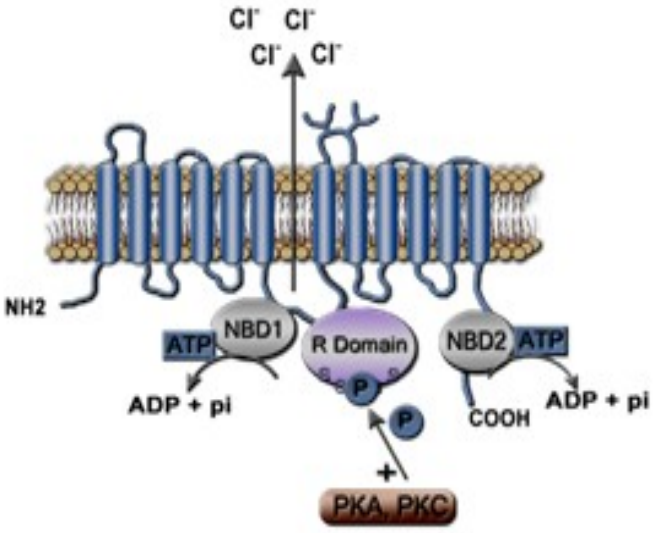

2. The CFTR Protein Life Cycle

The biogenesis of CFTR starts in the Rough Endoplasmic Reticulum (RER) ribosomes. From there the newly synthesized CFTR polypeptide chain is co-translationaly inserted into the ER membrane. CFTR is core-glycosylated by the addition of a glycoconjugates at Asn894 and Asn900, located in the fourth extracellular loop (Farinha *et al*., 2013). The N-glycosylation of CFTR at the ER creates the core-glycosylated immature form of the protein which plays a role in CFTR intracellular processes such as folding, sorting, and trafficking (Farinha *et al*., 2013). The CFTR polypeptide chain folding starts co-translationally where individual domains can achieve loosely folded conformations. In the cooperative domain folding model proposed by Lukacs G., the compactly folded, native tertiary structure of CFTR is formed post-translationally. In this model domain–domain interactions and energetic coupling are essential in CFTR co- and post-translational conformational maturation (Lukacs & Verkman, 2012). The compactly folded immature core glycosylated CFTR then passes to the Golgi apparatus for maturation where core sugars get glycosylated into complex sugar (complex glycosylated or mature CFTR) by the action of multiple Golgi glycosyltransferases. This complex glycosylation of the CFTR protein results in the presence of two bands on CFTR immunoblots: a high molecular weight C-band representing the mature protein (~ 180 kDa) and a lower molecular weight B-band (~ 140 kDa) representing the immature fraction or the core-glycosylated protein. After maturation at the Golgi level, CFTR traffics to the apical membrane. Some have reported the role of CFTR C-terminal domain in apical localization through PDZ domain interactions with scaffolding proteins (Moyer *et al*., 1999; Moyer *et al*., 2000; Milewski *et al*., 2001), however, this theory was challenged (Benharouga *et al*., 2003; Ostedgaard *et al*., 2003).

Although CFTR has a relatively long half-life: 16-24 h, WT-CFTR does not spend all its life at the membrane. It is well known that CFTR is rapidly internalized from the apical plasma membrane by clathrin-dependent mechanisms owing to the presence of a dileucine and tyrosine endocytotic signals in its C-terminal which interacts with the clathrine adaptor protein AP-2, to enter into clathrin coated pits (Prince *et al*., 1994;

Lukacs *et al*., 1997; Hu *et al*., 2001; Ameen *et al*., 2007). Once internalized from the plasma membrane, CFTR travels to early endosomes, from where it recycles back to the plasma membrane via recycling endosomes (Okiyoneda & Lukacs, 2007). The mature CFTR undergoes several cycles of endocytosis / recycling before its degradation by lysosomes.

The presence of CFTR in recycling endosomes provides an important submembranous pool of mature CFTR proteins, however, only those localized at the cell membrane participate in the trans-epithelial chloride secretion. Taking into account the slow CFTR biogenesis process and its relative long half-life, CFTR apical density, and therefore CFTR-dependent secretions, is reliant largely on the rate of endocytosis from the apical membrane and the exocytotic insertion (recycling) back to the membrane. Adapter proteins involved in CFTR endocytosis / recycling regulation have been studied in detail (Ameen *et al*, 2007; Okiyoneda and Lukacs, 2007), but its regulation by physiological agonists is far less well understood.

3. Regulation of CFTR Surface Expression by Scaffolding Proteins

PDZ domains, named after three proteins in which it was first described (Postsynaptic density 95 / Disk-large / Zonula occluden-1), are abundant protein-protein interaction modules in proteins of mammalian cells (Kennedy, 1995; Ponting, 1997). PDZ domains are usually 80-100 amino acid residues long and adopt similar topology (globular structure) with protein binding cleft (Lee & Zheng, 2010). The primary function of PDZ domains is to mediate protein-protein interactions by binding a short amino acid motif, usually found in C-termini of their interacting proteins, called PDZ interacting motif (Songyang *et al*., 1997).

The C terminus of CFTR contains a PDZ-interacting motif DTRL (the last four amino acids of CFTR) that is able to recognize and interact with PDZ domain containing proteins (Short *et al*., 1998). Seven PDZ proteins have been indentified so far to directly interact with CFTR: NHERF1, NHERF2, CAP70, PDZK1, CAL, Shank and MAST205 (Li & Naren, 2005; Li & Naren, 2010; Ren *et al*., 2013). These proteins exhibit

differential tissue distributions, suggesting that different PDZ proteins might interact with CFTR in different tissues.

The interaction of PDZ proteins with CFTR plays many roles including CFTR apical sorting (Moyer *et al*., 1999), the regulation of CFTR endocytosis / recycling, its surface expression and stability, and finally it mediates the interaction between CFTR and various ion channels like the sodium channel ENaC, the water channel AQP9, the MRP4 transporter (Multi drug Resistance protein 4), and some GPCR such as the adenosine and β-adrenergic receptors (Li & Naren, 2010).

3.1 NHERF1

3.1.1 Localization. The Sodium / Hydrogen Exchange Regulatory Factor 1 (NHERF1), also known as EBP50 (ERM-binding phosphoprotein 50), is a 50 kDa cytoplasmic phospho-protein first identified as a co-factor necessary for the protein kinase A mediated inhibition of the Na^+ / H^+ Exchanger activity in renal brush border membranes of Rabbits (Weinman *et al*., 1995). The human NHERF1 was identified in microvilli of the placental syncytiotrophoblast associated with Ezrin and actin (Reczek *et al*., 1997; Garbett *et al*., 2010). Immunoblotting experiments confirmed a widespread distribution of NHERF1 in many tissues including the kidney, intestine, placenta, lung and liver but not in the heart or skeletal muscles (Reczek *et al*., 1997; Short *et al*., 1998). Immunohistochemistry experiments then showed NHERF1 to be specifically localized to the polarized epithelia of these tissues (Reczek *et al*., 1997; Short *et al*., 1998). At the cellular level, NHERF1 is localized at the apical domain of epithelial cells and it is associated with actin-rich structures like membrane ruffles, microvilli, and filopodia. Immunohistochemical analysis of sections from human bronchi demonstrated intense staining of the apical cell surface including the cilia (Short *et al*., 1998), confirming apical localization of NHERF1 in airway epithelial cells (Reczek *et al*., 1997).

3.1.2 Regulation of NHERF1 Activity by Conformational Modifications

NHERF1 scaffolding ability to bind many proteins simultaneously, allowing it to assemble macromolecular complexes of signaling molecules, is related to its structural

organization. The human NHERF1 is a 358-residue protein organized into three protein-protein interaction domains (figure 1.3). Two PDZ domains (PDZ1, PDZ2) and a C-terminal ERM binding domain (Ezrin Radixin Moesin) also called Ezrin binding domain (EB) (www.ncbi.nlm.nih.gov/protein/NP). The PDZ1domain of NHERF1 binds to a variety of proteins including GPCR such as the parathyroid hormone receptor (PTHR) (Ardura & Friedman, 2011) and the β2-Adrenergic receptor (Hall *et al*., 1998; Hall, *et al*., 1998), and tyrosine kinase receptors such as the platelet derived growth factor receptor (PDGFR) (Maudsley *et al*., 2000). PDZ1 of NHERF1 was also shown to interact with receptors for Active C Kinase (RACK1) (Reczek *et al*., 1997; Reczek & Bretscher, 1998; Morales *et al*., 2004). The PDZ2 domain of NHERF1 binds specifically with Yes-associated protein 65 (Mohler *et al*., 1999) and β-catenin (Shibata *et al*., 2003). *In vitro*, both PDZ1 and PDZ2 bind to CFTR, however, PDZ2 has a higher binding affinity for CFTR than PDZ1 (Short *et al*., 1998). The C-terminal ERM domain of NHERF1 binds to ERMs proteins that bridge NHERF1 to the F-actin (Reczek *et al*., 1997; Reczek & Bretscher, 1998; Morales *et al*., 2004).

NHERF1 ability to mediate protein interactions is conformationally regulated (figure 1.4). Studies reported an intramolecular interaction between NHERF1 C-terminal EB domain and its PDZ2 (Li *et al*., 2007; Morales *et al*., 2007). This was later supported by structural study using NMR and circular dichroism (CD) (Cheng *et al*., 2009). Such interaction was shown to mask binding sites on both domains and to hold NHERF1 into an auto-inhibitory conformation.

Phosphorylation of NHERF1 was shown to increase its ability to assemble macromolecular complexes. Many kinases were reported to phosphorylate NHERF1 including G protein-coupled receptor kinase (GRK6A) at Ser-289 in the C-terminus (Hall *et al*., 1999) and Cyclin-dependent kinase 2 (Cdc2) at Ser-279 and Ser-301 in a cell-cycle dependent manner (He *et al*., 2001). NHERF1 is also phosphorylated by PKC (Deliot *et al*., 2005) on two amino acid residues (Ser-339 and Ser- 340) in its C-terminal domain (Li *et al*., 2007). Phosphorylation of NHERF1 disrupts the auto-inhibitory conformation providing an explanation for the molecular mechanism by which phosphorylation

activates NHERF1. Evidence came from studies using small-angle neutron scattering (SANS) experiments and binding assays showing that PKC phosphorylation of NHERF1 on Ser-339 and Ser- 340 disrupts the intramolecular interaction within NHERF1(Li *et al*., 2005; Li *et al*., 2007; Li *et al*., 2009). Similarly, PKC phosphorylation-mimicking mutants of NHERF1 (S339D/S340D) displayed a higher binding affinity for CFTR than WT-NHERF1 (Cheng *et al*., 2009).

Other than phosphorylation, NHERF1 ability to assemble complexes can be increased upon Ezrin interaction with its EB domain (Bhattacharya *et al*., 2010). A study by Zimei Bu showed that when the FERM domain of Ezrin binds to the C-terminal EB domain of NHERF1, the binding affinity of NHERF1 PDZ2 for CFTR C-terminal increases by 26 fold (Li *et al*., 2005). They also found that the mechanism responsible for NHERF1 activation after Ezrin interaction involves a disruption of the head-to-tail conformation within the dormant NHERF1 molecule leading to active NHERF1 (Li *et al*., 2009), providing a structural explanation for Ezrin allosteric control of NHERF1 activation.

3.1.3 Role of NHERF1 in Regulating CFTR Surface Expression and Stability

NHERF1 is known as a positive regulator for CFTR surface expression, stability and function (Moyer *et al*., 2000; Swiatecka-Urban *et al*., 2002; Broere *et al*., 2007). Studies over-expressing NHERF1 in human airway cells indicated a direct positive effect on both WT-CFTR and ΔF508-CFTR density at the membrane with subsequent increase in CFTR-dependent chloride secretion (Guerra *et al*., 2005; Favia *et al*., 2010). Down-regulating NHERF1 expression with RNA interference, reversibly reduced the surface expression of WT-CFTR without altering its total expression level and reduced both surface and total expression of temperature rescued ΔF508-CFTR with an accelerated degradation rate (Kwon *et al*., 2007). These studies indicated an important role of NHERF1 in regulating CFTR surface stability.

One mechanism for NHERF1 to stabilize CFTR at the membrane is by bridging CFTR to the actin cytoskeleton. With its PDZ2 domain, NHERF1 can bind to the DTRL

motif of CFTR (Short *et al*., 1998; Wang *et al*., 1998) while it interacts with the actin binding proteins ERM with its EB domain (Reczek & Bretscher, 1998; Bretscher *et al*., 2000; Morales *et al*., 2004). Such a multi protein interaction capacity (CFTR-NHERF1-ERMs-Actins) is thought to enable NHERF1 to control CFTR surface stability, preventing premature endocytosis.

NHERF1 was shown to play a role in the agonist-mediated increase of CFTR conductivity through its scaffolding ability. This includes the cAMP-mediated activation of CFTR, where PKA is brought in close proximity of CFTR through the Ezrin-NHERF1 complex (Dransfield *et al*., 1997) which enables PKA to phosphorylate CFTR. Evidence came from studies showing that PKA is localized in proximity to CFTR by an A-kinase anchoring protein (AKAP) like Ezrin (Dransfield *et al*., 1997; Huang, Trotter, Boucher, Milgram, & Stutts, 2000). Similarly, PKCε that regulates CFTR surface stability and function was shown to be tethered in close proximity to CFTR through NHERF1 interaction with RACK1 (Receptors for Activated C kinase) (Liedtke *et al*., 2002; Liedtke *et al*., 2004, Yarwood *et al*. 1999; Chang *et al*. 2001). Additionally, NHERF1 was shown to mediate the association of CFTR with some GPCR including the ß2-adrenergic receptor, allowing agonist-specific signaling (Hall *et al*., 1998; Naren *et al*., 2003).

3.2 CAL

3.2.1 Localization and Domain Arrangement

The CFTR-associated ligand (CAL) also known as PIST (PDZ domain containing protein interacting specifically with TC10), GOPC (Golgi-associated PDZ and coiled-coil motif containing), and FIG (fused in glioblastoma) is a PDZ adaptor protein known to interact with CFTR to regulate its trafficking and surface expression and therefore its function. CAL was identified as a CFTR interacting partner in yeast two-hybrid screens using the last 51 amino acids of the C terminus of rat CFTR (Cheng *et al*., 2002).The interaction between CFTR and CAL was confirmed in a yeast expression system and was shown to be dependent upon the terminal amino acids of CFTR (Cheng *et al*., 2002). Then full length human CAL was identified by screening human lung cDNA libraries.

CAL is an ubiquitous adaptor protein with a wide distribution in human tissues as first shown by Northern blot analysis (Cheng *et al*., 2002). Immunofluorescence labeling of CAL to determine its endogenous tissue distribution in rat trachea, showed CAL localization at the surface epithelium and in submucosal glands where CFTR is expressed. At the subcellular level, CAL is localized in the Golgi apparatus and in Golgi associated vesicles (Neudauer *et al*., 2001; Cheng *et al*., 2002; Cheng *et al*., 2004). It co-localizes with the trans-Golgi network marker TGN38 both in submucosal acinar cells and in kidney cells (Cheng *et al*., 2002).

CAL consists of 454-amino acid organized into three protein-protein interaction domains (figure 1.3), a C-terminal PDZ domain that is known to interact with CFTR and two coiled-coil domains that facilitate homo-multimerization and probably membrane association (Cheng *et al*., 2002). The interaction of the second coiled–coil domain with the GTPase TC10 (Neudauer *et al*., 2001), and the SNARE Syntaxin 6 (Charest *et al*., 2001) suggests that CAL might be involved in vesicle trafficking.

3.2.2 Role of CAL in the Regulation of CFTR Membrane Expression

The PDZ-dependent interaction of CAL and CFTR was confirmed by solution NMR spectroscopy (Piserchio *et al*., 2005) and structure-based mutagenesis experiments (Wolde *et al*., 2007). CAL is known as a negative regulator for both WT-CFTR and ΔF508-CFTR surface expression by mediating its lysosomal trafficking and degradation. Over-expression of CAL in the mammalian cell line COS-7 with WT-CFTR reduced CFTR surface expression and its activity. CAL over-expression also caused a dose-dependent reduction in mature CFTR which indicates that CAL not only retains CFTR in the cytoplasm but also mediates its degradation (Cheng *et al*., 2002). Inhibition of lysosomes by bafilomycin A1, a lysosomal proton pump inhibitor, reversed CAL-mediated CFTR degradation (Cheng *et al*., 2004). Inhibition of clathrin-mediated endocytosis by expression of the dominant negative dynamin prevented the CAL-dependent reduction of surface CFTR in CAL over-expressing cells suggesting that CAL interacts with CFTR after its endocytosis from the membrane.

Moreover, CAL was shown to limit the surface expression of ΔF508-CFTR. Suppression of endogenous CAL expression with RNA interference, increased ΔF508-CFTR surface expression and function in polarized human bronchial epithelial cell line (Wolde *et al*., 2007) suggesting that CAL is an important degradation mediator of ΔF508-CFTR. Studies have shown that the inhibitory effect of CAL on CFTR surface expression could be reversed by over-expressing NHERF1 (Cheng *et al*., 2002). This observation leads to the speculation that both CAL and NHERF1 compete for the same CFTR binding site to regulate CFTR surface expression in an opposite manner, however, the mechanism of such a competition is not clearly understood. Studies using fluorescence polarization, isothermal titration calorimetry, and surface-plasmon resonance analysis showed much higher affinity of the DTRL motif of CFTR for NHERF1 than CAL (Cushing *et al*., 2008). This might provide an explanation for the ability of the wild-type CFTR to recycle several time to the membrane, escaping CAL mediated degradation. The authors also speculated that the low affinity of CAL for CFTR C-terminal motif might be just enough for trapping the unstable mutant protein, limiting its surface expression and function (Cushing *et al*., 2008).

3.3 Ezrin / Radixin / Moesin (ERMs)

Ezrin / Radixin / Moesin (ERMs) are membrane-associated proteins which are involved in the dynamics of interactions between plasma membrane proteins and the actin cytoskeleton. The genes for the three proteins reside on different human chromosomes; the Ezrin gene is on chromosome 6, Radixin is on chromosome 11 and Moesin is on the X chromosome (Bretscher *et al*., 2000). However, the three proteins are closely related in terms of amino-acid sequence homology. Ezrin (82-kDa) was first purified from the chicken intestinal microvilli (at Ezra Cornell University, after which it was named) (Bretscher, 1983) and then was shown to be enriched in the actin rich cell surface structures in a wide variety of cells. The 75-kDa Moesin (Membrane-Organizing Extension Spike Protein) shares 74% amino acid homology with Ezrin and is also enriched in actin rich cell surface structures (Lankes & Furthmayr, 1991; Franck *et al*., 1993; Amieva & Furthmayr, 1995) while the 80-kDa Radixin, a barbed end-capping actin protein shares 77% amino acids homology with Ezrin (Tsukita*et al*., 1989; Amieva *et al*., 1994;). Based on the sequence homology, the three proteins constitute together the ERM

family that belongs to the band 4.1 superfamily by the virtue of the presence of a shared functional domain at the amino terminus called the FERM (Four-point one, ezrin, radixin, moesin) that was first identified in the band 4.1 protein.

3.3.1 Localization

Ezrin, Radixin and Moesin are co-expressed and co-localized in most cultured cells (Sato *et al*., 1992; Franck *et al*., 1993), however, they exhibit differential tissue specific distribution *in vivo*. For example, Ezrin is expressed in epithelial cells while endothelial and hematopoietic cells express Moesin. The brush border of intestinal epithelial cells expresses only Ezrin, while the hepatocytes express only Radixin (- , 2000). Radixin was first isolated from rat liver and shown to be localized at the hepaocyte adherens junctions (Tsukita *et al*., 1989). Later Radixin was shown to be also localized at the focal contacts in cultured cells and to the bile caniculi microvilli (Amieva *et al*., 1994).

At the subcellular level, Ezrin and Moesin have a similar subcellular apical distribution (Franck *et al*., 1993) where they are enriched in actin-rich surface structures such as microvilli (Franck *et al*., 1993; Amieva & Furthmayr, 1995) while Radixin shows slightly distinct distribution and is primarily localized to adherent junctions and in the cleavage furrow (- , 2000).

In cultured cells, the majority of Ezrin is present in the cytoplasm in a dormant state with only a small amount of active Ezrin localized beneath the plasma membrane and involved in cytoskeleton / plasma membrane proteins interaction. The association of Ezrin with the cytoskeleton is correlated with its phosphorylation on serine / threonine residues. Apoptosis induced serine / threonine dephosphorylation was shown to be associated with the translocation of the unphosphorylated Ezrin from the plasma membrane to the cytoplasm, inducing the disappearance of microvilli (Kondo *et al*., 1997). Immuno-detection with an antibody directed against conserved phosphorylated threonine residues (Moesin: Thr 558, Radixin: Thr 564 and Ezrin: Thr 567, collectively known as P-ERM) has shown that phosphorylated ERMs are highly concentrated in

microvilli (Hayashi *et al*., 1999). Thus P-ERMs represents the activated form of ERM proteins.

3.3.2 Domains Arrangement

ERMs are composed of three domains: an amino-terminal domain (FERM) that binds to the F-actin, a central α-helix domain, and a charged carboxy-terminal domain that binds to membrane or adaptor proteins (figure 1.3). Ezrin and Radixin have between the α-helix and the carboxy-terminal domain a poly-proline stretch.

The N-terminal 300-amino-acids (30-kDa) of the ERMs are highly conserved and form a functional domain. The FERM domain defines all members of the band 4.1 superfamily which contains five members (the band 4.1, the ERM family, talin, Protein Tyrosine Phosphatase family and the NBL4 family (- , 2000). This unique module binds to membrane proteins either directly or through adaptor proteins thus also defined as the membrane-cytoskeletal linking domain. The FERM domain is a cystein-rich, basic-charged globular domain that is formed of three structural units that together form a compact clover-shaped structure (- , 2000). The central α-helical domain has been shown to be important for PKA association (Dransfield *et al*., 1997) and the ~100 amino acids C-terminal domain binds to F-actin.

3.3.3 ERMs Function

ERM proteins, among which Ezrin is the most extensively studied, are well known as linkers of the actin cytoskeleton to the cell surface transmembrane proteins either directly, such as in the case of the hyaluran receptor CD44 and ICAM-2 (intercellular adhesion molecule-2) (Tsukita *et al*., 1994; Heiska *et al*., 1998), or indirectly through adaptor molecules such as NHERF1 in the case of CFTR and the β-adrenergic receptor (Reczek *et al*., 1997; Short *et al*., 1998). These large cytoskeleton-membrane protein complexes might in turn regulate important cellular activities including mediating cell-substrate and cell-cell adhesion, cell motility, membrane protein surface density and therefore membrane transport, trafficking and signal transduction.

The influence of ERMs on membrane associated signaling can be direct or indirect. The indirect influence results from the ability of ERMs to regulate membrane protein surface density by modulating endocytosis / recycling and surface stability (Bretscher *et al*., 2000; Li *et al*., 2005). The direct influence of ERMs on signaling results from their ability to scaffold cytoplasmic components of signal transduction cascades (Dransfield *et al*., 1997). Examples for the ERMs role include the regulation of PKA signaling by tethering the activated PKA near its downstream targets in cellular domains for efficient signaling (Dransfield *et al*., 1997). ERMs activation and recruitment to the membrane is also implicated in the regulation of insulin secretion by pancreatic β-cells (Lopez *et al*., 2010) and gastic acid secretion by stomach parietal cells (Ding *et al*., 2010).

ERMs are also implicated in maintaining the cell shape by facilitating the organization of morphologically distinct cell-surface domains by modulating the cortical actin cytoskeleton. ERMs are enriched in actin rich cell surface structures and are known to play a role in the formation of membrane associated projections like microvilli (Yonemura *et al*., 1999) that differentiate the apical domain of certain cells.

3.3.4 Conformational Regulation of the ERM Proteins

It is now well known that ERMs exist in two forms: a dormant and an active form (figure 1.4). The difference between these two states depends on the conformation of the proteins. In dormant Ezrin, the N-terminal domain binds very tightly to the C-terminal domain (Gary & Bretscher, 1995; Pearson *et al*., 2000), masking the binding sites for either NHERF1 or membrane proteins (Gary & Bretscher,
1995; Reczek & Bretscher, 1998).

Considerable evidences now exist to show that the activation of ERM proteins can be achieved by serine / threonine phosphorylation modulating the intramolecular interaction. For example, activation of dormant Moesin or Ezrin by PKC phosphorylation disrupts the intramolecular interactions and simultaneously unmasks both NHERF1 and F-actin binding sites (Simons *et al*., 1998; Larsson, 2006; Hong *et al*., 2011). Phosphorylation of Ezrin on T567 by EGF leads to cell polarization in the form of

lamellipodia and invasion (Orr Gandy *et al*., 2013). Similarly, activated PKA, after histamine stimulation, phosphorylates Ezrin within the FERM domain causing its activation which is important for gastric acid secretion (Neisch & Fehon, 2011). Other evidence for the conformational regulation of ERMs came from a recent study showing the importance of ERMs activation for the release of insulin from β-cells of the pancreas in response to high blood glucose level (Lopez *et al*., 2010). The study reported that Ezrin and Radixin were predominantly cytoplasmic in β-cells under low glucose condition. In response to high glucose stimulation both proteins became phosphorylated. Phosphorylation of Ezrin and Radixin was associated with their translocation to the plasma membrane where they play a role in insulin vesicle release (Lopez *et al*., 2010). Also, the over-expression of NHERF1 increased the phosphorylation of Ezrin with subsequent redistribution of phospho-Ezrin to the membrane fraction (Kwon *et al*., 2007).

Figure 1.3 NHERF1, CAL and ERMs Domain Arrangement.

The NHERF1 scaffolding protein contains two protein-protein interaction domains (PDZ1 and PDZ2) and a C-terminal Ezrin Binding domain (EB). CAL contains only one PDZ domain at the C-terminal along with two protein-protein interaction coiled-coil domains (CC). Ezrin, Radiaxin, Moesin (ERMs) are closely related proteins that all share a FERM domain that interacts directly or indirectly with a variety of membrane proteins, a central α helix and a C-terminal actin interacting tail. P: phosphorylation sites. Figure adapted from Chunying Lia and Anjaparavanda P. Naren, Integr. Biol., 2010, 2, 161–177.

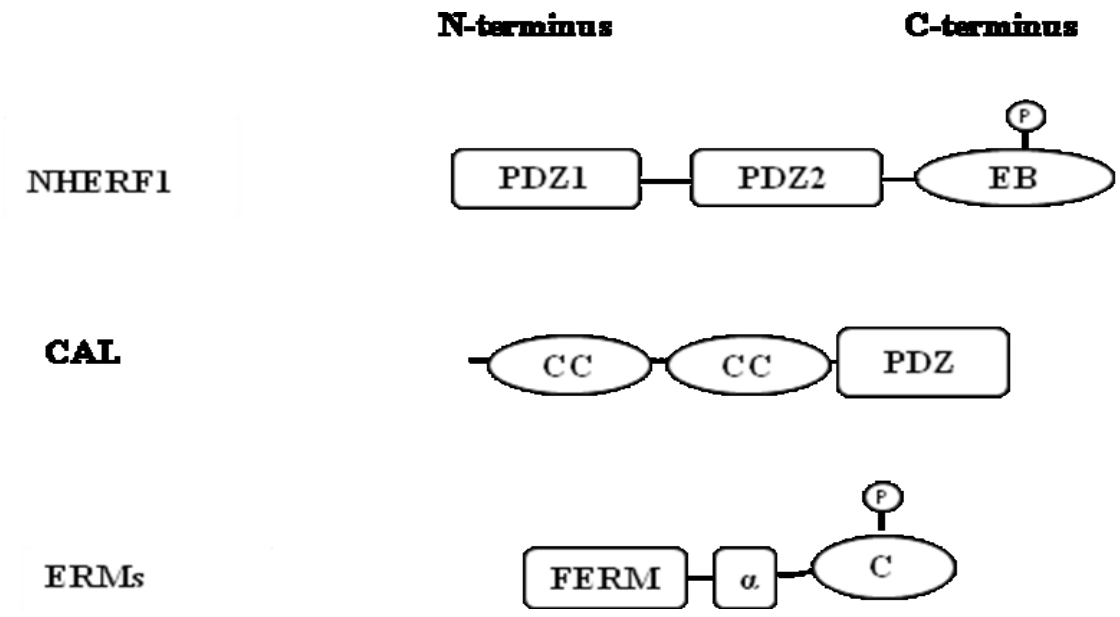

Figure 1.4 Conformationl Regulation of NHERF1 and ERM Proteins Activity.

A: Phosphorylation of ERMs carboxyl-termini and interactions with membrane lipids disrupt the intramolecular head-to-tail interactions that hold these proteins in the inactive state. **B**: NHERF1 scaffolding function is also regulated through conformational changes in the protein. Under basal condition most NHERF1 proteins are soluble in the cytoplasm where they adopt a head-to-tail inhibitory conformation (inactive state) due to intramolecular interaction between the EB and PDZ2 domains that mask the ligand binding sites on both PDZ1 and PDZ2. Phosphorylation or ERMs interaction release the intramolecular interaction, unmasking NHERF1 ligand binding sites on both PDZ domain. P: phosphorylation.

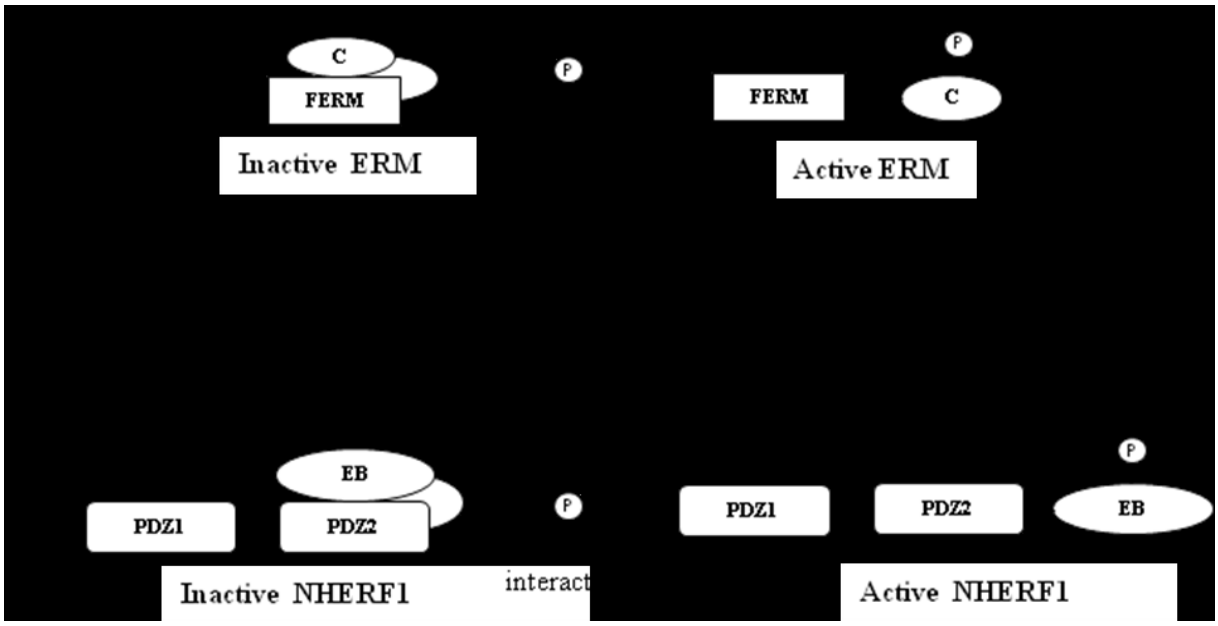

IV The Vasoactive Intestinal Peptide (VIP)

1. VIP Historical Background

The biological activity of VIP as vasodilator was noticed even before its discovery early in 1902 (Bayliss & Starling, 1902) when Bayliss and Starling reported that the dogs' Jejunum extract caused a dilation effect on the intestine. They attributed the effect to an unidentified substance in the intestinal extract. 50 years later the vasodilator substance was first discovered in the porcine lung for its vasodilator and muscle relaxant effect (Said & Mutt, 1969). The difficulty of collecting fresh lungs from the slaughter houses hampered its isolation from the lung at this time. Having in mind the early report on the intestinal extract vasodilator ability and the common embryonic origin for both lung and intestine Dr Said isolated the pure form of the vasodilator peptide from the porcine intestine for the first time in 1970 (Said & Mutt, 1970). Dr Said gave his new peptide discovery an identity after the first organ it was isolated from and it's first reported biological activity, Vaso-active Intestinal Peptide or VIP. VIP was then chemically characterized (Mutt & Said, 1974) with the sequence of the porcine VIP identified as His-Ser-Asp-Ala-Val-Phe-Thr-Asp-Asn-Tyr-Thr-Arg-Leu-Arg-Lys-Gln-Met-Ala-Val-Lys-Lys-Tyr-Leu-Asn-Ser-Ile-Leu-Asn-NH2.

After chemical characterization it became clear that this 28 amino-acid peptide with a molecular weight of 3,326 Da fits within the glucagon-growth hormone releasing factor superfamily which also includes PACAP, secretin, glucagon, helodermin, sauvagine, urotensin I, and gastric inhibitory peptide (glucose-dependent insulinotropic peptide) (Said, 2007). All members of this family are chemically and biologically associated with VIP, with the pituitary adenylate cyclase-activating polypeptide (PACAP) being the most closely related to VIP with 68% amino acid homology.

Immunohistochemical studies have shown that VIP immunoreactivity is localized primarily to neurons and nerve terminals in all VIP producing tissues (Uddman *et al*., 1978; Lundberg *et al*., 1980; Dey *et al*., 1981; Said, 1982). Later the plasma level of VIP was noticed to be increased in neuronal tumors (VIPomas). This observation encouraged Dr Said and his colleagues to look for VIP in neuronal tissues. His observation turned out

to be true when they identified VIP in the central and peripheral nervous systems. VIP was rediscovered as a neuropeptide with neurotransmitter or neuromodulator properties where its level only increases in proximity to its release site (Said *et al*., 1980). VIP blood level increases after exercise and in VIP-releasing tumors might also suggest that VIP act as a blood borne hormone on remote tissues (Said, 1991).

VIP is well appreciated as a very important peptide with pleiotropic effects such as immuno-regulator, vasodilator, smooth muscle relaxant, and mediator of water and ions secretion (secretagogue). Disturbed VIP levels in several human disorders also suggest that VIP plays roles in the pathogenesis of several diseases. For example its overproduction and elevated plasma level was seen in pancreatic cholera, watery diarrhea and in certain tumors while its underproduction was seen in cystic fibrosis and primary arterial hypertension (Said, 1991). VIP modulation thus presents a potential therapeutic benefit in a variety of disorders.

2. VIP Synthesis

The human gene encoding VIP is located on the chromosome 6, region 6q24. VIP is synthesized from a 170 amino acid long precursor molecule (Pro-VIP), which contains the VIP sequence and a sequence for a related peptide named PHM (peptide with N-terminal histidine and C-terminal methionine amide) in human or PHI (peptide with N-terminal histidine and C-terminal isoleucine amide) in rodents. VIP biosynthesis is stimulated by many factors including activation of PKA or PKC that can stimulate VIP gene transcription synergistically. Also, activation of muscarinic receptors by carbachol, PACAP and calcium were all reported to increase VIP mRNA synthesis (Dickson & Finlayson, 2009).

Under normal conditions, VIP is mainly degraded into inactive fragments by neural endopeptidase (NEP) while in case of inflammation VIP cleavage into inactive fragments is mainly the function of mast cell chymases and mast cell tryptases (Caughey*et al*., 1988; Goetzl *et al*., 1989; Groneberg *et al*., 2001).

3. VIP Receptors

Receptors for VIP were first described through [125I]-VIP ligand binding techniques (Carstairs & Barnes, 1986) and measurements of cAMP production (Frandsen *et al*., 1978). Three receptors have been cloned and identified for VIP: VPAC1, VPAC2 and PAC1 (Ishihara *et al*., 1992). Both VPAC1 and 2 bind both VIP and PACAP with equal affinity while PAC1 shows high affinity for PACAP and low affinity for VIP. VIP receptors show a differential distribution in different tissues with PAC1 present predominantly in the brain, while VPAC1 is expressed in brain and in peripheral tissues such as liver, lung and intestine, as well as immune cells. VPAC2 is expressed in the CNS and in a number of peripheral tissues, including the pancreas, skeletal muscle, lung, heart, kidney, adipose tissue, testis, and stomach, blood vessels, the GI and reproductive tract. The wide distribution of VIP receptors represents the pleiotropic effect of VIP on many systems including both the CNS and the periphery.

In human airways, the distribution of VIP receptors follows the pattern of VIP containing nerve distribution in the smooth muscle layer of larger but not smaller airways, pulmonary vascular smooth muscles, airway epithelium and submucosal gland serous cells. In the nasal mucosa, VIP receptors are found in epithelial cells, submucosal glands, and arterial but not sinusoidal vessels. VIP receptors are also found in immune cells (Wu *et al*., 2011).

VIP receptors belong to the class II GPCR family of 7 transmembrane domain receptors. It has been shown that VPAC1 and VPAC2 receptors can couple to Gαs, Gαq or Gαi, however, PAC1 receptor can only couple to Gαs and Gαq but not Gαi. Upon activation and Gαs, the three receptors produce an increase in the intracellular cAMP level with subsequent activation of cAMP-dependent protein kinases which leads to smooth muscle relaxation (Lincoln *et al*., 1990). The rise in cAMP after VIP receptors activation also activates CFTR-dependent secretions (Martin & Shuttleworth, 1994). Additionally, the three receptors can also activate the PLC signaling cascade, leading to an increase in intracellular Ca^{2+} and PKC activation, via coupling to Gαq/i. (Dickson & Finlayson, 2009)(figure 1.5).

Figure 1.5 Transduction Pathways for VIP Receptors.

VPAC1 and VPAC2 receptors are coupled to Gαs, Gαq or Gαi. However, PAC1 receptor can only couple to Gαs and Gαq but not Gαi. Upon VIP binding to VPAC1, 2 or PAC1, the PKA and/or PKC signaling cascades are stimulated.

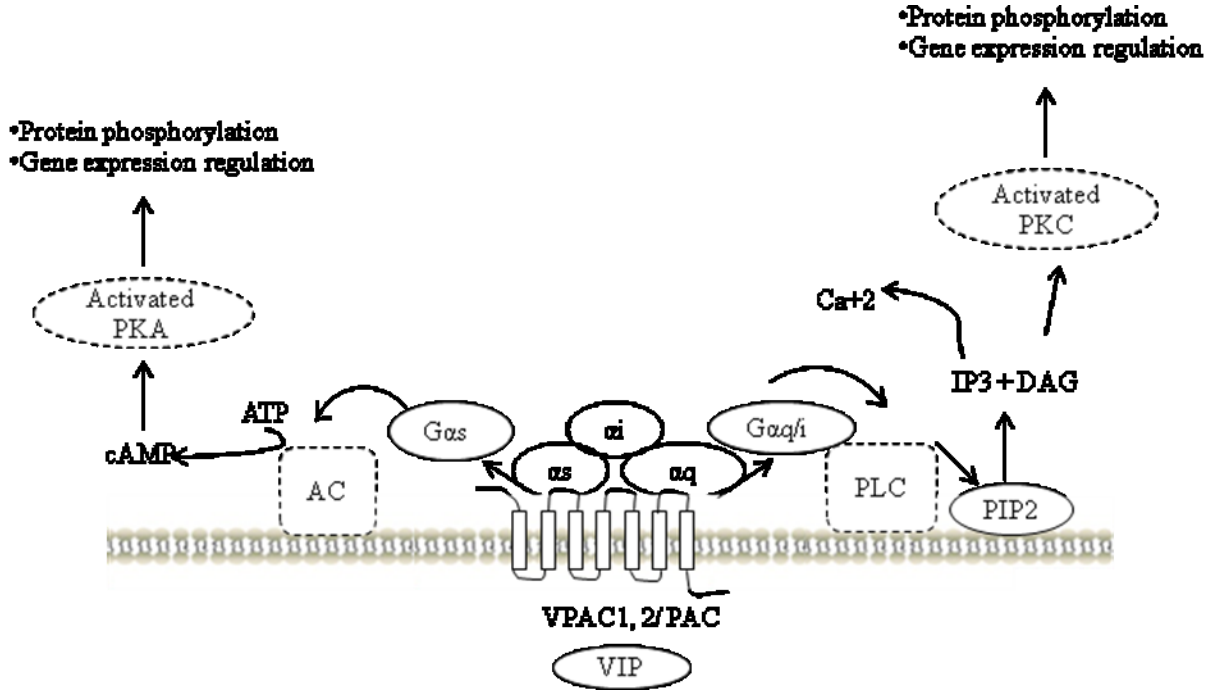

4. VIP Distribution with Special Attention to the Airways

Immunohistochemical and radioimmunoassays have demonstrated the widespread distribution of VIP in many tissues including the central and peripheral nervous systems. VIP containing nerves are co-localized with acetylcholine secreting neurons surrounding exocrine glands (Lundberg *et al*., 1980; Heinz-Erian *et al*., 1986).VIP also can be released by endocrine and immune cells (Aliakbari *et al*., 1987; Cutz *et al*., 1978).

In the airways, VIP is localized primarily to sensory neurons and nerve terminals (Uddman *et al*., 1978; Dey *et al*., 1981) suggesting that its release is intrinsic to the lung and not related to the CNS (Said, 1982). VIP containing nerves are found as a branching network (Ghatei *et al*., 1982) in the human airway with more abundant distribution in the upper airways and less abundant distribution in the lower airways (Laitinen *et al*., 1985). The pattern of VIP releasing nerves distribution follows that of cholinergic nerves, consistent with the co-localization of VIP and acetylcholine in human airway nerve fibers (Laitinen *et al*., 1985). VIP releasing nerves are present mainly in the smooth muscle of large, but not smaller airways, pulmonary vascular smooth muscle layer, around the mucus and serous glands of the airways as well as in airway epithelium and in alveolar walls. VIP was also reported in ganglion-like structures containing clusters of VIP-rich neuronal cell bodies near the bronchi (Dey *et al*., 1981).

In the lung, VIP is a potent relaxant of airway smooth muscle and thus a very potent bronchodilator. VIP is also a fluid secretagogue for the human airway submucosal glands by its direct regulation of CFTR function (Wine, 2007). VIP also augments the antibacterial substance secretion by serous cells of the airway submucosal glands (Wu *et al*., 2011).

5. VIP as Gland Fluid Secretagogue

Studies using direct VIP application *in vitro* clearly demonstrated the VIP ability to induce gland secretions in ferret, cat, rat, pig and human tracheal glands (Joo *et al*., 2002; Groneberg, *et al*., 2006). VIP was then shown to stimulate an active secretion of chloride and $HCO3^-$ ions in the dog trachea that is not blocked by atropine, suggesting an

additive effect to the acetylcholine-dependent secretion. Also VIP was shown to increase lactoferrin secretion from human nasal mucosal cells (Groneberg *et al*., 2006). Then it became clear that the ability of VIP to induce glandular fluid secretion is mediated through activating CFTR-dependent secretions because CF glands, where CFTR is defective, do not secrete fluid in response to VIP (Joo *et al*., 2002; Joo *et al*., 2010), but do respond to carbachol (Choi *et al*., 2007; Ianowski *et al*., 2007; Joo *et al*., 2010). Also cAMP elevating agonists e.g. forskolin, mimic the secretion response to VIP (Joo *et al*., 2002; Ballard *et al*., 2006). Studies then indicated that human and pig airway glands secrete maximum mucus when stimulated by low concentration of both VIP and ACh and this synergistic mode between VIP and ACh was lost in CF submucosal glands (Choi *et al*., 2007).

An *in vivo* study utilizing VIP-KO mice as a model for VIP deficiency provided direct evidence for the importance of VIP stimulation for CFTR function on the health of the lung. In this study, CFTR-dependent chloride secretion was lost and VIP-KO mice developed CF-like lung pathology with inflammation and goblet cells metaplasia (Alcolado, 2010; Chappe and Said, 2012). Thus absence of VIP regulation of CFTR in CF could potentially play an important role in the development of the disease. VIP deficiency and its disturbed regulation of CFTR might contribute to the disturbed ion/ fluid secretion seen in CF.

6. VIP Deficiency in CF Tissues

Observation of exocrine dysfunction in CF disease was hypothesized to originate from a lack of VIP secretion before the gene encoding the CFTR protein was discovered and CF characterized as a monogenic disease. The hypothesis was proven to be true when Heinz-Erian showed that innervations by VIP immune-reactive nerves surrounding the acini and collecting ducts of sweat glands of CF patients were almost absent compared to tissue samples from normal human subjects (Heinz-Erian *et al*., 1985). The deficient VIP secretion in CF exocrine tissues was then confirmed by several other groups showing reduced innervations of VIP in skin, nasal mucosa and intestinal mucosa of CF patients

(Wattchow*et al*., 1988; Savage *et al*., 1990). Additionally, deficiency of VIP binding sites was also seen in human CF lung (Sharma *et al*., 1995).

The absence of several biological functions attributed to VIP could be related to CF pathogenesis including the absence of its anti-inflammatory and immunomodulatory activities. However, the absence of VIP function as a gland fluid secretagogue drew the attention of many researchers to explain the basic defect in CF because this action is mediated through VIP direct regulation of CFTR function which presents the primary defect in CF. Researchers are devoted to understand how the absence of VIP regulation of submucosal gland fluid secretion (through CFTR) could potentially contribute to the development of the disease pathology.

7. Role of VIP in Regulating CFTR Membrane Expression and Function

7.1 VIP signaling pathways regulating CFTR

Stimulation of VIP receptors initiates signaling cascades that stimulate PKA and/or PKC. In the Calu-3 cell line, the most widely used model of airway submucosal gland serous cells, that endogenously express CFTR on the apical membrane and VPAC1 receptors for VIP on the basolateral membrane, both Gαs and Gαq/i signaling pathways are activated by VIP and play different roles in CFTR regulation (Derand *et al*., 2004; Chappe *et al*., 2008;) (figure 1.6).

Gαs activation: Activated Gαs dissociates from the receptor and activates Adenyl cyclase enzymes with subsequent increase in intracellular cAMP concentration and PKA activation. Activated PKA is held in CFTR compartment by its interaction with a PKA-anchoring protein; such as Ezrin (Dransfield *et al*., 1997; Huang *et al*., 2000) where it can directly phosphorylate CFTR on the R domain to stimulate its ATP-dependent gating. It has also been proposed that activated PKA is implicated in CFTR trafficking regulation through an unidentified mechanism (Ameen *et al*., 2003; Rafferty *et al*., 2009), however, conflicting results are found perhaps due to disparity in the cell types studied.

Gαq/i activation: Activation of the Gαq/i signaling pathway activates phospholipase C (PLC) located at the plasma membrane. PLC hydrolyzes Phoshpatidylinositol 4, 5-bisphosphate (PIP2) into Insitol 1, 4, 5-triphosphate (IP3) and Diacylglycerol (DAG). IP3 binding to receptors in the membrane of smooth endoplasmic reticulum promotes the opening of Ca2+ channels, whereas DAG activates PKC. PKCε was identified as the exclusive PKC isoform involved in regulating CFTR activity in Calu-3 cells (Okiyoneda *et al*., 2004). Similarly, Chappe V. and her group identified PKCε as the isoform selectively activated after VIP stimulation of the VPAC1 receptor (Alcolado *et al*., 2011; Chappe and Said, 2012). The activated PKCε is held in the apical compartment of cells through NHERF1 interaction with the PKCε shuttling protein RACK1 (Liedtke *et al*., 2002; Liedtke *et al*., 2004; Liedtke & Wang, 2006). The activated PKCε can then phosphorylate CFTR to produce minimal channel activation but a significant increase in CFTR responsiveness to PKA activation (Chappe V *et al*., 2003; Jia *et al*., 1997; Liedtke & Cole, 1998; Liedtke *et al*., 2001; Seavilleklein *et al*., 2008). Chappe and her group also reported that activated PKCε, after VIP stimulation, plays a role in modulating ΔF508-CFTR membrane stability in JME/CF15 cells. The role of PKCε activation after VIP stimulation was shown to lead to a significant increase in CFTR membrane density through stabilizing CFTR at the membrane by reducing its endocytosis by more than 50% (Chappe *et al*., 2008), however the detailed mechanism was not known and was the main focus of this research thesis.

7.2 Chronic VIP Stimulation is Needed for CFTR Membrane Localization and Function

In a study using VIP-KO mice as a model of VIP deficiency (Chappe and Said, 2012), CFTR membrane localization was lost and CFTR was mainly intracellular. The absence of CFTR from the membrane was associated with lung pathology similar to that seen in the CF lungs, with inflammatory cells infiltration, thickening of the alveolar wall as well as the bronchiolar mucosa and goblet cells hyperplasia. The lung pathology was corrected with external VIP intraperitoneal administration for 3 weeks and CFTR membrane localization was restored. This study confirmed that VIP chronic stimulation is

necessary for CFTR membrane localization and function *in vivo* and thus its dependent secretion necessary for healthy lungs (Alcolado, 2010).

7.3 Prolonged VIP Stimulation Increases CFTR Membrane Density by Modulating its Recycling

To demonstrate the effect of prolonged VIP stimulation on regulating CFTR surface expression, the Chappe research group (Chappe *et al*., 2008) used cell surface biotinylation assays to quantify the amount of CFTR at the cell membrane under control condition or after VIP stimulation in polarized Calu-3 cells. They found that prolonged VIP stimulation (15-120 minutes) increased the number of CFTR channels at the membrane of the cells after 15 minutes. The effect of VIP stimulation on CFTR membrane density could be sustained for up to 2 hours. The increase in apical CFTR density was associated with an increase in CFTR-dependent function as measured by iodide efflux assays. The authors concluded that the increase in apical CFTR occurred through modulation of CFTR recycling because the total content of mature (fully glycosylated) CFTR was not altered under any of the tested conditions. Measuring the rate of CFTR endocytosis from the membrane with internalization assays, they found that VIP stimulation was associated with much less CFTR being internalized from the membrane compared to control unstimulated cells, suggesting that VIP-dependent increase in CFTR membrane density occured via stabilizing CFTR at the membrane.

7.4 Role of PKCε in Mediating CFTR Surface Stability

To explore the molecular mechanism responsible for VIP-dependent increase in CFTR membrane density, the Chappe group (Chappe *et al*., 2008) tested the role of PKA or PKC kinases known to be activated after VPAC1 receptors activation by VIP. Treating the cells with forskolin to activate PKA did not change the amount of surface CFTR. Similarly, VIP-dependent increase in apical CFTR protein was unaffected by the PKA inhibitor H89, indicating that PKA signaling was not a major contributor to VIP effect. On the contrary, pre-treating cells with two structurally distinct PKC inhibitors (bisindolylmaleimide X or chelerythrine chloride) abolished the VIP-stimulated increase

in surface CFTR. Moreover, treating the cells with phorbol 12-myristate 13-acetate; PMA, a general activator of PKC, mimicked VIP-dependent increase in CFTR membrane density. The study concluded that the VIP-dependent increase in CFTR membrane density through stabilizing CFTR at the membrane by reducing its endocytosis depends on the activation of PKC through Gαq/i signaling pathway (Chappe *et al*., 2008; Rafferty *et al*., 2009).

Later the Chappe group identified the activated PKCε as the exclusive isoform responsible for the VIP-dependent increase in CFTR membrane density in the human nasal epithelial cell line JME/CF15 derived from a CF patient homozygous for the ΔF508 mutation and in recombinant BHK cells (Alcolado *et al*., 2011). However the downstream events after PKCε activation were still unknown.

Figure 1.6 VIP Signaling Cascade Regulating CFTR Surface Expression and Function. After binding to VPAC1 receptors on the basolateral membrane of Calu-3 cells, VIP activates both PKA and PKCε. Activated PKA phosphorylates CFTR R domain leading to channel activation. Activation of PKCε is thought to directly phosphorylate CFTR R domain. Also PKCε activation was shown to stabilize CFTR at the cell membrane by inhibiting the endocytosis. Figure adapted from Chappe & Said, 2012. ISBN: 978-953-51-0287-8.

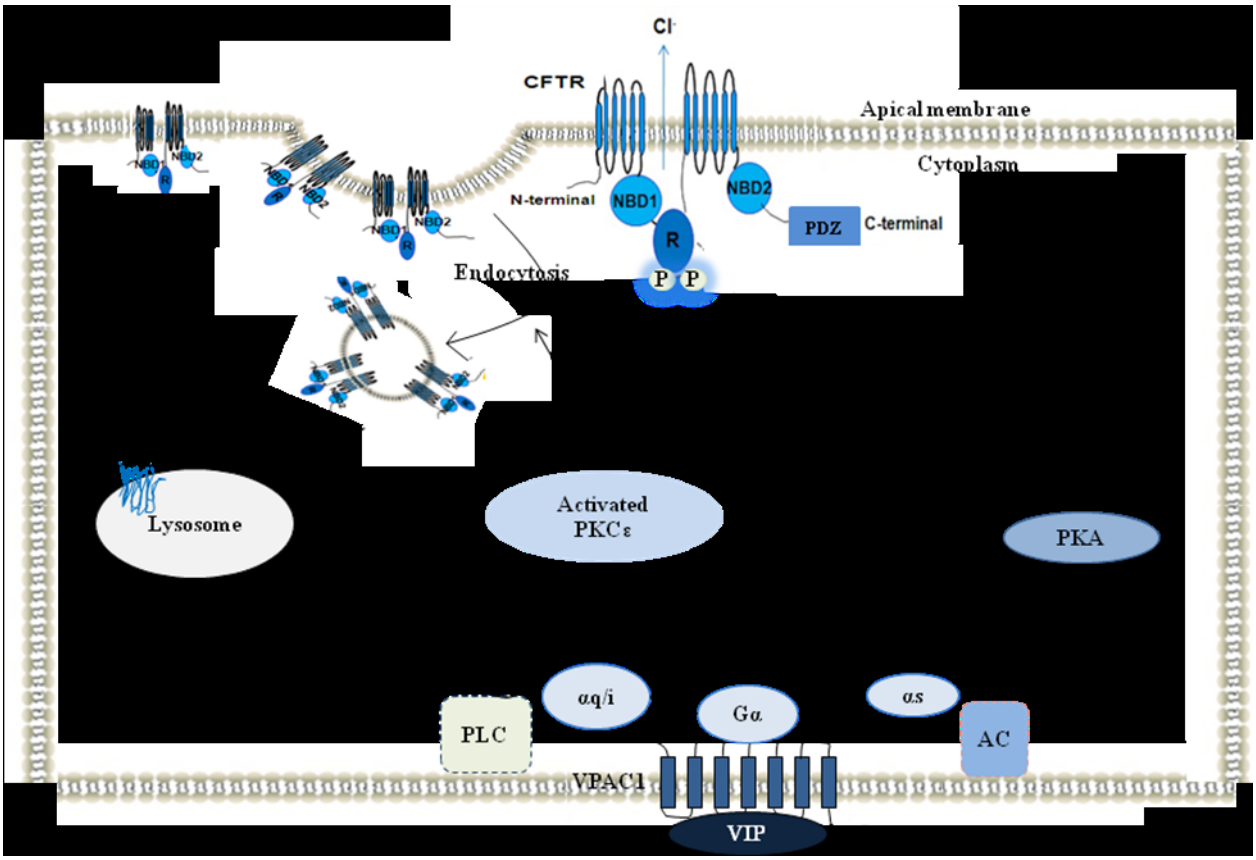

Research Objectives

Many CFTR mutations are characterized by surface instability that leads to reduced CFTR surface expression and thus reduced CFTR-dependent function. VIP stimulation was shown to increase both WT-CFTR and ΔF508-CFTR surface stability which contributed to increase their number at the cell surface with functional consequences (Chappe *et al*., 2008; Alcolado *et al*., 2011). PKCε activation through Gαq/i signaling pathway was shown to relay the VIP-dependent effect (Alcolado *et al*., 2011). The aim of this work was to identify the molecular mechanism by which PKCε activation, after VIP stimulation of VPAC1 receptors, stabilizes CFTR at the membrane.

1- We hypothesized that scaffolding proteins, known to positively regulate CFTR surface turnover, anchor CFTR to the actin cytoskeleton following VIP-dependent PKCε activation.

2- We also investigated if the VIP-dependent PKCε activation regulates certain PDZ domain mediated interactions that are known to play several roles in CFTR life cycle.

Chapter 2: Materials and Methods

I. Materials

1. Chemicals and Buffers

Antibodies: Monoclonal anti-NHERF1 (A-7), polyclonal anti PIST (Q-23) and monoclonal pan-Cytokeratin antibody were from Santa Cruz Biotechnology Inc. (Santa Cruz, CA, USA). The monoclonal anti-CFTR antibody M3A7 and the monoclonal anti-CFTR (MM13-4) were from Millipore / Upstate (Charlottesville, VA, USA) while the monoclonal Anti-GAPDH-Peroxidase was from Sigma (St. Louis, MO, USA). The P-ERM antibodies were purchased from Cell Signaling Technology (Danvers, MA, USA). The goat anti-Mouse secondary antibody conjugated to peroxidase was from Jackson ImmunoResearch Lab., Inc. (West Grove, PA,USA), the Rabbit Ploclonal Secondary IgG conjugated to Dylight 650 was from Abcam (Cambridge, USA) and the goat anti-Mouse secondary antibody conjugated to either Cy5or Cy3 were from Jackson ImmunoResearch (west Grove, PA, USA).

Immunolabeling Buffers: The Blocking/permeabilizing buffer was composed of PBS / 0.1% Triton X-100 / 2% bovine serum albumin (BSA) all came from Sigma (St. Louis, MO, USA). The antibody buffer was composed of PBS / 0.1% Triton X-100 / 0.2% BSA while the wash buffer was composed of PBS / 0.1% Triton X-100. The Vybrant® CM-DiI Cell-Labeling Solution was from Invitrogen™ (Carlsbad, CA, USA)**.**

RNA Extraction: RNeasy mini kit was from Qiagen (Mississauga, ON, Canada).

cDNA Synthesis : Bio-Rad iScript™ cDNA Synthesis Kit (Mississauga,ON, Canada)

RT-PCR: The iTaq™ DNA Polymerase kit was from Bio-Rad (Mississauga, ON, Canada). The 10 mM dNTP mix was also purchased from Bio-Rad. Finally, both NHERF1 and CAL primers were from Invitrogen™ (Carlsbad, CA, USA).

Table 2.1- Primer Sequences for NHERF1, PIST along with their Expected Product Sizes in base pairs (bp) and annealing Temperature (Tm) used in the RT-PCR Reaction.

protein	**Primer Sequence (5'-> 3')**	**Product size (Pb)**	**Tm (°C)**
NHERF1	Forward Primer: CTCTGCTGCGCTCCCGGTTC Reverse Primer: GCAGGGGACCATTCAGGTGCT	869	58.8
PIST	Forward Primer: CCCCTCTGTGGAGGAGCTGGAAA Reverse Primer: AGCGGAGTTTCACTTGCAGTGCC	873	60
PKC Aplha (+ Control)	Forward Primer: TGCCGGCCAGTGGATGGTAT Reverse Primer: TGCACATCCCAAAGTCGGCG	651	57.9

Agarose Gel Electorphoresis: The UltraPure™ Agarose and the Ethidum Bromide Solution (10 mg/ml) came from Invitrogen™ (Carlsbad, CA, USA) while the10x Tris-Borate-EDTA (TBE) buffer was from Sigma (St. Louis, MO, USA). The 6x Loading dye and the phiX174 DNA/BsuRI (HaeIII) Marker were from Thermo Fisher Scientific (Burlington, ON, Canada).

Bradford Assay Buffers: The lysis buffer, Radio Immuno Precipitation Assay (RIPA) was prepared from 0.15 m nacl, 10 mm tris, 1 mm EDTA, 1% tritonx-100, 0.08% deoxycholic acid, 0.01% SDS with a protease inhibitor cocktail (Roche, Laval, Qc, Canada) to prevent protein degradation with 7.5 adjusted PH. The Quick Start™ Bradford protein assay was from Bio-Rad (Mississauga, On, Canada).

Buffers for Immunoblotting: The following chemicals were all supplied by Bio-Rad (Mississauga, ON, Canada): 30% acrylamide / Bis solution, 29:1 (3.3% C), 10x TGS (Tris/ Glycine/ SDS) running buffer (0.25 M Tris ,1.92 M Glycine, 1% SDS, pH 8.3), 10x TG (Tris /Glycine) transfer buffer (0.25 M Tris and 1.92 M Glycine, pH 8.3) and 10x Tris Buffered Saline (TBS) (0.2 M Tris, 5 M NaCl, pH 7.5) and the Kaleidoscope Prestained Protein Standards. Benchmark™ Prestained Protein Standards was from Invitrogen (Burlington, ON, Canada). Methanol, Ammonium Per-Sulfate (APS), 10% sodium dodecyl sulphate solution (SDS) and tetra-methyl-ethylene-diamine (TEMED) were all from Sigma (St. Louis, MO, USA). 5x sample buffer and Restore™ PLUS Immunoblot Stripping buffer were from Thermo Fisher Scientific (Burlington, ON, Canada). Immun-Star™ Western C™ Chemiluminescence Kit containing luminal/enhancer and peroxide solution was purchased from Bio-Rad (Mississauga, ON, Canada).

siRNA Transfection Reagents: NHERF-1 siRNA (h), ERM siRNA (m), Control siRNA-A (non-targeting scrambled-siRNA) as well as the control fluorescein conjugated siRNA along with siRNA transfection medium, siRNA dilution buffer and siRNA transfection reagent were all purchased from Santa Cruz Biotechnology Inc. (Santa Cruz, CA, USA).

Immunopreciptaion (IP) Reagents: Protein G IGg binding buffer, Elution Buffer, 50% immunopure protein G slurry, DSS (disuccinimidyle suberate) as well as 0.6 ml handee spin cup column all were from Pierce thermo scientific (Rockford, USA). Quenching buffer for IP was made of 0.025 M Tris, 0.15 M NaCL with PH adjusted to 7.2 while the lysis buffer for IP was made of PBS / 1% triton-100 and protease inhibitor.

Cross-linking Experiment Reagents: The amine crosslinker, disuccinimidyle suberate, (DSS) was from Pierce Thermo Scientific (Rockford, USA). Borate buffer was made with 10mM boric acid, 154 mM NaCl, 7.2 mM KCl and 1.8 mM CaCl2 with PH adjusted to 8. The quenching buffer was made of 192 mM glycine, 2.5mM tris with PH 8.3. dimethyl sulfoxide (DMSO) for dissolving the DSS, glycine and boric acid were from sigma (St. Louis, MO, USA). Tris Base was from Bio-Rad (Mississauga,ON, Canada).

***In Situ* Proximity Ligation Assays Reagents:** Duolink *In Situ* Detection Reagents Orange kit was purchase from Sigma-Alorich (St. louis, Mo, USA). The kit contains 5 x Ligation stock, 1× Ligase, 5 × Amplification Orange (amplification stock) and 1× Polymerase. All the other reagents were also from Sigma-Aldrich (st. lois, Mo, USA) including the Duolink *In Situ* Mounting Medium with DAPI, the Duolink *In Situ* PLA Probe Anti-Mouse MINUS, the Duolink *In Situ* PLA Probe Anti Rabbit PLUS, the Duolink *in Situ* Wash Buffer, Brightfield (wash buffer A) and the Duolink *In Situ* Wash Buffers, Fluorescence (Wash buffer B).
Wash buffer A or B came in ready to use pouches of powders. The working buffers were prepared by dissolving the content of 1 pouch of powdered buffer in 1 litre of dd H_2O. The 1× wash buffer was stored at 4 °C and brought to the room temperature before use.

Cell Culture Media: Cell culture medium and supplements were purchased from GIBCO (Invitrogen, Burlington, ON, Canada) or Sigma (St. Louis, MO).

Other Reagents: The Vasoactive Intestinal Peptide (VIP) was from Tocris BioScience (Burlington, ON, Canada). PKCε translocation inhibitor peptide EAVSLKPT was from

Calbiochem (EMD Chemical Inc., USA) and the phorbol 12-myristate 13 acetate (PMA) was from Sigma (St. Louis, MO, USA).

II. Methods

2.1 Cell Culture

The human bronchial serous cell line Calu-3 was cultured in α-minimum essential medium supplemented with 15% FBS, 1% penicillin-streptomycin, 1% nonessential amino acids, and 1% sodium pyruvate in a 37°C incubator with 5% CO2 and 95% humidity.

2.2 RNA Extraction from Cells

Calu-3 cells were cultured in 6 cm petri dishes and allowed to grow until forming a confluent monolayer. After media aspiration, cells were washed with PBS-EDTA three times and dislodged with trypsin at 37°C before collection in PBS. Cells were centrifuged at 3,500 rpm at 4°C for 15 min and the supernatant was discarded. The pellet was resuspended in 1 ml PBS then transferred to RNase-free tube and centrifuged at 13,000 rpm for an additional 20 min. The final pellet was then stored at -80 °C. Later, RNA extraction was carried-out with the RNeasy mini kit (Qiagen, Mississauga, ON, Canada) according to the manufacturer's instructions for the protocol: Purification of Total RNA from cells. Cell pellets were removed from the -80°C freezer and allowed to thaw at room temperature. 350µl of RTL buffer containing 1 M Dithiothreitol in a 1:30 dilution was added to the pellet. The cells were homogenized by passing 20-50 times through RNAase-treated needle attached to 1ml syringe. Then 350 µl of 70% ethanol was added to the cell lysate and thoroughly mixed by repeated pipetting. 700 µl of the mixed sample was transferred to an RNeasy spin column placed inside a 2 ml collection tube and centrifuged for 15 seconds at 10,000 rpm. The flow through was discarded and 700 µl of RW1 buffer was added to the spin column and centrifuged for 15 seconds at 10,000 rpm and the flow through was discarded. 500 µl of RPE buffer was added to the spin column and centrifuged 15 seconds at 10,000 rpm and the flow through was discarded. An additional 500 µl of RPE buffer was added to the spin column and centrifuged for 2 min at 10,000 rpm. The spin column was placed in a new 1.5 ml tube and 34 µl of RNase-free

water was added to the spin column and centrifuged for 1 min at 10,000 rpm to collect the RNA. Recovered RNA concentration and purity was determined using Unico UV-VIS spectrophotometer (NJ, USA) by measuring optical density (OD) at 260 nm and 280 nm. Samples with a 260/280 ratio between 1.8 and 2.2 were considered of good purity and stored at -20°C until further use.

2.3 Conversion of RNA to cDNA

The iScript™ cDNA Synthesis Kit was used to convert RNA to cDNA according to manufacturer instructions. An ice cold PCR reaction tube containing 4 µl of 5x iScript reaction mix, 1 µl of iScript reverse transcriptase, 1 µg of RNA and Nuclease-free water to bring the total volume of the mixture to 20 µl was placed in the thermocycler (MyCycler™, Bio-Rad) and underwent 1 cycle of the following program: 5 min at 25°C, 30 min at 42°C and 5 min at 85°C. The reaction tube containing the newly synthesised cDNA was removed from the thermocycler and immediately stored at -20°C until further use.

2.4 Reverse Transcriptase Polymerase Chain Reaction (RT-PCR)

Reactions were prepared in PCR tubes using the iTaq™ DNA Polymerase kit, on ice, according to the manufacturer instructions. Briefly, the following was added to a PCR tube: 5 µl of 10x iTaq buffer, 1.5 µl $MgCl_2$ (50 mM), 1 µl of forward primer (50 mM), 1 µl of reverse primer (50 mM), 1 µg cDNA template, 1 µl dNTP mix (10 mM), 0.25 µl iTaq DNA Polymerase and sterile ddH20 to bring the total reaction volume to 50 µl. Reaction tubes were placed into a thermo cycler (MyCycler™, Bio-Rad) and subjected to the following heat-cycle program for DNA amplification: 95°C for 3 min for polymerase activation, 95°C for 30 seconds to denature DNA (40 cycles), 55-60°C for 30 seconds for primer annealing and 72°C for 50 seconds for product elongation. After the previously stated cycles were completed an additional incubation at 72°C for 4 min was applied to allow elongation of any incomplete products before the temperature was decrease to 4°C to stabilize DNA until storage at -20°C.

2.5 Agarose Gel Electrophoresis

RT-PCR reaction products were visualized in agarose gel electrophoresis experiments. 1.5% agarose gel was prepared by mixing 0.45 g of agarose and 30 ml of 1x TBE buffer and microwaving for 1 min with swirling every 15 seconds. The agarose mixture was then cooled down to a warm temperature before the addition of 1.3 µl of Ethidum Bromide Solution (10 mg/ml) and thorough mixing. The agarose mixture was poured into a horizontal casting gel system with a 10 well comb in place and allowed 30 min to solidify at room temperature. The PCR samples were prepared on ice using 2µl of 6x loading dye and 18µl of PCR product and mixed by gentle pipetting. The Φx ladder was prepared using 2 µl of stock Φx molecular weight marker, 2 µl of 6x loading dye and 3 µl ddH20. After polymerization, the gel was placed in electrophoresis cell (Mini-Sub Cell GT Cell, Bio-Rad) filled with TBE buffer. Then after the marker and samples were loaded, the gel was run at 89 V for about 1.5 hour or until samples had migrated a sufficient distance to allow imaging. PKCα was used as a positive control for the PCR reaction. Negative controls were prepared by omitting the primers from the RT-PCR reaction. Gels were imaged using an ultraviolet imaging box and digital camera in combination with the AlphaDigiDoc® (Cell Biosciences, Toronto, ON, Canada) software-imaging program.

2.6 Protein Assay

The Bradford protein assay was used to determine protein concentration in Calu-3 cell lysates. A standard curve was made using bovine serum albumin (BSA) standards at increasing concentrations of 0, 2, 5, 10, 15 µg. Protein standards were made from BSA stock (2µg/µl) diluted in ddH20 to a final volume of 10 µl for each concentration and added to 480 µl of ddH20 and 10 µl of RIPA (diluted to 1:4 in ddH20). 500 µl of Quick Start™ Bradford dye reagent (Bio-Rad, Mississauga, ON, Canada) was then added. Similarly, 10 µl of each cell lysate sample, diluted 1:4 in ddH20, were added to 490 µl ddH20 and 500 µl Bradford dye. Standards and samples were quickly vortexed and incubated at room temperature for 15-60 min before reading the optical densities (595 nm) using a Unico® 2802 UV/VIS Spectrophotometer. Duplicates of each sample were measured. To obtain the standard curve, optical densities of BSA samples were plotted as

a function of their concentration and a linear standard curve was drawn using the Protein & DNA Assays Software (copyrights: Frederic Chappe & Valerie Chappe). Optical densities from cell lysate samples were plotted against the standard curve to determine the protein concentration of each sample.

2.7 Immunoblotting

10 wells polyacrylamide gels were made for all immunoblots with a 5% stacking gel and either 6% resolving gel for samples from cross-linking experiments or 7.5% resolving gel for all other samples. Cells were lysed in RIPA buffer by vigorous pipetting and incubated for 30 min on ice with vortexing every 15 min. The lysate was then centrifuged 15 min at 13,000 rpm. The supernatant containing soluble proteins was transferred into a new 1.5 ml tube and protein concentration was measured as indicated above with the Bradford assay method. Samples containing defined protein concentrations (20 µg for NHERF1 and CFTR, 40µg for P-ERMs and CAL) were mixed with half volume of 5x sample buffer. Samples used to detect NHERF1, CAL or P-ERMs were boiled at 95°C for 5 min to expose the antigenic sites on the proteins before loading into the gel. Samples to detect CFTR were not heated as CFTR degrades at high temperatures. Prestained Protein Standards were loaded along with the samples and subjected to SDS-PAGE (sodium dodecyl sulfate polyacrylamide gel electrophoresis). The gels were run to 90 V in running buffer until samples had migrated into the resolving gel and the voltage was increased to 120 V for the remaining part of migration (resolving gel). After gel migration, proteins were transferred onto nitrocellulose membranes using a blotting chamber (Thermo Scientific OWL, Rochester, NY, USA) at 45 V for 2 h in ice cold transfer buffer containing 20% Methanol. Membranes were then blocked with 5% milk in TTBS for 1 hour at room temperature with gentle shaking. The blocking solution was then rinsed off the membrane and the membrane was incubated with the primary antibody against the protein of interest in TBS / 0.2% BSA (NHERF1 1/2,000, CAL 1/600, CFTR 1/1,000 or P-ERMs 1/1,000) overnight at 4°C with gentle shaking. After primary antibody removal, the membrane was washed 3 times with TTBS for 15 min each and one time with TBS for 15 min, at room temperature with moderate shaking. The membrane was then incubated with 1/10,000 secondary antibody (peroxidase-conjugated,

goat anti-Mouse for NHERF1 and CFTR, or peroxidase-conjugated goat anti-Rabbit IgG for P-ERMs and CAL) in TBS / 0.5% milk with gentle shaking at room temperature. After 2 hours of incubation with the secondary antibody the membrane was washed 5 times with TTBS 10 min each and one time with TBS for 15 min at room temperature with moderate shaking. Proteins were revealed using The Immun-Star™ WesternC™ Chemiluminescence Kit with 750 µL luminal enhancer and 750 µL peroxide solutions mixed together in a light protected tube. The 1.5 ml mixture was spread evenly over the membrane and incubated for 3-5 min before exposing Kodak X-Ray films and development using an X-Ray processor. X-Ray films were scanned and protein band density measured with Image J software (National Institute of Health, http://rsbweb.nih.gov/ij/). Initial experiments were conducted to determine the appropriate mutual concentration of both proteins and antibodies for best results; for NHERF1 (figure 2.1 and 2.2) for CAL (figure 2.3) for P-ERMs (figure 2.4).

The membrane was then stripped of antibodies, using 10 ml of immunoblot stripping buffer, protected from light, with gentle shaking for 30 min at room temperature. The membrane was then washed three times with TTBS 15 min each with moderate shaking and blocked with 5% milk in TTBS for 1 hour with gentle shaking. After removal of the blocking solution, the membrane was incubated with another primary antibody for the protein of interest overnight at 4°C, washed and incubated with the corresponding secondary antibody as before. Membranes were then imaged and scanned as described above.

Figure 2.1 Representative Immunoblots Testing the Endogenous Expression of NHERF1 in Calu-3 Cells. Blotting membranes were labeled with the mouse monoclonal anti-NHERF1 antibody at varying concentrations as indicated under each image. The secondary peroxidase conjugated goat anti-Mouse was used and detected by chemiluminescence. Expected size (kDa) NHERF1:50.

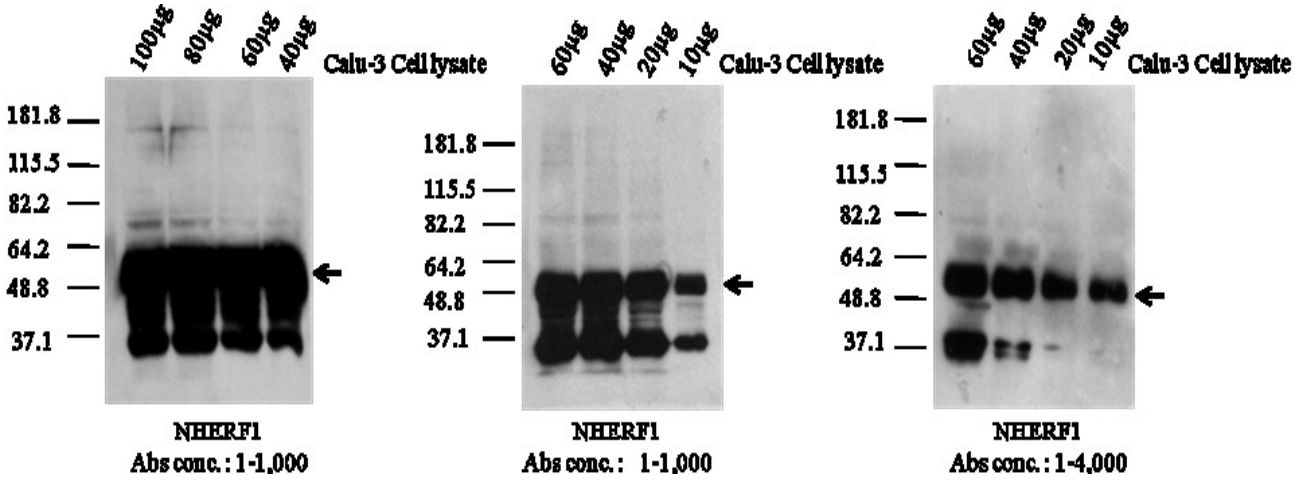

Figure 2.2 Representative Immunoblots Testing the Endogenous Expression of NHERF1 in BHK Cells. Blotting membranes were labeled with the mouse monoclonal NHERF1 antibody at varying concentrations as indicated on each image. The secondary peroxidase conjugated goat anti-Mouse was used and detected by chemiluminescence. The membranes were reprobed for GAPDH. Expected sizes (kDa): NHERF1:50 and GAPDH: 37.

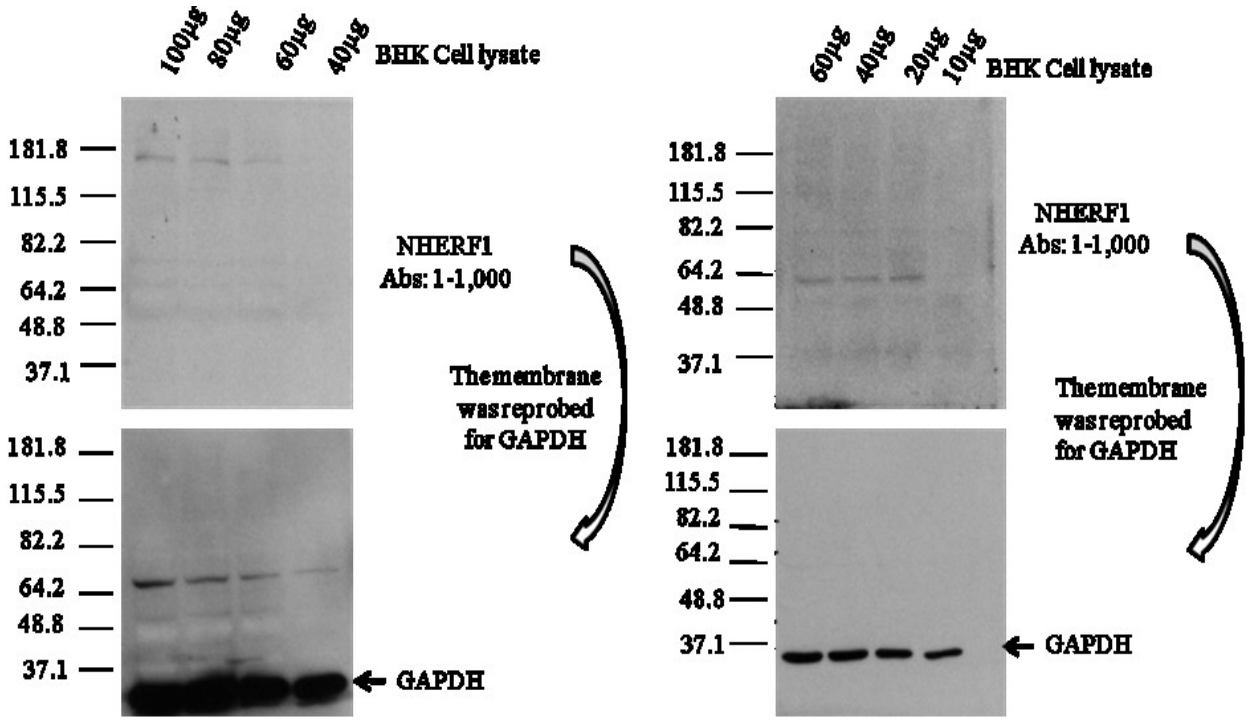

Figure 2.3 Representative Immunoblots Testing the Endogenous Expression of CAL in Calu-3 Cells (A) or BHK Cells (B). Blotting membranes were labeled with the polyclonal anti CAL antibody at varying concentrations as indicated under each image. The secondary peroxidase conjugated goat anti- Rabbit was used and detected by chemiluminescence. Expected sizes (kDa) CAL: 60/35.

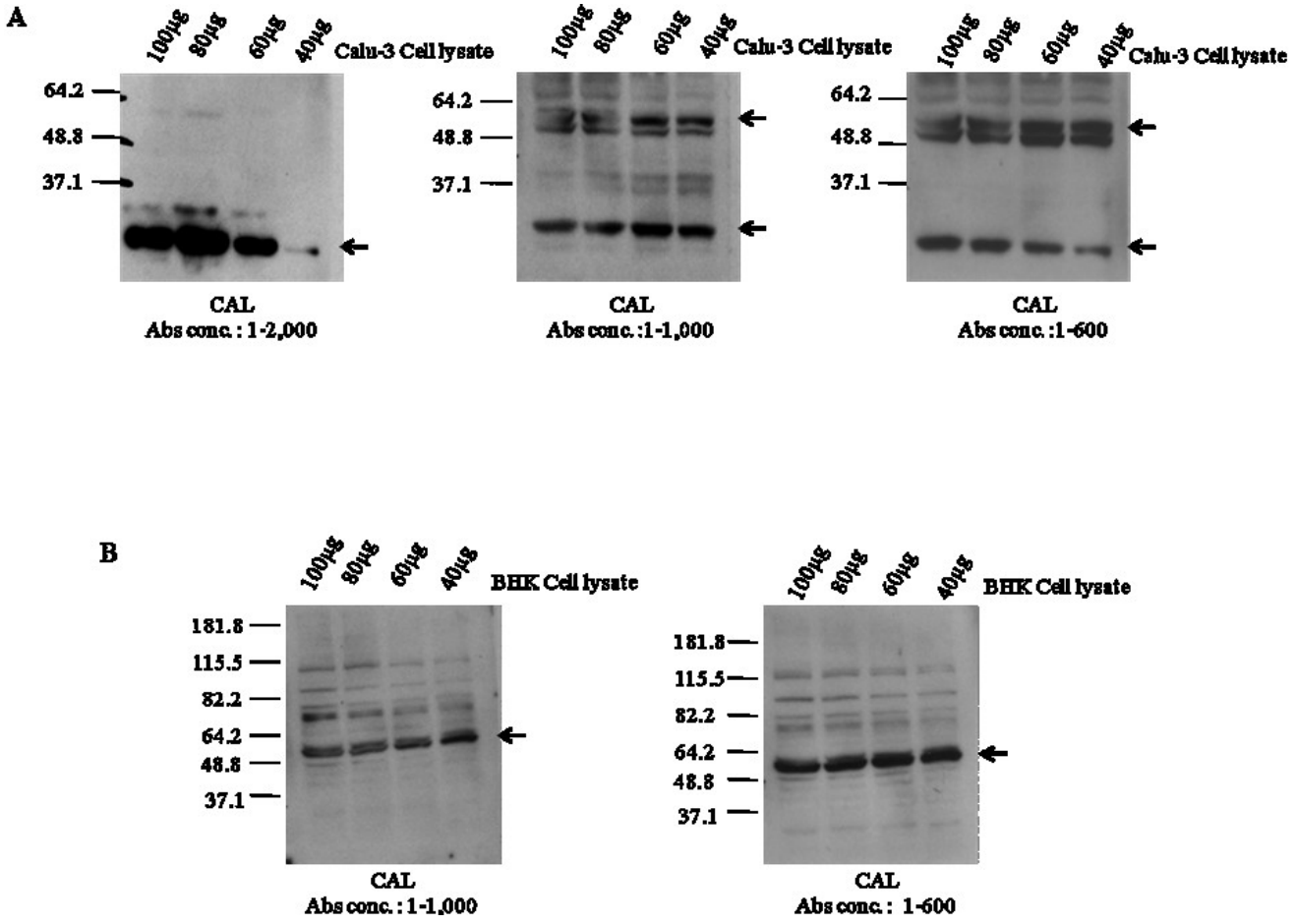

Figure 2.4 Representative Immunoblots Testing the Endogenous Expression of P-ERMs in Calu-3 Cells. Blotting membrane was labeled with the polyclonal anti -P-ERM antibodies (1:1,000). The varying amounts of cell lysate are indicated on the image. The secondary peroxidase conjugated goat anti-Rabbit was used and detected by chemiluminescence. The membrane was reprobed for GAPDH. Expected sizes (kDa) Ezrin: 82, Radixin: 80, Moesin: 75 and GAPDH: 37.

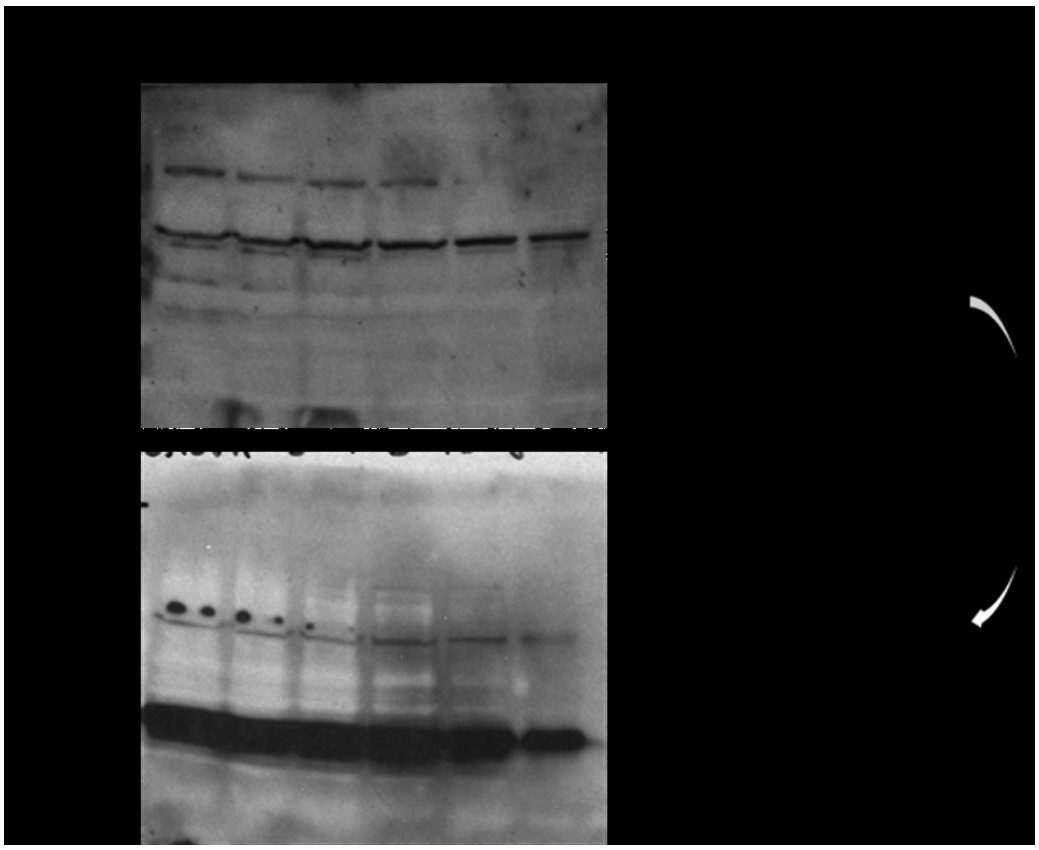

2.8 Immuno-Localization

Calu3 cells were cultured at 37°C on glass coverslips at low density. The treatment with 300 nM VIP for 30 min took place just before staining. The culture medium was removed; cells were then washed with PBS three times, fixed in 2% paraformaldehyde at room temperature or with 10% TCA on ice for P-ERMs labeling. Cells were then permeabilized in antigen blocking solution containing 0.1% Triton X-100 and 2% BSA for 45 min. The blocking / permeabilizing solution was removed and cells were incubated for 1 hour at RT with anti-CFTR M3A7 (1:1,000), anti NHERF1 (1/1,000), anti-PIST (1/600) or anti P-ERMs (1/100) antibodies in PBS/0.1% Triton X-100/0.2% BSA buffer. The antibody containing buffer was then removed and cells were washed 3 times in PBS / 0.1% Triton X-100 and incubated with goat anti-Mouse secondary antibody conjugated to Cy3 (1:100) for CFTR labeling or to Cy5 (1/200) for NHERF1, or a Rabbit Ploychonal Secondary IgG conjugated to Dylight 650 (1/100) for PIST and P-ERMs labeling, in 0.1% Triton X-100 and 0.2% BSA. After one hour, the secondary antibody was removed and cells were washed again with PBS containing 0.1% triton X-100 three times 10 min each. Cells were then incubated with a second primary antibody for double labeling experiments or mounted with antifade lmmuno-Fluore mounting Medium, dried and stored at -20 C until viewed with a Zeiss LSM 510 confocal microscope. Negative controls were performed by omitting the primary antibody or by staining cells and tissues that do not express the targeted protein (figure 2.5).

Confocal Microscopy

Zeiss LSM 510 Meta Confocal Microscope (CMDI facility, 13th floor Sir Charles Tupper Building, Faculty of Medicine, Dalhousie University) was used to monitor the cellular distribution of all fluorescently labeled proteins. Images were taken at 40X objective under oil immersion and captured with the LMS computer software. Differential Interface Contrast (DIC) images were taken to allow visualization of cells' nuclei and cells' membranes.

Confocal microscope setting: the pinhole was ~ 90 µm for all images. Detector gain was between 500 to700 and digital offset was between 7 to -0.1. Filter was LP 650 and the

laser emission wavelength was 633 nm at 26% for CY5 and Dylight 650, and 543 nm and 80% for CY3.

Fluorescence Microscopy

Zeiss axiovert 200M inverted fluorescence microscope (CMDI facility, 13th floor Sir Charles Tupper Building, Faculty of Medicine, Dalhousie University) was used. Images were taken at the 40X objective and captured with the AxioVision 4.7 Multi Channel Fluorescence software. Excitation was 546 nm and emission was 575-640 nm for CY3 and for DAPI excitation was 365nm and emission was 420 nm.

2.9 Down regulation of NHERF1 and ERM Proteins Expression by siRNA Electroporation

Calu-3 cells were grown in culture to 60-80% confluency. Cells were then collected by trypsinization, re-suspended in wash media to stop the trypsin action and the cell suspension was centrifuge at 1,200 rpm for 5 min. The supernatant was discarded and 10 X 10^7 cells (estimated by cell counting of an aliquot of the cell suspension) were re-suspended in 100 µl of transfection mixture which contained 80 pmols of NHERF1-siRNA, ERM-siRNA or scrambled non targeting siRNA and an equal volume of transfection reagent in 100 µl of transfection medium. The transfection mixture was then transferred to a 2 mm electroporatin cuvette and cells were electroporated using the ECM 830 electroporator at 310 V for 20 ms with a single pulse. Electroporated cells were immediately diluted in culture media pre-warmed to room temperature and incubated at 37°C with 5% CO_2. Cells were assayed 48 hours post electroporation using immunoblotting and immuno-staining methods. Preliminary experiments enabled us to determine that 48 hours after electroporation was the optimal incubation period for NHERF1 and ERM proteins down-regulation (figure 2.6).

Figure 2.5 Testing the Best Time for Maximal Down-regulation of NHERF1 Expression. Representative immunoblot of NHERF1 after transfection with specific NHERF1-siRNA delivered into Calu-3 cells by electroporation. 20 μg of cell lysate were loaded into 7.5% gel, separated by SDS PAGE and detected with a monoclonal NHERF1 antibody followed by peroxidase conjugated secondary antibody and detected by chemiluminescence. Time post transfection is indicated on the image. The membrane was stripped and re-probed for CFTR. Expected sizes (kDa) for NHERF1: 50 and for CFTR: 180.

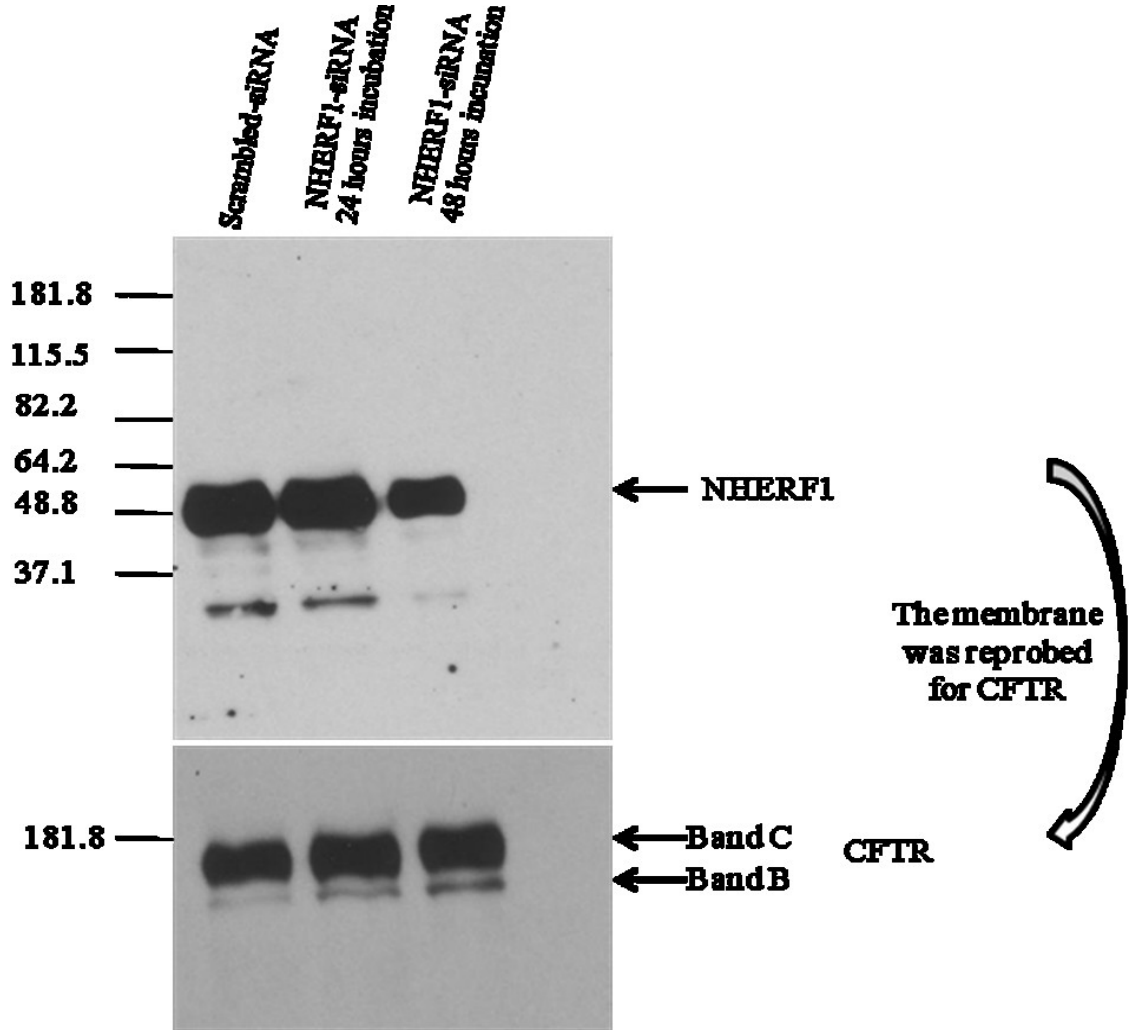

2.10 Immunopreciptations

Calu-3 cells were cultured in 850 cm^2 roller bottles to confluency and stimulated with 300 nM VIP for 30 min before collection. Cells were washed 3 times with ice cold PBS, dislodged from the bottle surface by scrapping and collected in 15 mL tubes followed by centrifugation for 15 min at 3,500 rpm at 4°C. After discarding the supernatant, cell pellets were stored at -20 °C until further use.

Preparation of the immunoprecipitation columns: 0.2 ml of 50% immunopure protein G slurry were loaded into 0.6 ml handee spin cup column and spun 1 min to remove the buffer. The beads were washed (3X) with 0.4 ml binding buffer with gentle rocking for 2 min followed by 1 min spinning. 12µg of MM13-4 monoclonal antibody against the N-terminal of CFTR diluted in 0.2 ml of binding buffer were loaded to the column. The beads and the antibodies were allowed to interact for 45 min with gentle rocking at room temperature. The column was then spun for 1 min to remove the binding buffer followed by 3 washes with binding buffer. 0.09 mg of DSS dissolved in 15µL DMSO was added to each column containing 0.2 ml binding buffer and incubated for 2 hours with gentle rocking at room temperature to allow the cross-linking of the antibodies to the beads. The column was then spun for 1 min to remove the buffer and incubated with quenching buffer for 10 min with gentle rocking. The column was washed with quenching buffer followed by 1 min spinning. The column was then washed with elution buffer 4 times to remove any non-cross linked antibodies. Lastly, columns were washed 4 more times with quenching buffer and stored in quenching buffer over night at 4°C.

On the next day, Calu-3 cells' pellets were lysed and proteins solubilized in PBS / 1% X100-triton supplemented with protease inhibitors to prevent protein degradation, by passing the lysate 30-50 times though a needle attached to a syringe and incubated for 30 min on ice. Lysates were then centrifuged for 30 min at 13,000 rpm at 4°C and the supernatant containing soluble proteins was collected and diluted in an equal volume of binding buffer. Diluted samples were placed on a rocker with gentle agitation at room temperature to allow protein interaction for 2 hours. A Bradford protein assay was run to measure protein concentration of each sample and a total of 8-10 mg of proteins were loaded in 500 µl aliquots to antibody-linked column. Each aliquot was allowed to interact with the antibody-linked column on a rocker under gentle agitation, at room temperature,

for 15 min before removal by 1 min centrifugation. After the entire volume for each sample was loaded, columns were washed 7 times with quenching buffer. Columns were then transferred to clean 1.5 ml eppendorf tubes and incubated with 110 µL of elution buffer for 3 min before centrifugation. The flow through were collected for analysis. 3 sequential elutions were collected. 5X sample buffer supplemented with 1M DTT was added to each collected elution and stored at -20 °C until assayed by immunoblotting.

2.11 Cross-linking experiments

After removal of the media, Calu3 cells were washed three times with pre-warmed (37 °C) PBS and one time with pre-warmed (37°C) borate buffer (PH 8). 4 mM DSS dissolved in DMSO and solubilized in borate buffer was added to the cells with or without 20 mM PMA treatment. After 30 min incubation at 37 °C, the DSS/ borate buffer was removed and cells were washed 3 times with quenching buffer and incubated 15 min with quenching buffer at room temperature. Cells were then washed three times with ice cold PBS, scrapped, collected in 1.5 ml tubes and centrifuged 20 min at 13,000 rpm at 4 °C. After centrifugation the supernatant was discarded and the cell pellet stored at -20°C until analyzed by SDS-PAGE immunoblotting.

2.12 *In Situ* Proximity Ligation Assays

Calu3 cells were cultured at 37°C on glass cover slips at low density and treated with 300 nM VIP for 30 min before starting the assay. The culture medium was removed; cells were washed 3 times with PBS, fixed with either 2% paraformaldhyde for 20 min at room temperature or 10% TCA for 15 min on ice for P-ERMs labeling. Cells were then permeabilized in antigen blocking solution containing 0.1% Triton X-100 and 2% BSA for 45 min at room temperature with gentle shaking. Primary antibodies for the two proteins of interest (must have been raised in two different species) , diluted in PBS / 0.1% triton X-100 / 0.2% BSA were added to the cells and incubated over night at 4°C. On the next day, the primary antibodies were removed and cells were washed with PBS / 0.1% triton X-100 / 0.2% BSA three times 10 min each with gentle agitation. The PLA probes were diluted 1:5 in PBS / 0.1% triton X-100 / 0.2% BSA and allowed to sit 20 min at room temperature before applying to the cells for 60 min at 37 °C. After removal of

the PLA probes, cells were washed with wash buffer A twice 5 min each with gentle agitation. During the wash period, the ligation mixture was prepared by diluting the 5X ligation stock in ultrapure distilled water. Immediately before applying to the cells, the ligase 1:40 was prepared in the ligation mixture, vortexed and incubated with the cells for 30 min at 37 °C. After removing the ligation mixture, cells were washed with wash buffer A twice 2 min each with gentle agitation. During the wash, in a light protecting zone, the amplification mixture was prepared by diluting the amplification stock 1:5 in high purity water with polymerase 1:80 added just before applying to the cells and incubating for 100 min at 37°C protected from light. Cells were then washed with wash buffer B twice 10 min each followed by another one time wash with 0.01X wash buffer B for 1 min. Finally, cells were mounted with the Duolink *in situ* mounting medium containing DAPI for nuclei staining, sealed with nail polish and left on the bench for 15 min to dry before imaging using a fluorescence microscope (CMDI) as indicated above. Excitation was 546 nm and emission was 575-640 nm for CY3 and for DAPI excitation was 365nm and emission was 420 nm. Slides were stored at -20 °C. protected from light.

2.13 Statistic

Results were reported as the mean ± S.E.M., N= number of independent experiments. Diffrences were assessed using student's t-tset or ANOVA, with $p \geq 0.05$ considered non significant (ns), $p \leq 0.05$ * and $p \leq 0.01$ **.

.

Chapter 3: Results

I. VIP Simulation Increases CFTR Membrane Localization

VIP is a well-known agonist for CFTR-dependent secretions by directly activating CFTR and by its ability to increase CFTR surface expression (Ameen *et al*., 1999; Bewley *et al*., 2006; Chappe *et al*., 2008; Qu *et al*., 2011). Here, with immuno-labeling experiments using the anti-CFTR monoclonal antibody M3A7 followed by confocal microscopy, we confirmed that VIP stimulation (300 nM) of Calu-3 cells for 1 h resulted in a clear increase in CFTR expression at the cell membrane (figure 3.1 B) compared to control unstimulated cells where CFTR signal was distributed between the cytoplasm and the membrane (figure 3.1 A). Negative controls to test the specificity of the M3A7 anti-CFTR antibody were done before in cells not expressing the CFTR protein (Chappe *et al*., 2005; Seavilleklein *et al*., 2008) and confirmed here by labeling lung and intestine tissues from CFTR-KO mice (figure 3.1 E and F). Additional negative controls were performed by omitting the primary antibody to detect the background noise associated with the secondary antibody (figure 3.1 G). To further confirm this result, we labeled Calu-3 cells with the CM-DiI membrane dye and immunolabled CFTR with the M3A7 antibody as before. Our results show that CFTR co-localization with the membrane dye increases after VIP treatment (figure 3.1 D).

Using immunoblotting experiments we showed that the total amount of CFTR and its maturation (as monitored by the unchanged ratio between band B and band C of CFTR on the immunoblot membrane) did not change after the 1 h VIP stimulation (figure 3.2), confirming that the increase in CFTR surface expression after VIP stimulation was not a result of *de novo* synthesis or changes in CFTR maturation (as observed by the unchanged B immature band to the C mature band) but rather due to the modulation of membrane recycling and surface stability (figure 3.2).

II. VIP-Stimulated Increase in CFTR Surface Stability Depends on PKCε

Previously, our group has shown that PKC is responsible for the VIP-dependent reduction in CFTR endocytosis from the membrane (Chappe *et al*., 2008). Among the 11 known PKC isoforms, the calcium-independent novel isoform epsilon (PKCε) was identified to relay the VIP-dependent increase in ΔF508-CFTR membrane stability in the human nasal epithelial cell line JME/CF15 (Alcolado *et al*., 2011). Here in Calu-3 cells, to confirm the role of PKCε, we used immuno-labeling experiments to detect CFTR cellular expression after PKCε inhibition. We found that the VIP-dependent increase in CFTR membrane expression was almost lost in cells pre-treated with 15 μM PKCε inhibitor peptide EAVSLKPT for 30 min before VIP stimulation (figure 3.1 C) confirming that PKCε activation is important for VIP effect in Calu-3 cells. Decreased CFTR co-localizations with the CM-Dil membrane dye in cells pre-treated with the PKCε inhibitor peptide before VIP stimulation (figure 3.1 D) confirmed the involvement of PKCε in VIP mediated increase in CFTR membrane expression.

Figure 3.1 Immuno-localization and Confocal Microscopy Pictures of CFTR in Calu-3 Cells. Cells were labeled with anti-CFTR antibody M3A7 (1:1,000) followed by secondary anti-Mouse conjugated to CY3 (1-100) (red signal) **A**: Control untreated cells. **B**: Cells were treated with 300 nM VIP for 1 h. **C**: Cells were treated with 15 μM EAVSLKPT PKCε inhibitor peptide for 30 min before VIP treatment. **D**: Cells were labeled with the membrane dye CM-Dil (red signal) followed by immuno-labeling for CFTR (green signal). Overlapping signals (yellow) indicates membrane localization.

E and **F:** The M3A7 antibody for CFTR was tested on tissue sections from CFTR-KO mice. **E**: Intestine, **F**: lung. Paraffin embedded mouse tissues were sliced into 5 μm thick sections and mounted onto microscopy slides before staining with the M3A7 anti-CFTR antibody followed by secondary antibody conjugated to CY3. Corresponding DIC images are shown beside each confocal microscopy image.

G: Calu-3 cells were only labeled with secondary antibody conjugated to CY3 while the M3A7 antibody was omitted from the immuno-labeling experiment.

Images were visualized using the LSM 650 confocal microscope. N= 3 experiments.

A

Control

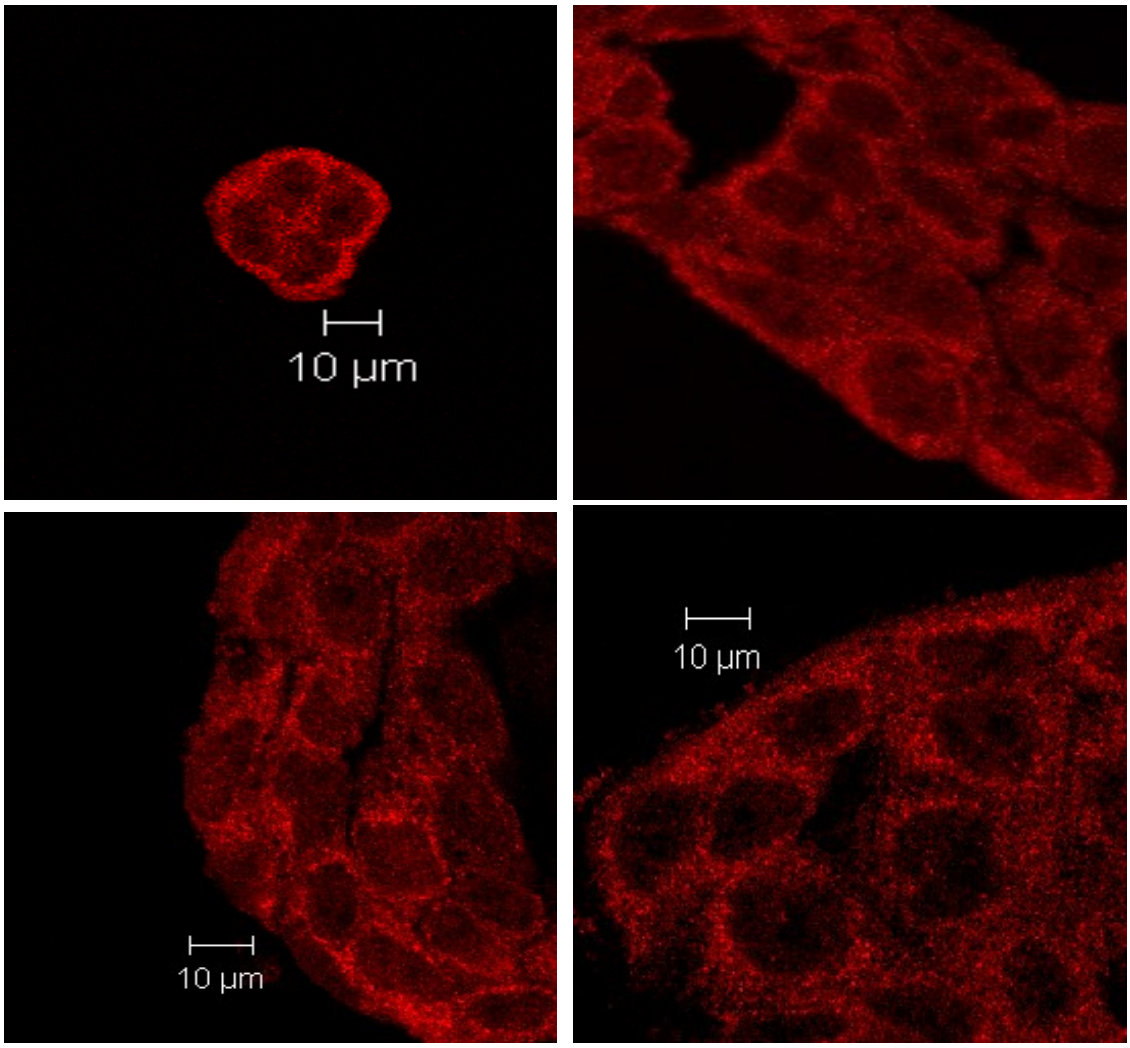

CFTR

VIP treated cells

B

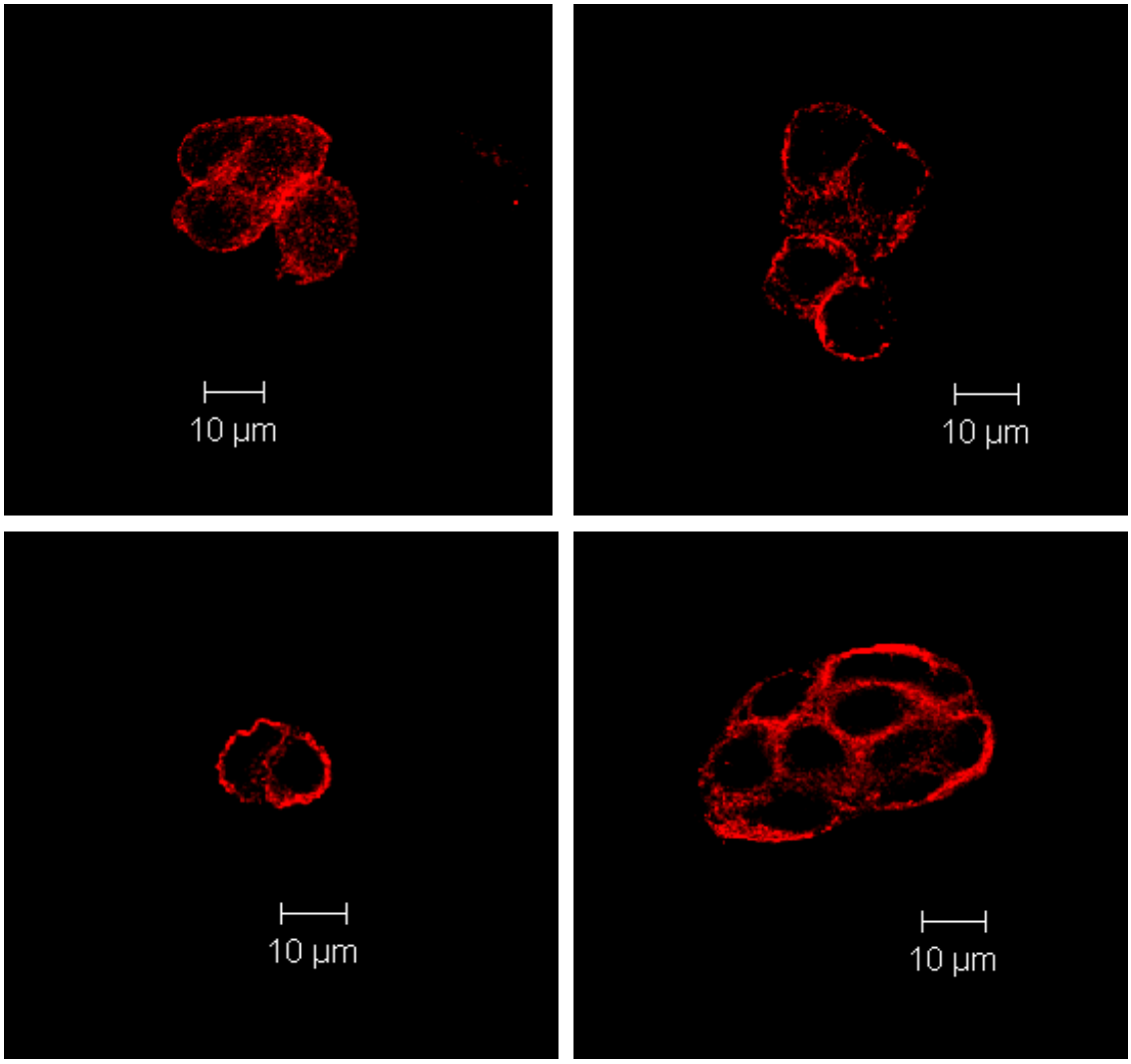

CFTR

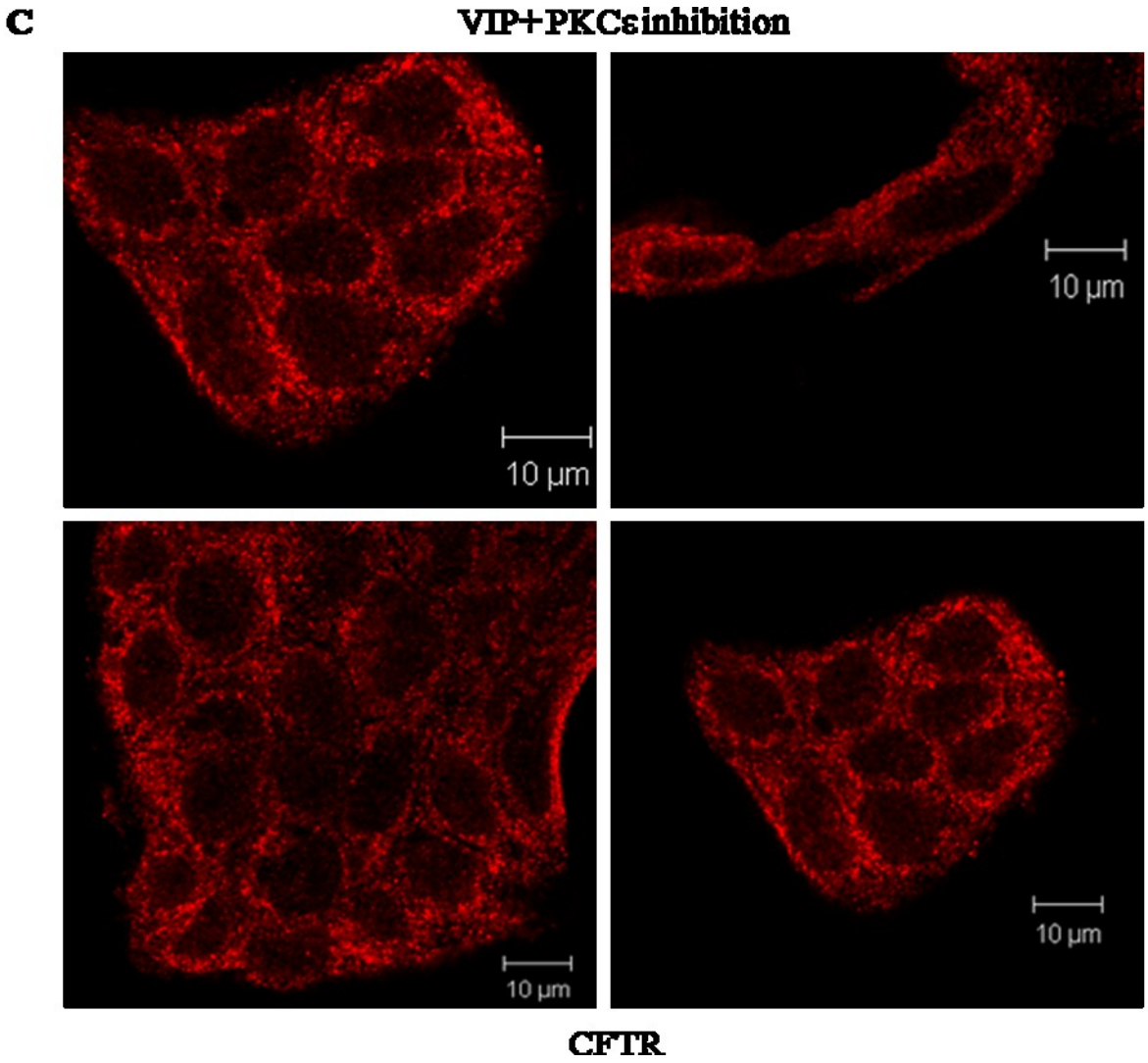
C
VIP+PKCεinhibition
10 µm
10 µm
10 µm
10 µm
CFTR

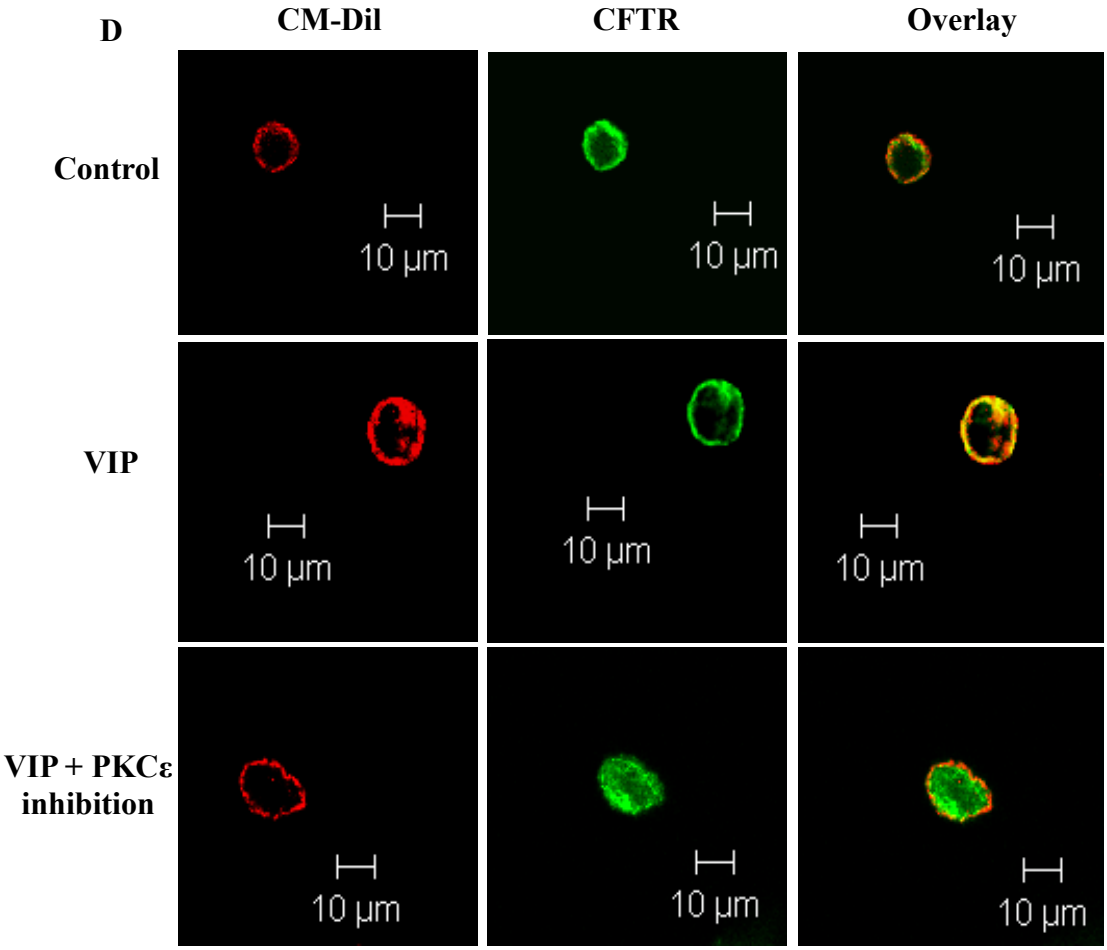
D
CM-Dil
CFTR
Overlay
Control
VIP
VIP + PKCε inhibition
10 µm

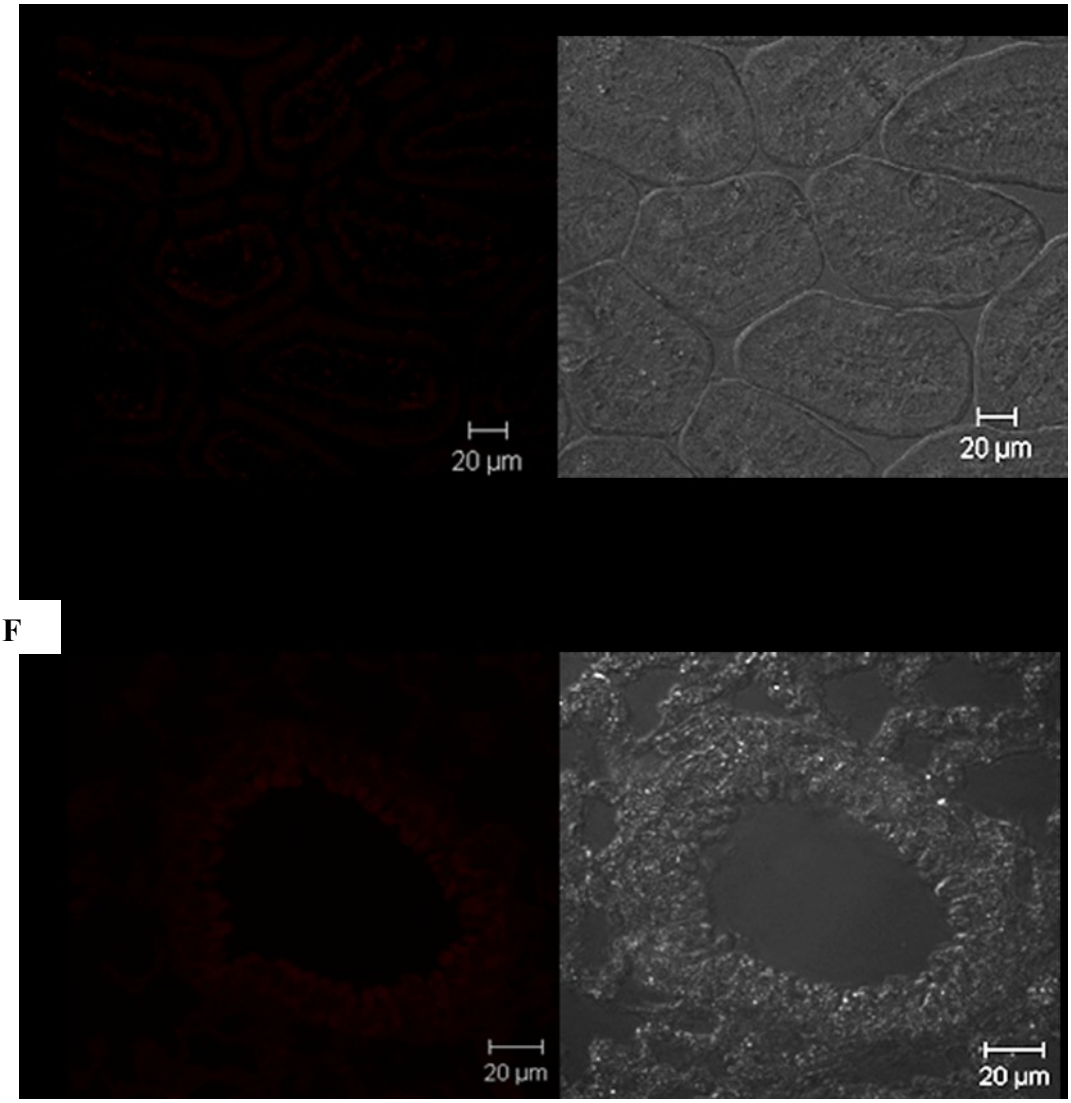

F

G

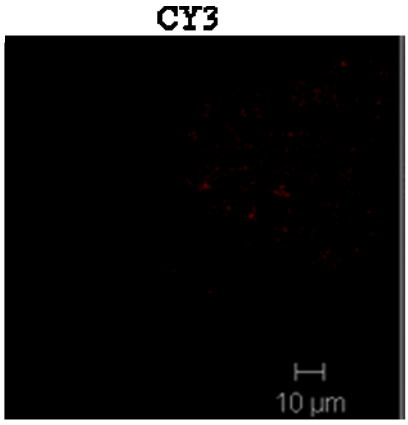

Calu-3 cells

Figure 3.2 Neither the Amount of Total CFTR nor its Maturation were Affected by VIP Stimulation. A: Representative immunoblot of CFTR expression in Calu-3 cells. Cells maintained at 37°C were treated by 300 nM VIP (1 h) or 20 nM PMA (1 h) or 15μM EAVSLKPT PKCε inhibitor peptide for 30 min before VIP stimulation or 15μM EAVSLKPT PKCε inhibitor peptide alone for 90 min. 20 μg of cell lysate was loaded to 7.5% gel, separated by SDS-PAGE and detected by the monoclonal CFTR antibody M3A7 followed by peroxidase conjugated secondary goat anti-Mouse antibody and visualized by chemiluminescence. **B**: Quantification of CFTR expression by densitometry of scanned immunoblots. N= 1.

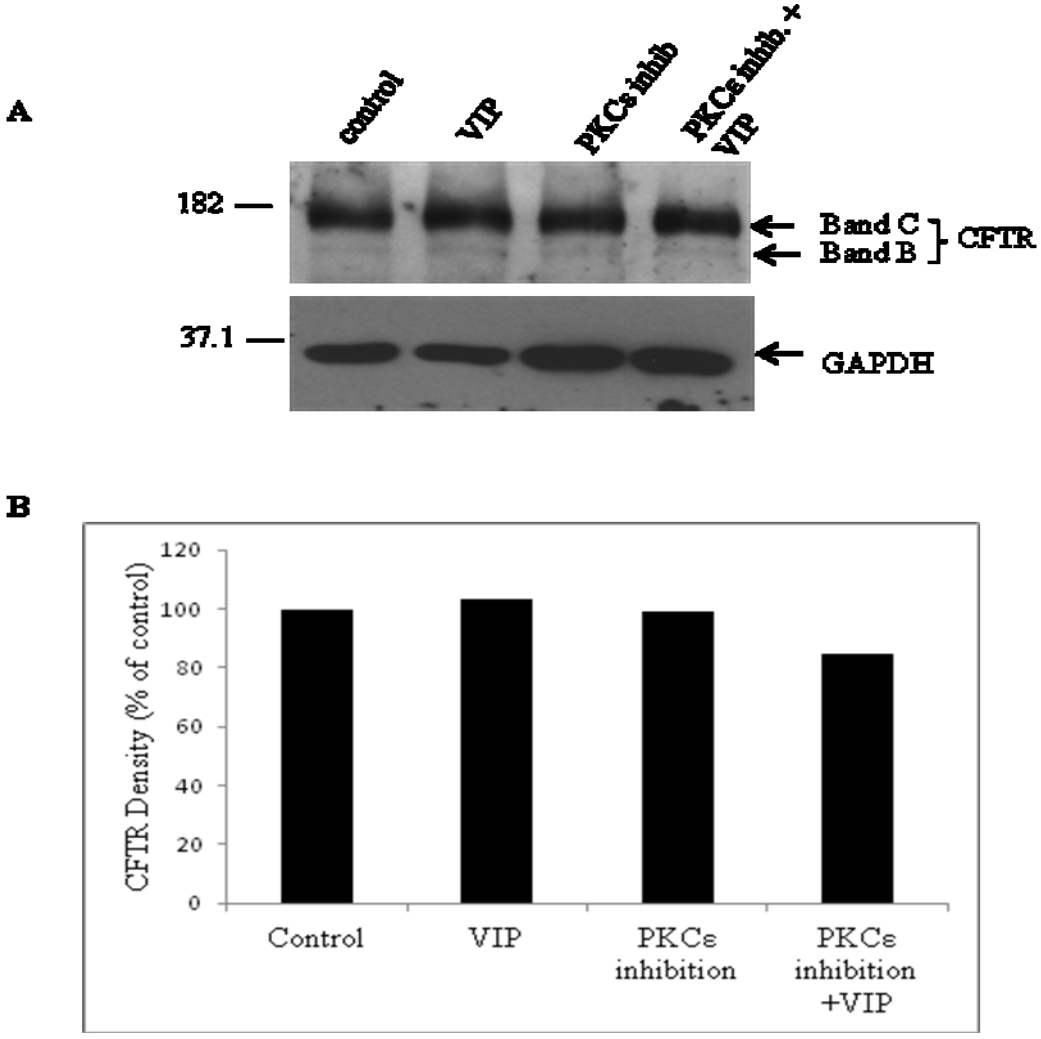

III. VIP induced Phosphorylation of ERM Proteins by PKCε

Calu-3 cells express VPAC1 receptors for VIP on the basolateral membrane (Chappe *et al*., 2008; Derand *et al*., 2004) that is coupled to both Gαs and/or Gαq/i signaling pathways. Activation of PKCε through Gαq/i signaling pathway was shown to increase CFTR surface stability (Chappe *et al*., 2008; Rafferty *et al*., 2009; Alcolado *et al*., 2011). To understand how PKCε activation after VIP stimulation of the VPAC1 receptors mediates CFTR membrane stability, we investigated the possibility of an activation of ERMs by PKC following VIP stimulation. The role of ERMs in regulating the membrane density of many membrane proteins, including CFTR, by their ability to link them to the actin cytoskeleton, either directly or indirectly, has been widely recognized (Bretscher, 1999; Bretscher *et al*., 2000; Bretscher *et al*., 2002). We measured the phoshorylation level of ERMs upon either VIP stimulation or activation of PKC directly by phorbol ester (phorbol 12-myristate 13-acetate; PMA).

Treatment of Calu-3 cells with 300 nM VIP or 20 nM PMA for 1 h increased the phosphorylation level of ERMs as measured by immunoblotting experiments using the widely used P-ERM antibodies that only detect ERM proteins when they are phosphorylated on threonine residues: Ezrin (T567) / Radixin (T564) / Moesin (T558) (Hayashi *et al*., 1999; Koss *et al*., 2006). Both VIP and PMA stimulation were shown to double the phoshorylation level of ERMs as measured by densitometry of scanned immunoblots (224.7 ± 82.9% of control, n=3, $p < 0.02$ and 258.7 ± 52.5% of control, n=3, $p < 0.005$, respectively) (figure 3.3 A and B).

Next we investigated the role of PKCε in VIP-dependent ERMs phosphorylation. Once again we used immunoblotting experiments and measured the phosphorylation level of ERMs using anti P-ERM antibodies. Our results showed that the VIP-induced increase in P-ERMs phosphorylation was significantly reduced in cells pre-treated with 15μM PKCε inhibitor peptide EAVSLKPT as measured by densitometry of scanned immunoblots (158.2695 ± 10.78 % of control, $p \leq 0.005$ and 103.82 ± 7.94 % of control $p \leq 0.6613$, n=3) (figure 3.3 C and D) confirming the involvement of PKCε. These results were also confirmed by immuno-labeling experiments. In control, unstimulated condition

(figure 3.4 A), P-ERMs staining was minimal. Whereas 1 h stimulation with PMA (20 nM) or VIP (300 nM) resulted in an increase in P-ERMs staining (figure 3.4 C). The P-ERMs staining returned to the control level when the cells were pretreated with 15μM PKCε inhibitor peptide EAVSLKPT before VIP stimulation (figure 3.4 D).

Figure 3.3 VIP Stimulation Increases the Phosphorylation Level of ERMs Through PKCε Activation. **A** and **C**, Representative immunoblots of P-ERM proteins in Calu-3 cells. Cells maintained at 37°C were treated with 300 nM VIP or 20 nM PMA for the indicated periods or with 15μM EAVSLKPT PKCε inhibitor peptide for 30 min before VIP stimulation (1 h). 40 μg of cell lysate were loaded into 7.5% polyacrylamide gel, separated by SDS-PAGE, and detected by polyclonal P-ERM antibodies and peroxidase conjugated goat anti-Rabbit secondary antibody and visualized by chemiluminescence. Immunoblotting membranes were stripped and re-probed for GAPDH. Expected sizes (kDa) for Ezrin: 82, Radixin: 80, Moesin: 75, and GAPDH: 37. **B** and **D**: Quantification of P-ERMs expression by densitometry. Results were normalized to corresponding GAPDH expression level. Values are means ± S.E.M for N= 3 independent experiments (* $p \leq 0.05$, **, $p \leq 0.01$).

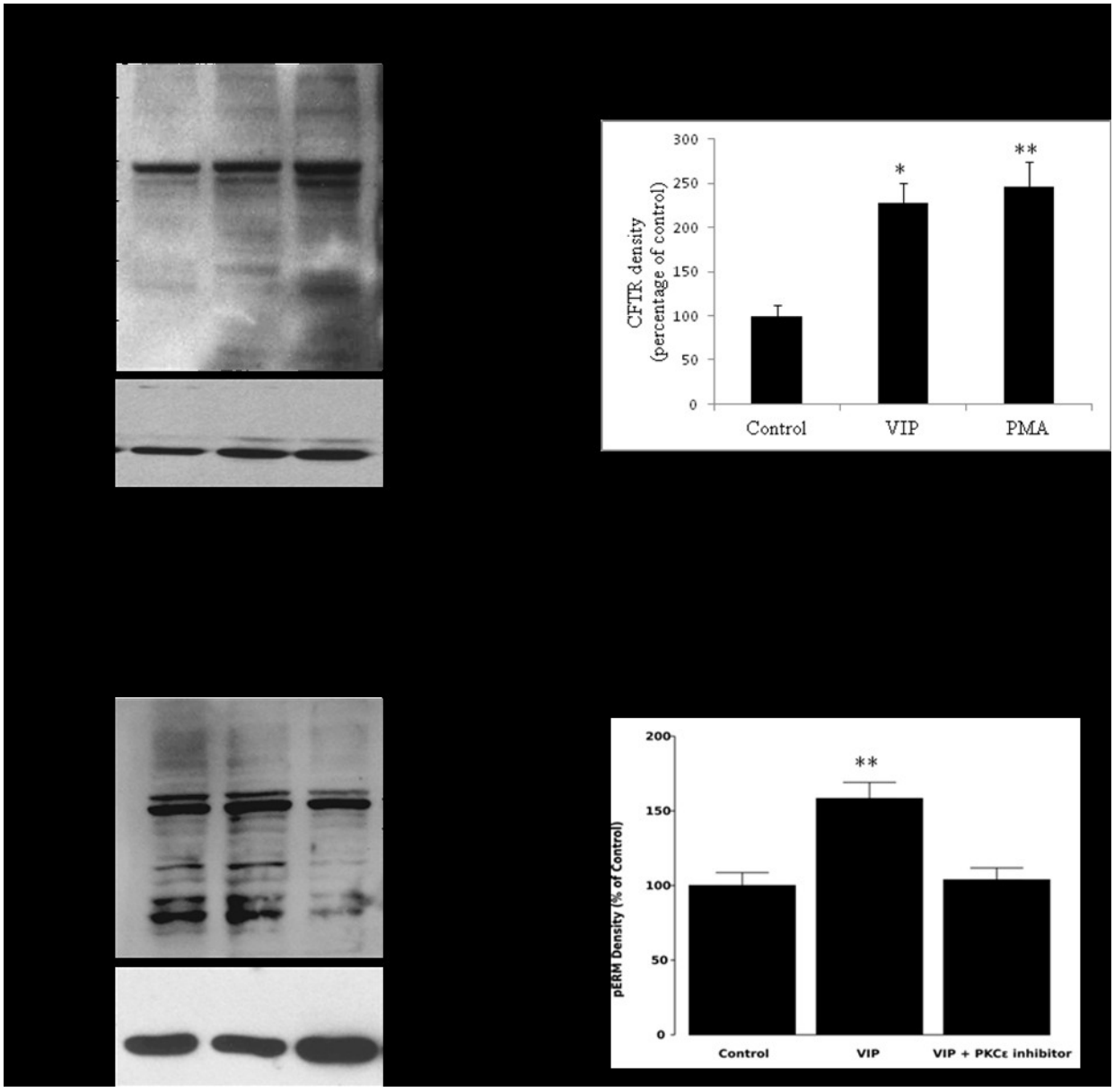
CFTR density
(percentage of control)
300
250
200
150
100
50
0
*
**
Control
VIP
PMA
pERM Density (% of Control)
200
150
100
50
0
**
Control
VIP
VIP + PKCε inhibitor

Figure 3.4 Confocal Microscopy Pictures of P-ERMs Immuno-Localization in Calu-3 Cells. Cells were labeled with anti-P-ERM antibodies (1:1,000) followed by a secondary antibody conjugated to dylight 650 (1-100) (blue signal). **A**: Control untreated cells. **B**: Cells treated with 20 nM PMA for 1 h. **C**: Cells treated with 300 nM VIP for 1 h. **D**: Cells treated with 15µM EAVSLKPT PKCε inhibitor peptide for 30 min before VIP treatment. Images were visualized using the LSM 650 confocal microscope. N= 3 independent experiments.

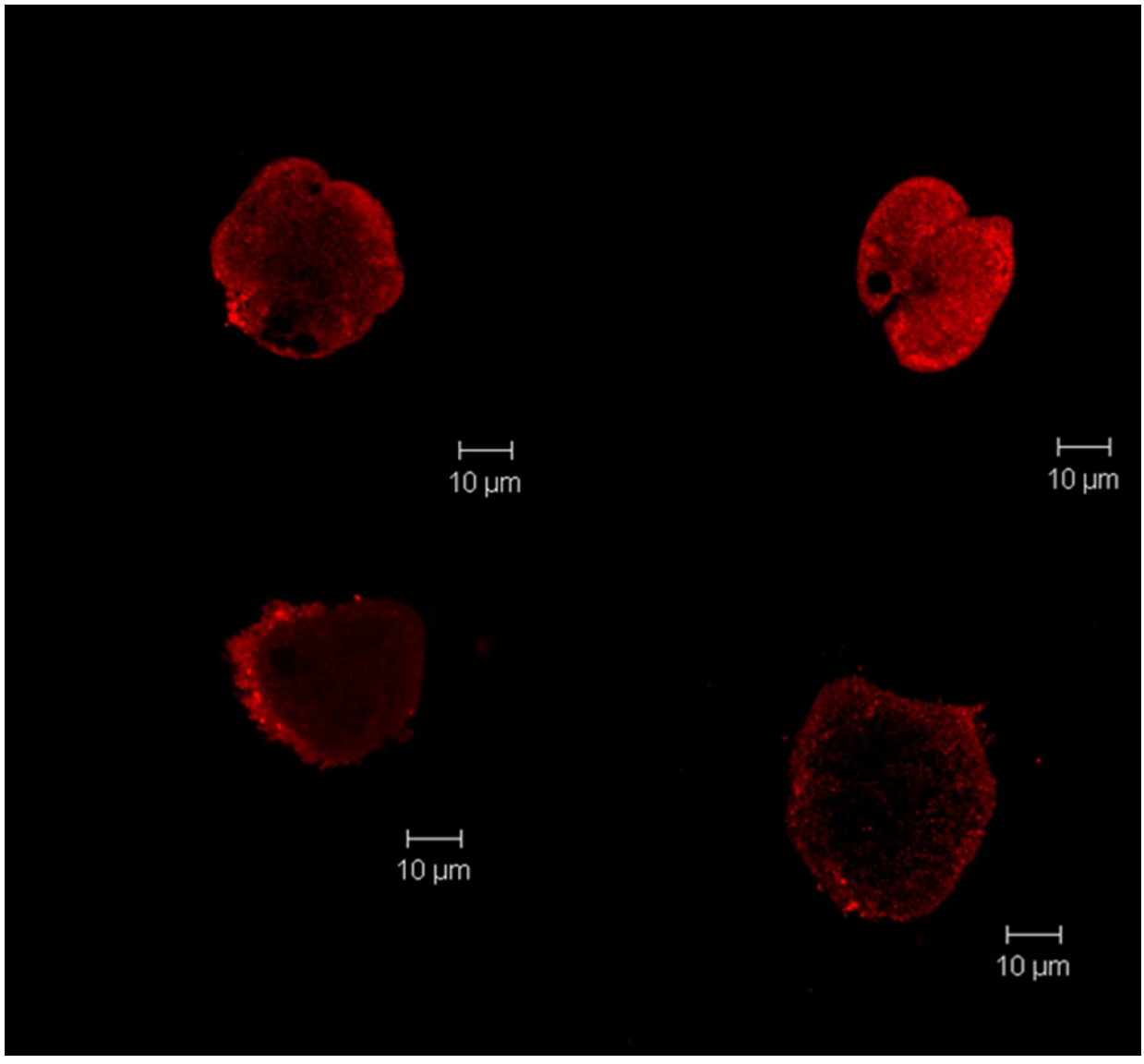
10 µm
10 µm
10 µm
10 µm

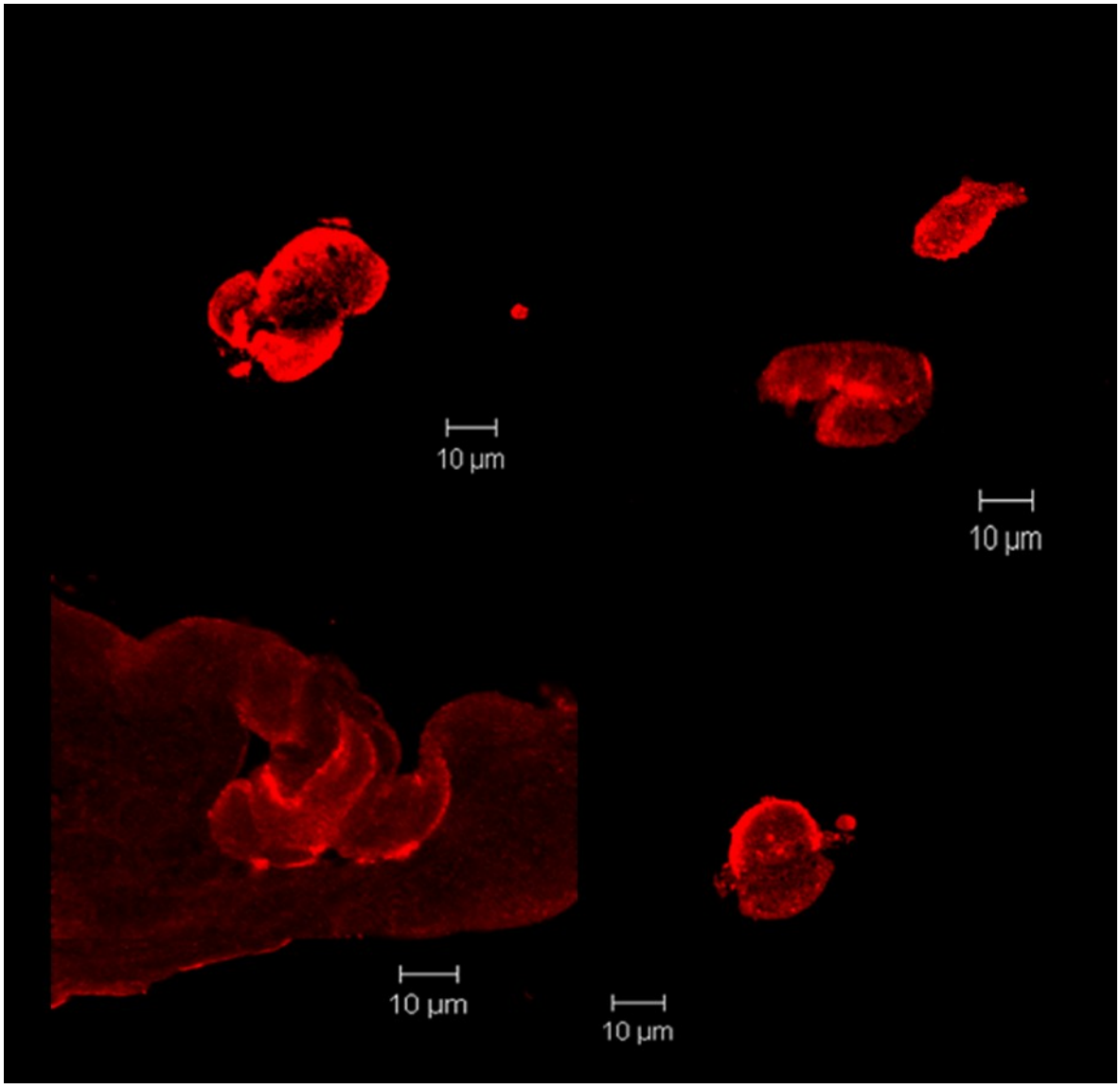
10 µm
10 µm
10 µm
10 µm

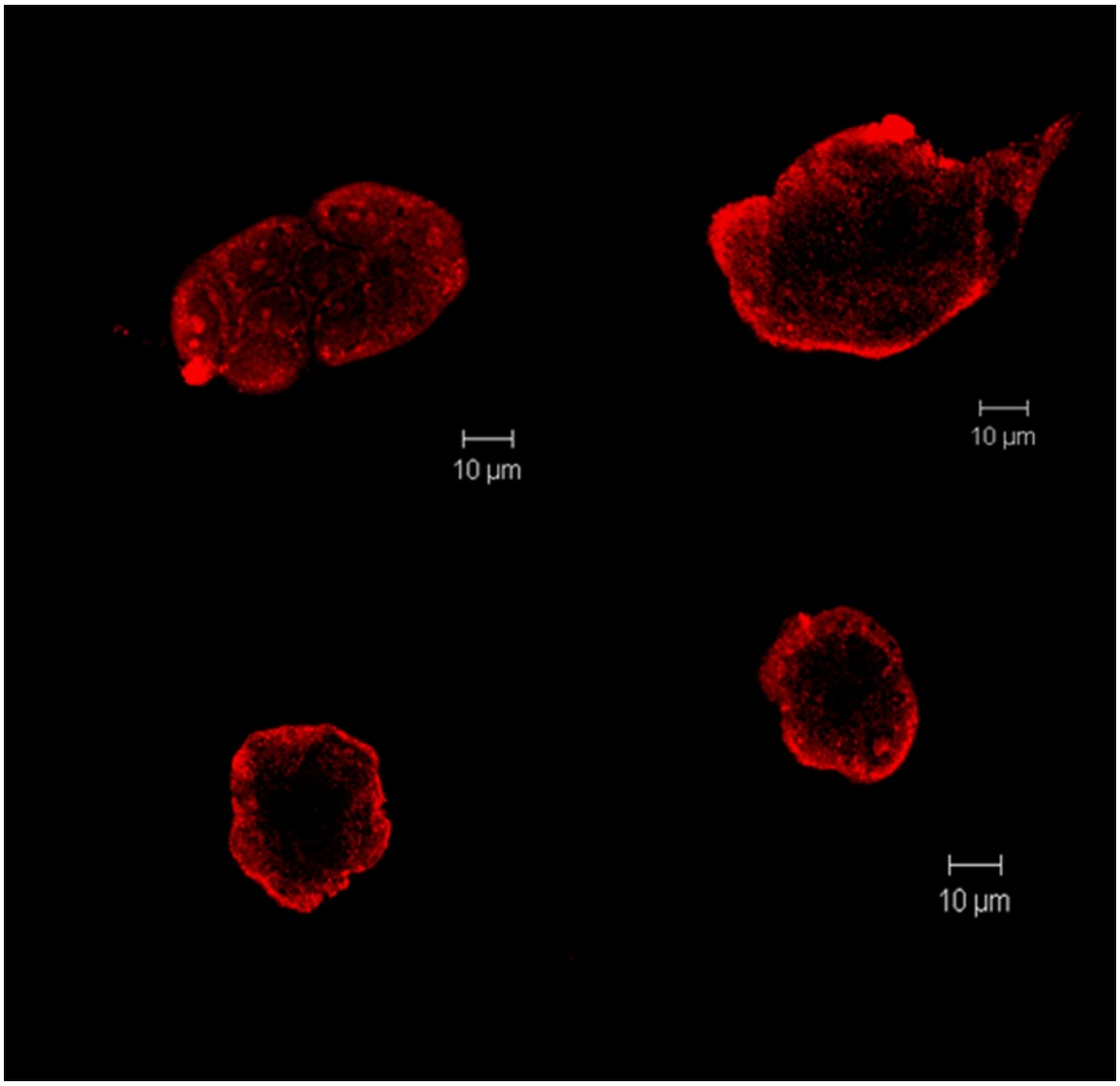
10 µm
10 µm
10 µm

D **VIP+PKCεinhibition (P-ERMs)**

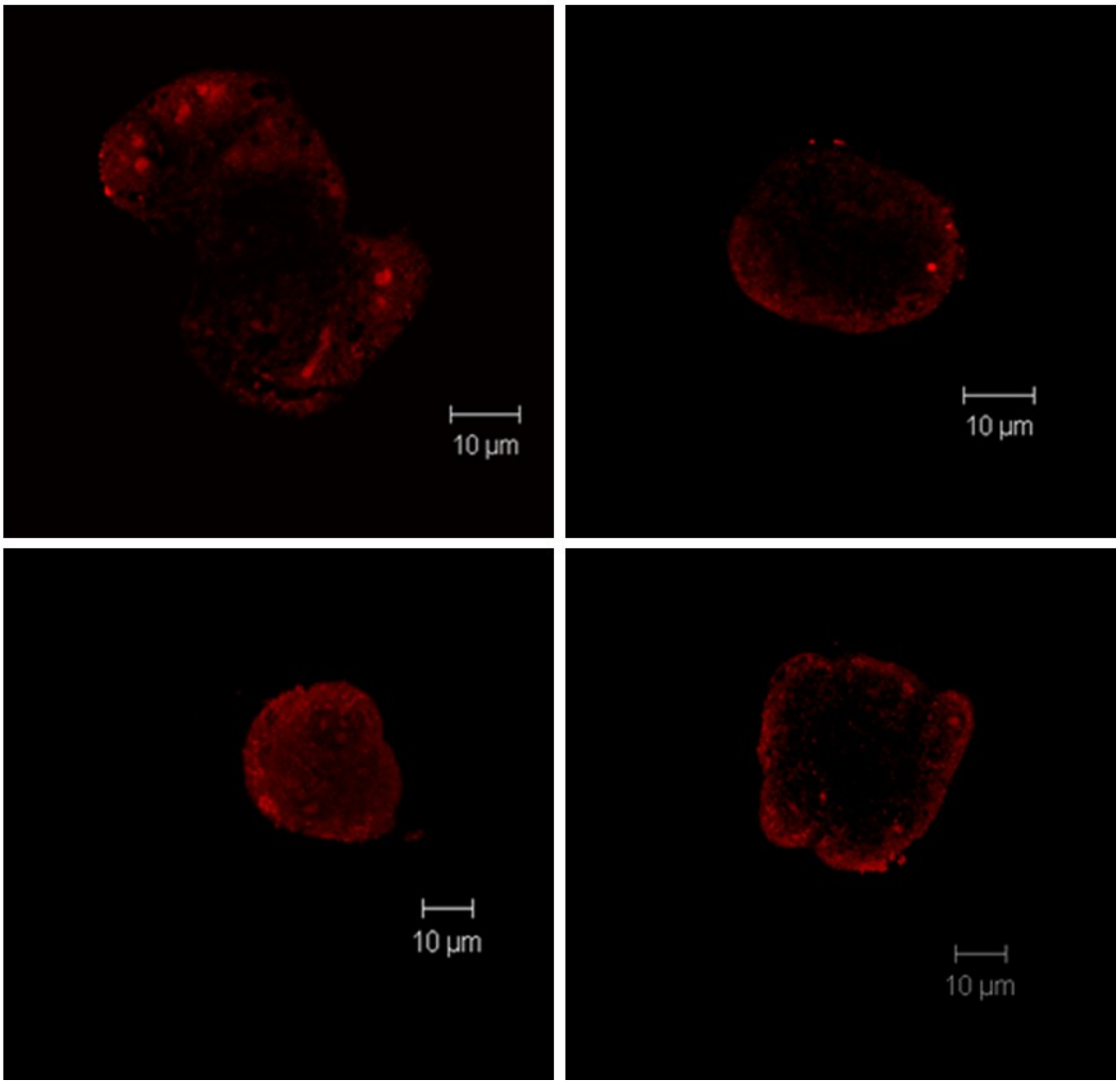

IV. Time Course of VIP Effect on ERMs Phosphorylation

Previous studies in which the amount of CFTR at the membrane was measured with the cell surface biotinylation assays, showed that the VIP-dependent increase in CFTR membrane density followed a time order with maximal CFTR membrane density obtained after 30 min of VIP stimulation that could be sustained for up to 2 h (Chappe *et al*., 2008). We hypothesized that if ERMs phosphorylation plays a direct role in the VIP-dependent increase in CFTR membrane density, it should follow a similar time course. To investigate this possibility, we performed time-course experiments of VIP stimulation (300 nM) from 15 min to 2 h and measured ERMs phoshorylation level as before. Interestingly, a time-dependent increase in ERMs phoshorylation by VIP was obtained, (figure 3.5 A and B) with maximum phosphorylation obtained after 30 min of VIP stimulation (205.24 ± 47.08 % of control, $n = 3$, $p < 0.007$), consistent with the previous report. The increase in ERMs phosphorylation was sustained for 1 h (152.68 ± 37.64 % of control, $n=3$, $p < 0.04$) and decreased after 2 h (141.15 ± 39.02 % of control, $p > 0.37$).

Figure 3.5 Time Course Experiments for ERMs Phosphorylation by VIP.

A: Representative immunoblot of P-ERM proteins in Calu-3 cells. Cells maintained at 37°C were treated with 300 nM VIP for the indicated periods. 40 µg of cell lysate were separated by SDS-PAGE and detected by the polyclonal P-ERM antibodies followed by peroxidase conjugated goat anti-Rabbit secondary antibody and visualized by chemiluminescence. **B**: Quantification of P-ERMs expression by densitometry. The immunoblotting membranes were stripped and re-probed for GAPDH. Expected sizes (kDa) for; Ezrin: 82, Radixin: 80, Moesin: 75 and GAPDH: 37. Results were normalized to corresponding GAPDH expression level. Values are means ± S.E.M for N= 3 independent experiments, * $p \leq 0.05$, ** $p \leq 0.01$.

A

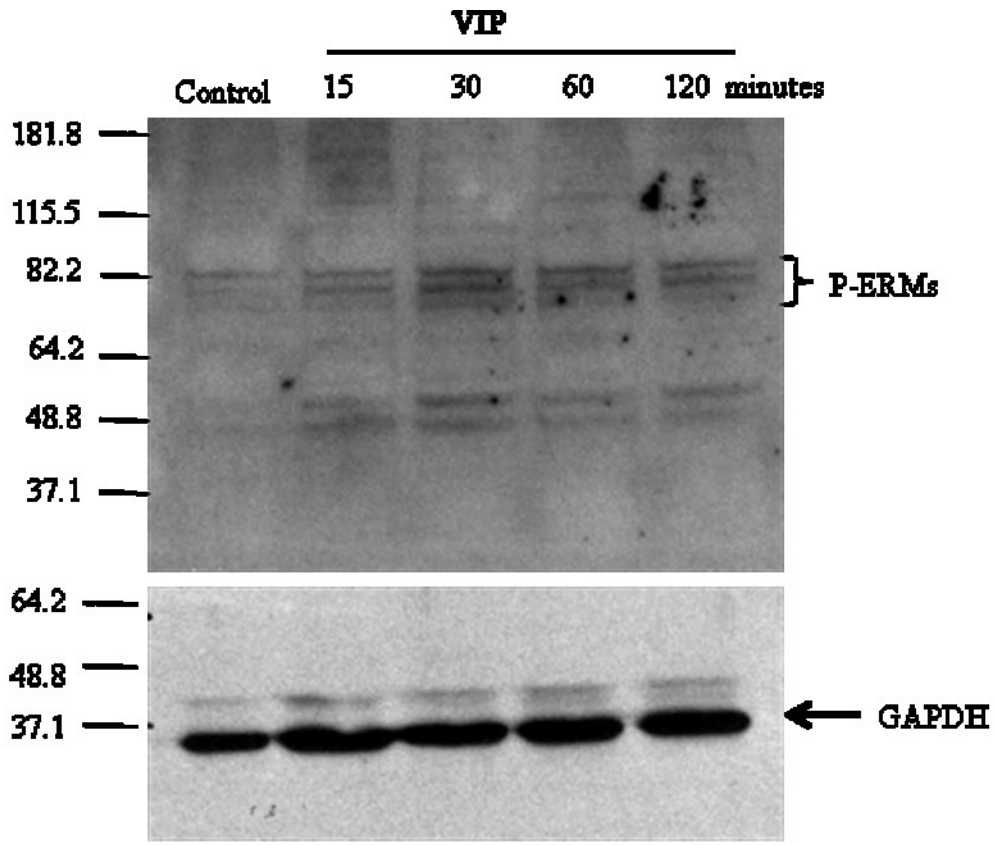
VIP
Control
15
30
60
120 minutes
181.8
115.5
82.2
64.2
48.8
37.1
P-ERMs
64.2
48.8
37.1
GAPDH

B

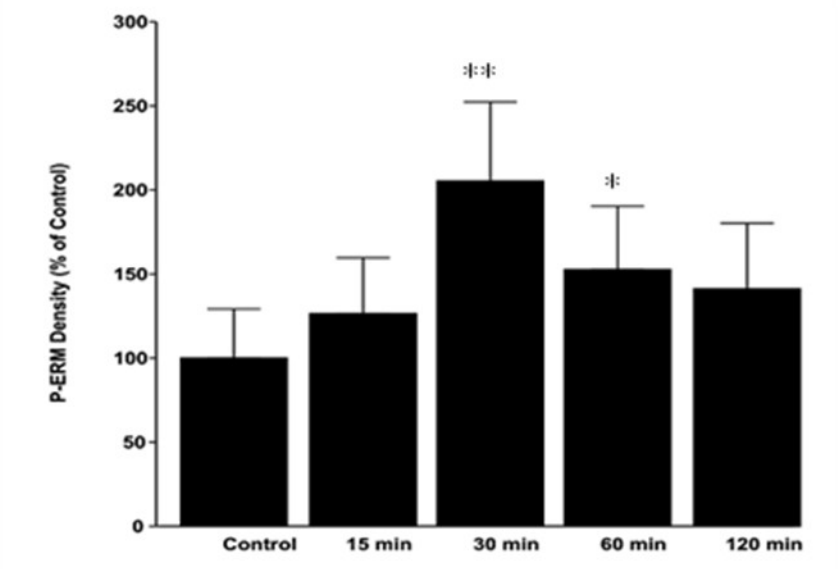
P-ERM Density (% of Control)
300
250
200
150
100
50
0
**
*
Control
15 min
30 min
60 min
120 min

V. ERM-siRNA Transfection Prevents VIP-dependent Increase in CFTR Surface Expression

To further confirm the involvement of ERMs in the VIP signaling cascade that regulates CFTR membrane density, we used specific siRNA against ERM proteins to reduce their expression level. ERM-siRNA electroporated into Calu-3 cells and ERM expression levels were assessed 48 h after the electroporation. Immunoblotting results showed a reduction in total P-ERMs expression of ~44 % (56.54202 ± 10.03% of control, n=3, $p < 0.001$) as measured by densitometry of scanned immunoblots, without changing GAPDH expression (figure 3.6 A and B). Although this seemed to be a low efficiency, this average value reflected a mixed population of transfected and untransfected cells. To overcome the low transfection efficiency, we used immunolabeling experiments to assess the effect of ERMs deficiency in VIP mechanism. We selected cells which displayed efficient siRNA transfection as indicated by very low or no fluorescence signal in confocal microscopy images for the targeted proteins and looked for the VIP effect on CFTR membrane expression in these cells.

Immuno-labeling experiments for CFTR and confocal microscopy analysis confirmed that the electroporation method did not affect CFTR cellular distribution or VIP-dependent increase in membrane CFTR. The ERM-siRNA specificity was confirmed by using scrambled non-coding siRNA (figure 3.7 A and C). Interestingly, VIP treatment (1 h, 300 nM) failed to induce the intended increase in CFTR membrane density in cells transfected with ERM-siRNA (figure 3.7 D), suggesting the requirement of P-ERMs proteins for VIP mechanism. The loss of the VIP ability to increase CFTR membrane density in ERM-siRNA transfected cells was confirmed by the decreased co-localization of CFTR with the CM-Dil membrane dye compared to cells transfected with the non-targeted scrambled-siRNA (figure 3.8).

Figure 3.6 ERM-siRNA Decreased ERMs Expression Level.

A: Representative immunoblot of P-ERMs after ERM-siRNA electroporation into Calu-3 cells. 40 μg of cell lysate were separated by SDS PAGE and detected by P-ERM antibodies followed by peroxidase conjugated secondary antibody and detected by chemiluminescence. **B**: Quantification of P-ERMs expression by densitometry. The immunoblotting membranes were stripped and re-probed for GAPDH. Expected sizes (kDa) for; Ezrin: 82, Radixin: 80, Moesin: 75 and GAPDH: 37. (* $p \leq 0.05$) N=3.

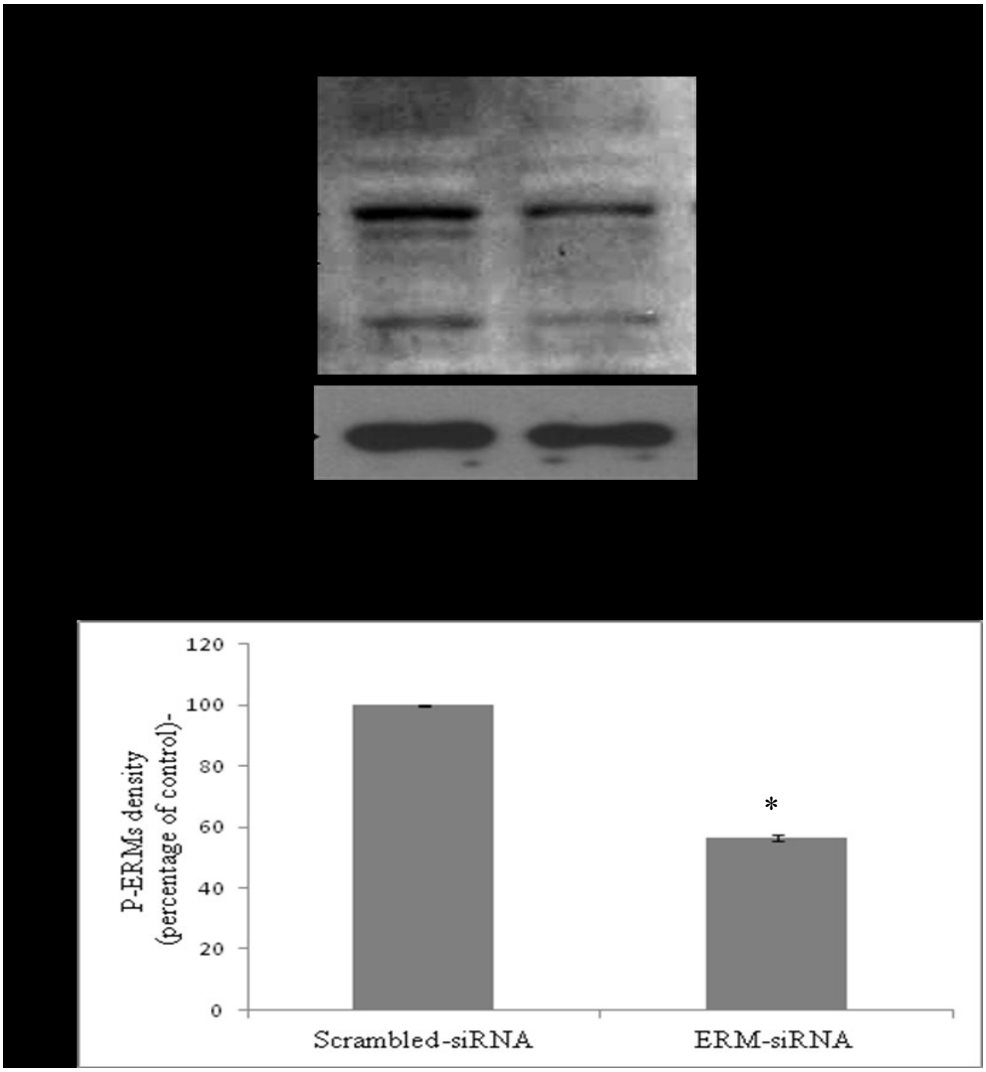

Figure 3.7 VIP stimulation Failed to Increase CFTR Membrane Expression in ERM-siRNA Transfected Cells.

Immuno-localization and confocal microscopy pictures of CFTR in Calu-3 cells. Cells maintained at 37°C were transfected with ERM-siRNA or scrambled-siRNA. 48 h after transfection, the cells were labeled with anti-CFTR antibody M3A7 (1:1,000) followed by a secondary antibody conjugated to CY3 (1-100) (red signal) **A**: Control cells transfected with scrambled-siRNA. **B**: Control cells transfected with ERM-siRNA. **C**: Cells transfected with scrambled-siRNA and treated with 300 nM VIP for 1 h before immuno-labeling. **D**: Cells transfected with ERM-siRNA and treated with 300 nM VIP for 1 h before immuno-labeling. Images were visualized using LSM 650 confocal microscope. N= 3 experiments.

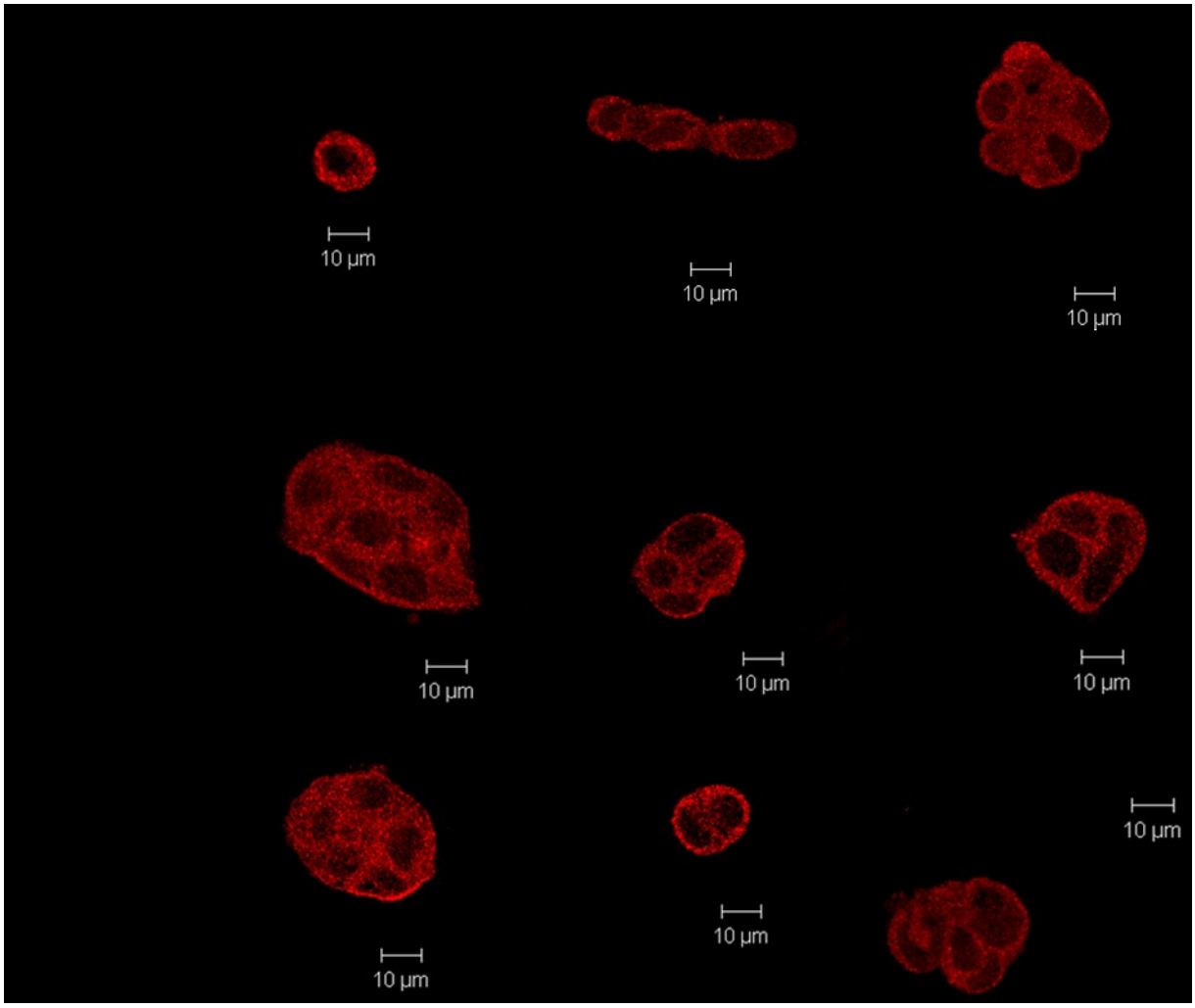
10 µm
10 µm
10 µm
10 µm
10 µm
10 µm
10 µm
10 µm
10 µm

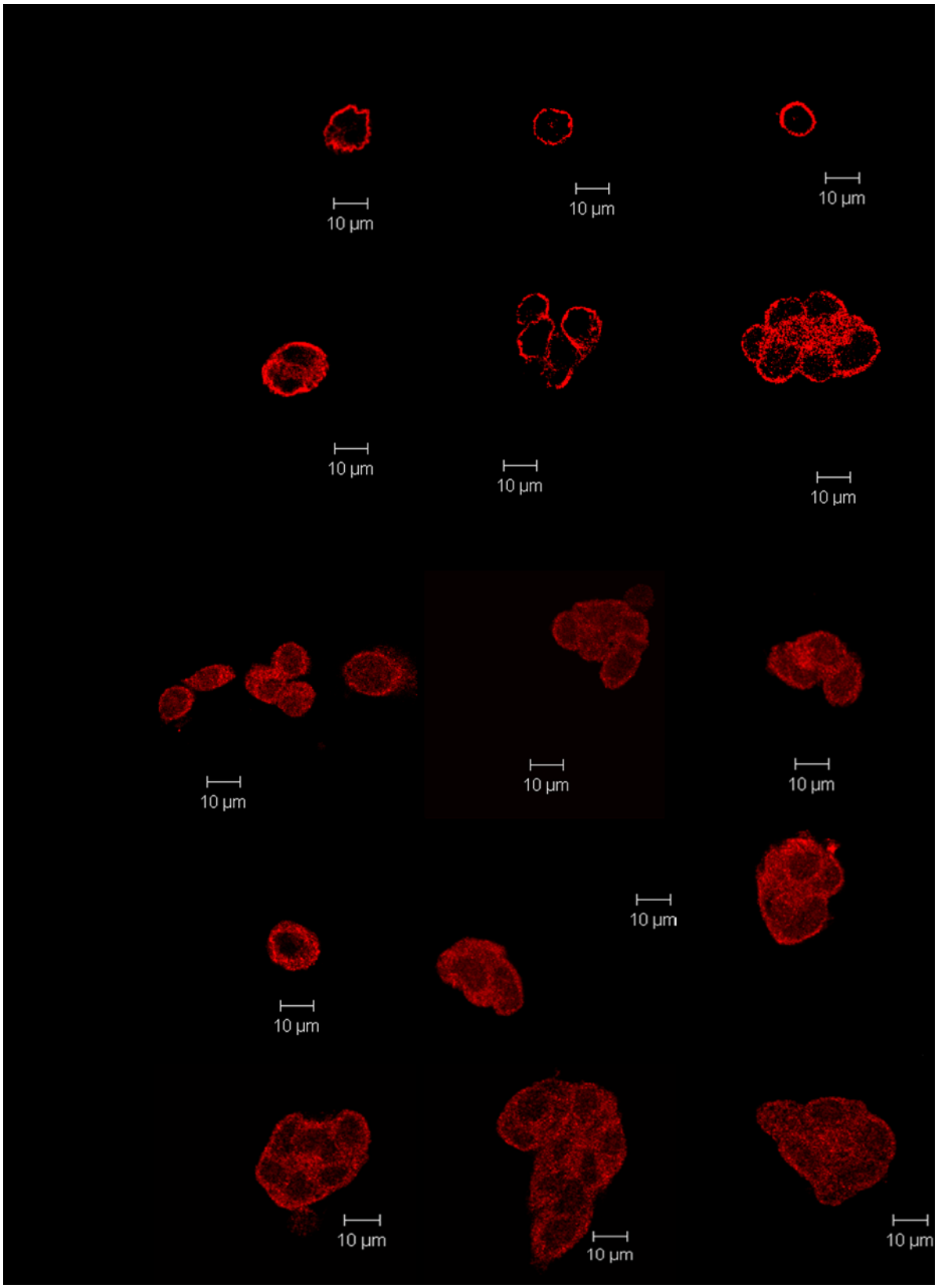
10 µm
10 µm
10 µm
10 µm
10 µm
10 µm
10 µm
10 µm
10 µm
10 µm
10 µm
10 µm
10 µm
10 µm

Figure 3.8 Dowm-regulating ERMs by siRNA Transfection Prevented VIP-dependent Increase of CFTR Membrane Localization. 48 h after ERM-siRNA or scrambled-siRNA transfection**,** Calu-3 cells maintained at 37°C were labeled with the membrane dye CM-Dil (red signal) followed by immuno-labeling for CFTR (green signal). Overlapping signals (yellow) indicate membrane localization. Images were recorded by LSM confocal microscope. The different stimulation conditions are indicated on the figure.

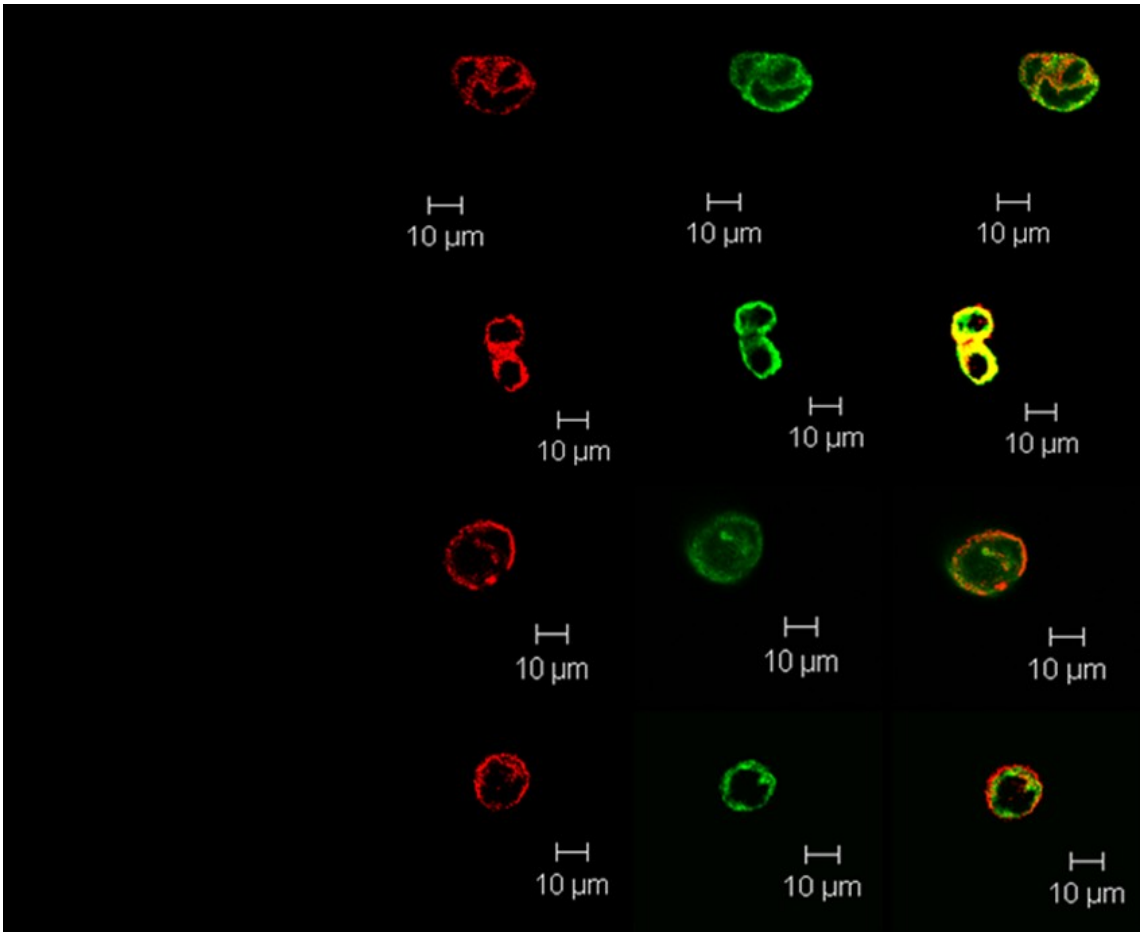

VI. VIP Stimulation Increases NHERF1 membrane Localization

Previous studies have shown that the interaction between ERMs and CFTR is indirect through PDZ scaffolding proteins such as NHERF1 that can bind both proteins simultaneously (Short *et al*., 1998; Moyer *et al*., 1999; Bretscher *et al*., 2000; Ladias, 2003). So we next investigated the role of NHERF1 in VIP signaling cascade to regulate CFTR membrane density.

We used RT-PCR experiments to detect NHERF1 mRNA in Calu-3 using primers designed to detect human NHERF1 as described in the method section. NHERF1 mRNA was detected in Calu-3 cells while no signal was detected when the primer was omitted from RT-PCR reaction. PKCα was used as positive control (figure 3.9 A). Using immunoblotting experiments, we determined the amount of endogenous NHERF1 protein expression level in Calu-3 cells (figure 3.9 B and figure 2.1 in method section).

We then tested whether VIP stimulation (1 h, 300 nM) has an effect on NHERF1 cellular localization. NHERF1 is a membrane associated cytoplasmic protein that was shown to translocate from the cytoplasm to the plasma membrane when activated (Kreimann & Cabrini, 2013). Here, we labeled Calu-3 cells for NHERF1 using specific monoclonal anti-NHERF1 antibody and examined the cellular localization of NHERF1 using the laser scanning confocal microscopy. We found that under control condition, NHERF1 staining was distributed between the cell membrane and the cytoplasm as expected (figure 3.10 A). After VIP stimulation, for 1 h there was a noticeable increase in NHERF1 membrane localization (figure 3.10 B). Negative controls to test the specificity of anti-NHERF1 antibody were done in BHK cells that do not express the NHERF1 protein (figure 3.10 C). Additional negative controls were performed by omitting the primary antibody to detect the background noise associated with the secondary antibody (figure 3.10 D).

Figure 3.9 NHERF1 mRNA and Protein Expression in Calu-3 Cells.

A: NHERF1 mRNA was detected by RT-PCR after RNA extraction from Calu-3 cells. PCR products were subjected to 1.5% agarose gel electrophoresis for analysis. Lane 1: DNA ladder Ø, Lane 2: PKCα (positive control), Lane 3: NHERF1. Lane 4: negative control where primers are omitted from the RT-PCR reaction. Specific primers for the human NHERF1 were used, see materials and methods. Expected sizes (bp) of amplified products are indicated under the figure. **B**: Representative immunoblot of NHERF1 protein expression in Calu-3 cells. Expected size for NHERF1 (kDa): 50.

A

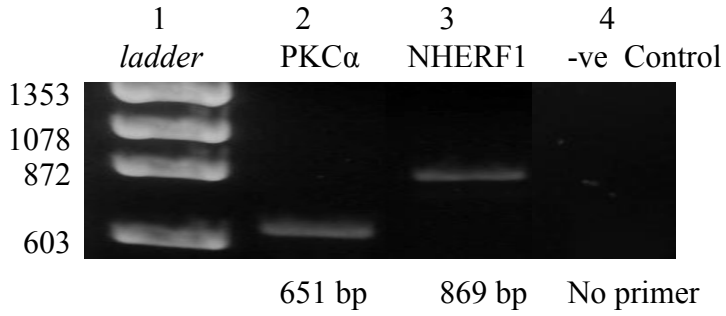

B

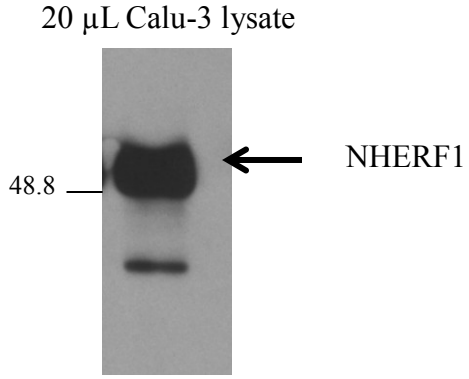

Figure 3.10 Immuno-localization and Confocal Microscopy Pictures of NHERF1 in Calu-3 Cells. Calu-3 cells maintained at 37°C were labeled with anti-NHERF1 antibody followed by a secondary antibody conjugated to CY5 (blue signal). Images were visualized using LSM 650 confocal microscope. **A**: Control untreated cells, **B**: Cells treated with 300 nM VIP (1 h) before immuno-labeling, N= 3 independent experiments. **C** and **D:** Negative controls for the anti-NHERF1 antibody. **C**: BHK cells that do not express NHERF1 were labeled with anti-NHERF1 antibody followed by a secondary antibody conjugated to CY5 (blue signal). **D**: No primary antibody was incubated with Calu-3 cells followed by incubation with secondary antibody conjugated to CY5.

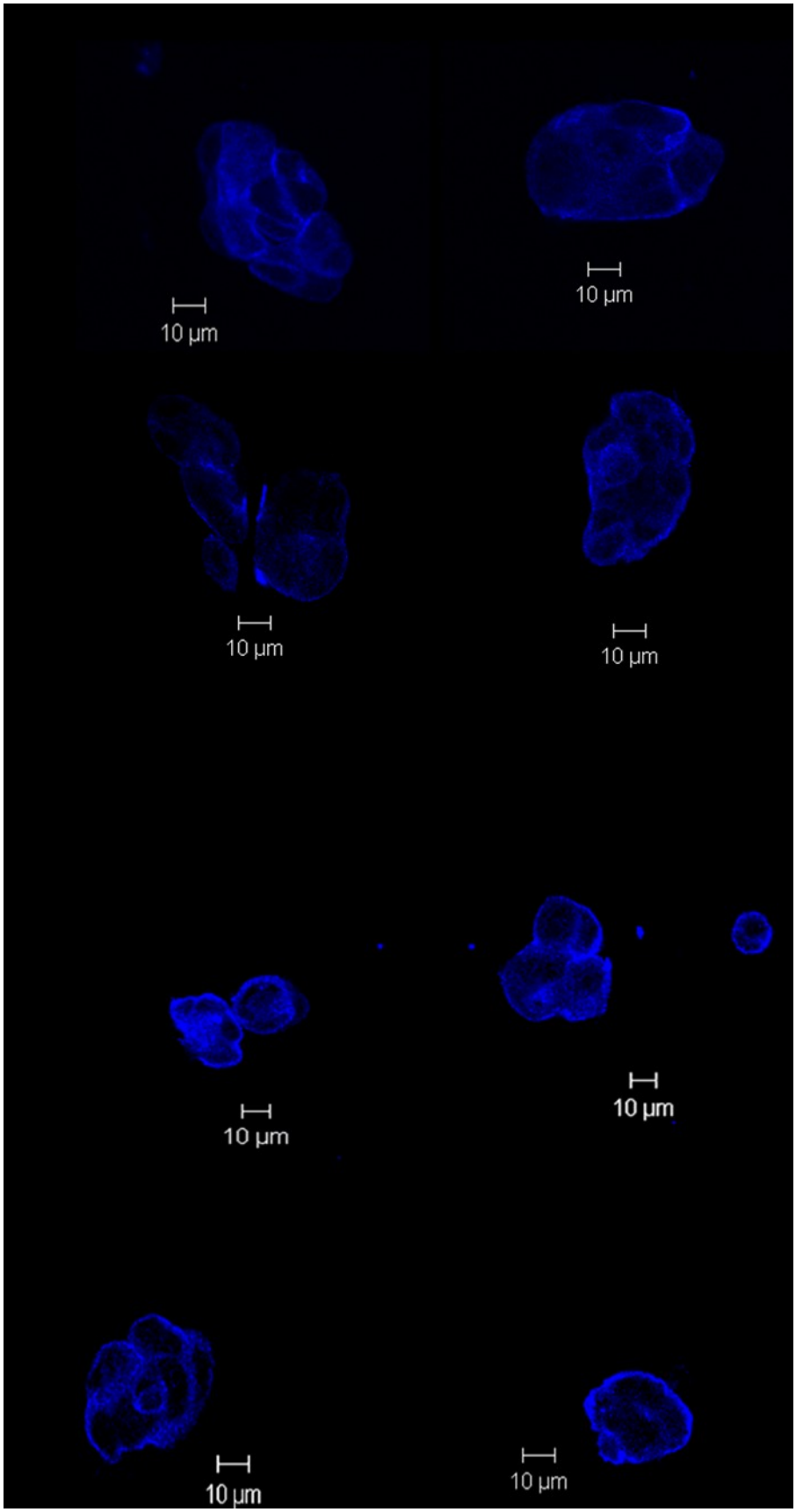
10 µm
10 µm
10 µm
10 µm
10 µm
10 µm
10 µm
10 µm

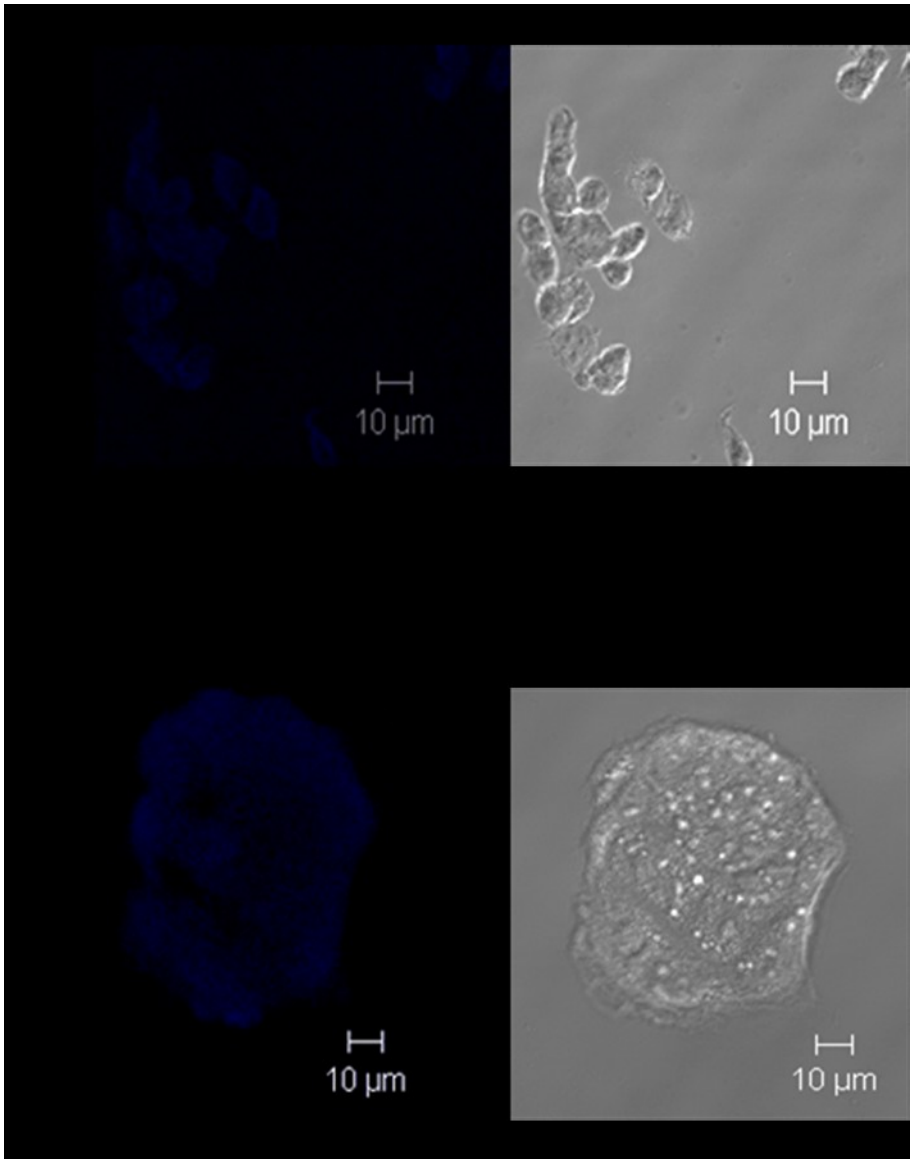
10 µm
10 µm
10 µm
10 µm

VII. VIP Increases CFTR and NHERF1 Interaction at the Membrane of Calu-3 Cells

To examine the effect of VIP on NHERF1-CFTR interaction, we labeled Calu-3 cells for both CFTR and NHERF1 using the monoclonal anti-CFTR M3A7 and anti-NHERF1 antibodies. Interestingly, we found that treating Calu-3 cells with 300 nM VIP for 1 h resulted in a noticeable increase in CFTR-NHERF1 co-localization at the cell membrane (figure 3.11 B) compared to the control unstimulated cells (figure 3.11 A).

To further confirm that NHERF1 is part of the VIP signaling cascade, we used specific siRNA against NHERF1 transfected into Calu-3 cells by electroporation as indicated in the method section. NHERF1-siRNA electroporation resulted in reduction of NHERF1 expression by ~ 40 % (61.8% ± 3.9 % of control, n=3, $p < 0.003$) as measured by densitometry of scanned immunoblots with no effect on the expression of CFTR or GAPDH, confirming the specific effect of the NHERF1-siRNA (figure 3.12). Also, CFTR-NHERF1 expression pattern (figure 3.11 A) and VIP-dependent increase in membrane CFTR-NHERF1 co-localization (figure 3.11 B) were not different between control non-transfected cells or cells transfected with the non-targeting scrambled-siRNA. This confirms that the transfection method did no disturbed Calu-3 cells. Additionally, to confirm that the cells with no or low NHERF1 signal, after siRNA transfection, were viable, Calu-3 cells transfected with NHERF1-siRNA were labeled for cytokeratin and nuclei were stained with DAPI. Our results show that cells with no NHERF1 signal (incorporated the siRNA) were not morphologically different from control cells (figure 3.13 A and B).

Using confocal microscopy, we selected the cells that incorporated NHERF1-siRNA as shown by minimal to none NHERF1 signal, and examined VIP ability to increase CFTR membrane expression in these cells. The absence of NHERF1 in Calu-3 cells did not compromise CFTR localization, although the fluorescence signal seemed slightly reduced compared to control cells (figure 3.14 C). Interestingly, in cells with minimal NHERF1 expression, VIP failed to increase CFTR membrane expression (figure

3.14 D), once again suggesting the involvement of NHERF1 in VIP-dependent increase in CFTR membrane density. The loss of VIP ability to increase CFTR membrane expression in NHERF1-siRNA transfected cells was confirmed by the decreased co-localization signal between CFTR and the membrane dye CM-DiI compared to the cells transfected with scrambled-siRNA before VIP stimulation (figure 3.15).

Figure 3.11 VIP Stimulation Increases CFTR-NHERF1 Co-localization at the Membrane. Immuno-localization and confocal microscopy pictures of CFTR and NHERF1 in Calu-3 cells. Cells maintained at 37°C were labeled with the anti-CFTR antibody M3A7 followed by secondary antibody conjugated to CY3 (red signal) and with the anti-NHERF1 antibody followed by secondary antibody conjugated to CY5 (green signal).Yellow signal represents the overlapping signals. Images were visualized using the LSM 650 confocal microscope. **A**: Control untreated cells, **B**: Cells treated with 300 nM of VIP before staining. N= 3-4 independent experiments.

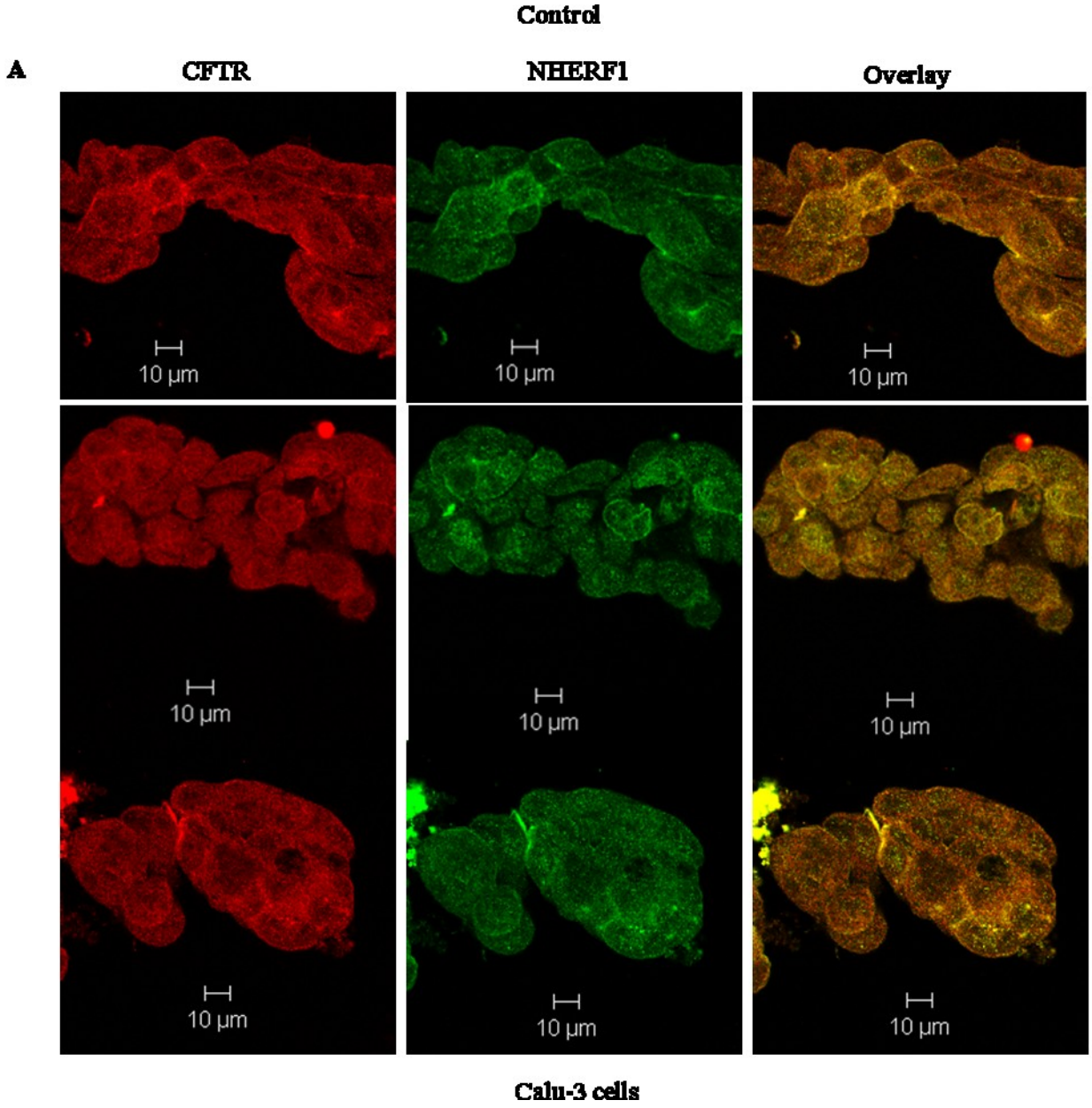
Control
A
CFTR
NHERF1
Overlay
10 µm
10 µm
10 µm
10 µm
10 µm
10 µm
10 µm
10 µm
Calu-3 cells

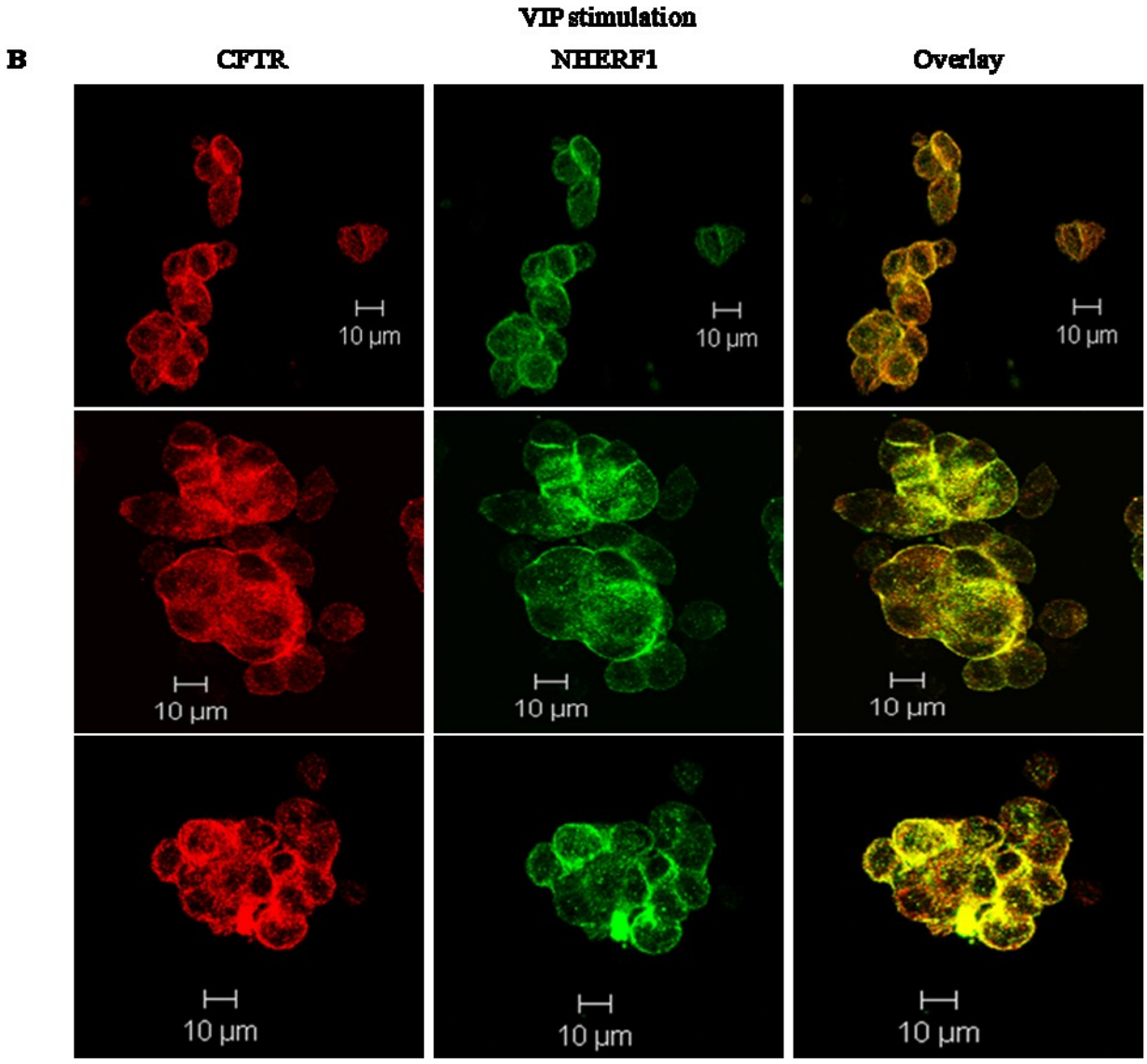
VIP stimulation
B
CFTR
NHERF1
Overlay
10 µm
Calu-3 cells

Figure 3.12 NHERF1-siRNA Decreased NHERF1 Expression by 40%.

A: Representative immunoblot of NHERF1 expression after transfection of Calu3 cells by electroporation with specific NHERF1-siRNA. 20 µg of cell lysate were separated by SDS PAGE and detected by monoclonal anti-NHERF1 antibodies followed by peroxidase conjugated secondary antibodies and visualized by chemiluminescence. Blotting membranes were stripped and re-probed for GAPDH and CFTR. **B**: Quantification of NHERF1 expression by densitometry of scanned immunoblots. Expected sizes (kDa) for NHERF1:50, CFTR: 180 and GAPDH: 37. Values are means ± S.E.M (* $p \leq 0.05$), N= 3.

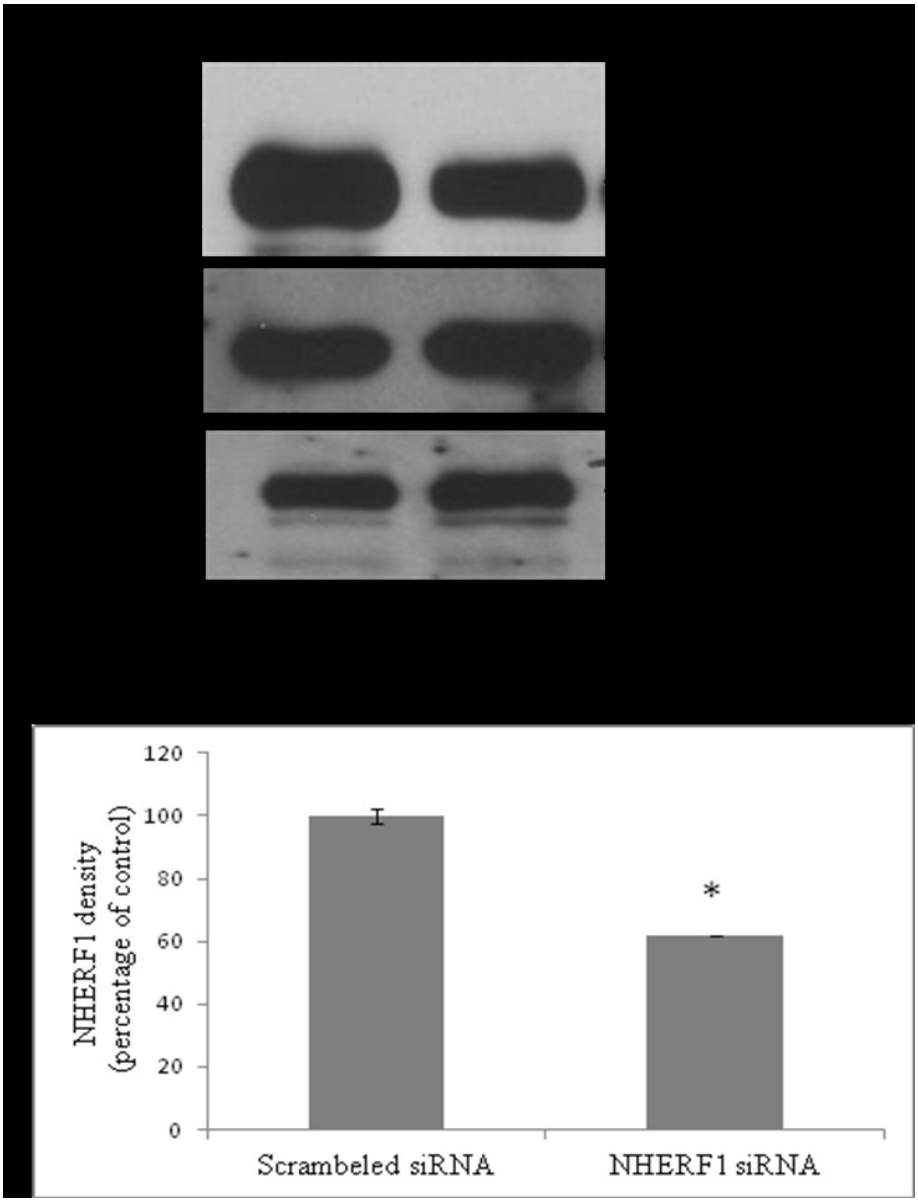

Figure 3.13 siRNA Trasnfection Did Not Affect the Cells Morphology or viability. Immuno-localization and fluorescence microscopy pictures of NHERF1 and cytokeratin in Calu-3 cells. Cells maintained at 37°C were transfected with NHERF1-siRNA. 48 h after transfection, the cells were labeled with anti-NHERF1 antibody (1:1,000) followed by secondary antibody conjugated to CY5 (1-200) (green signal) and with pan-cytokeratin antibodies (1-200) followed by secondary antibody conjugated to CY3 (1-100) (red signal). Images were visualized using the Zeiss Axiovert 200 fluorescence microscope. **A**: Group of cells expressing NHERF1, **B**: Group of cells with no/minimal NHERF1 expression following NHERF1-siRNA incorporation.

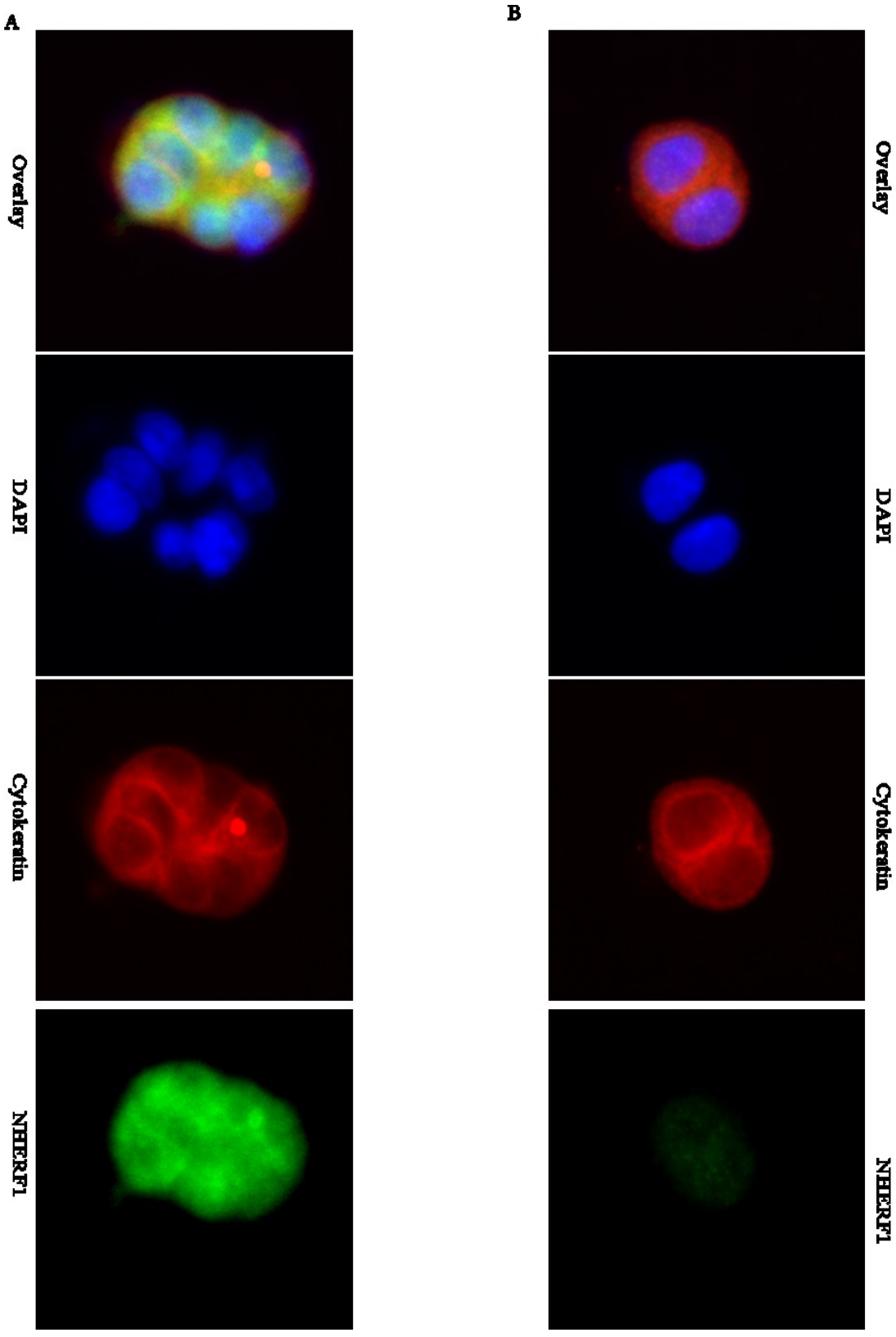
A
Overlay
DAPI
Cytokeratin
NHERF1
B
Overlay
DAPI
Cytokeratin
NHERF1

Figure 3.14 VIP Stimulation Failed to Increase CFTR Membrane Density in NHERF1-siRNA Transfected Cells.

Immuno-localization and confocal microscopy pictures of CFTR and NHERF1 in Calu-3 cells. Cells maintained at 37°C were transfected with NHERF1-siRNA or with scrambled-siRNA. 48 h after transfection, cells were labeled with anti-CFTR antibody M3A7 (1:1,000) followed by secondary antibody conjugated to CY3 (1-100) (red signal) and with anti-NHERF1 antibody (1-1,000) followed by secondary antibody conjugated to CY5 (1:200) (green signal). **A**: Control cells transfected with scrambled-siRNA. **B**: Control cells transfected with NHERF1-siRNA. **C**: Cells transfected with scrambled-siRNA and treated with 300 nM VIP for 1 h before the immuno-labeling. **D**: Cells transfected with NHERF1-siRNA treated with 300 nM VIP for 1 h before the immuno-labeling. Images were visualized using the LSM 650 confocal microscope. N= 3 independent experiments.

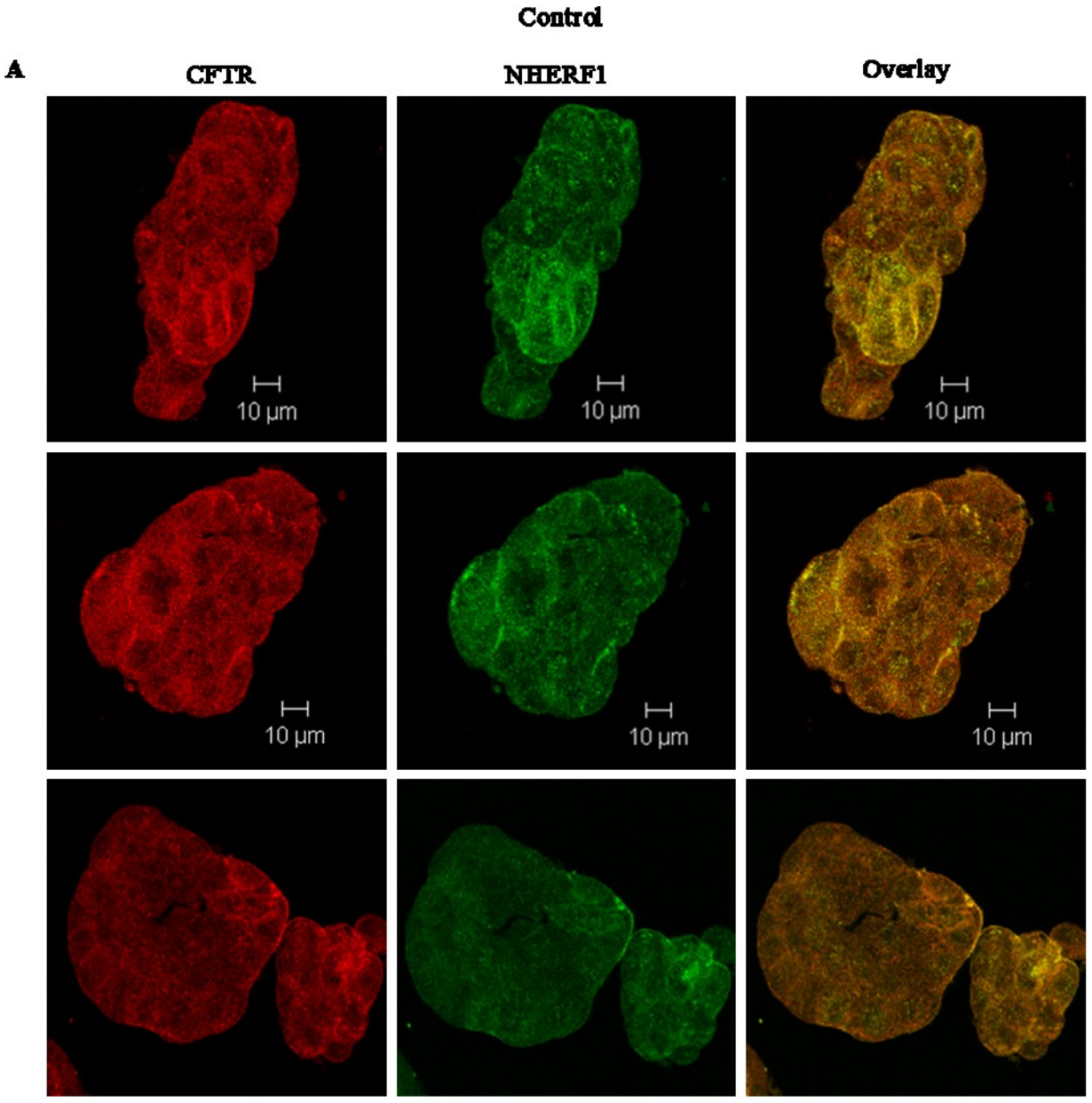

Calu-3 cells transfected with scrambled-siRNA

B

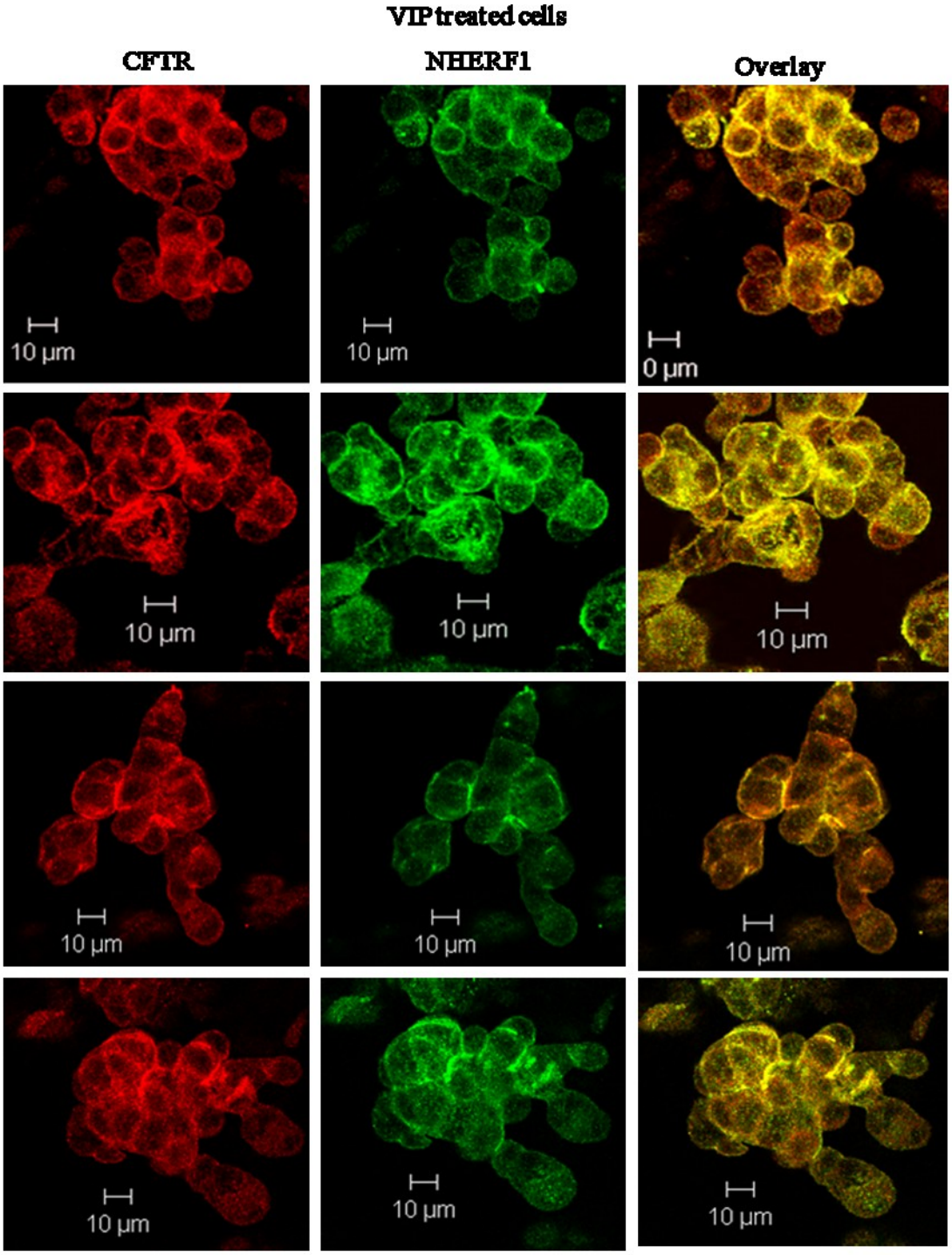

Calu-3 cells transfected with scrambled-siRNA

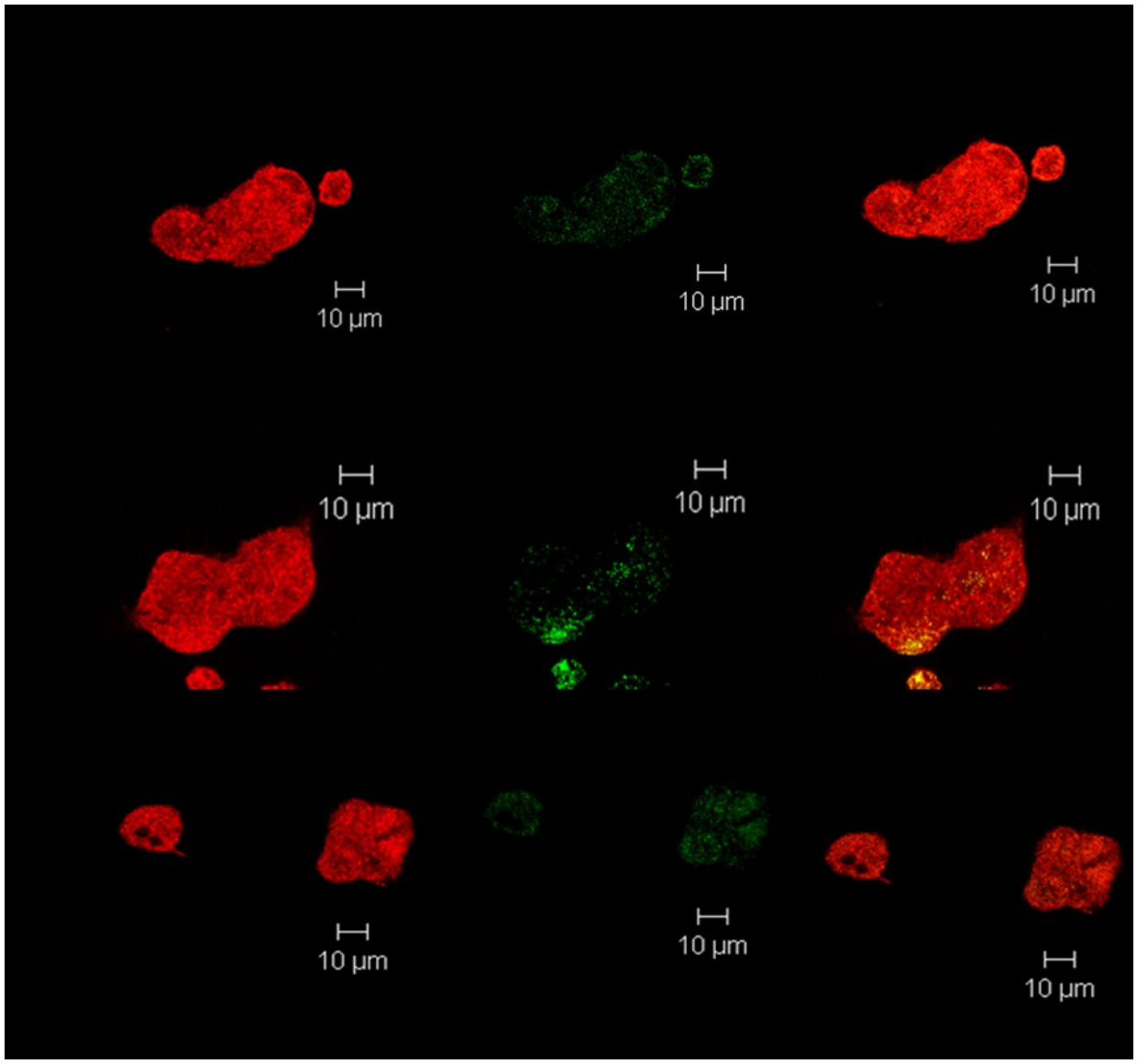
10 µm
10 µm
10 µm
10 µm
10 µm
10 µm
10 µm
10 µm
10 µm

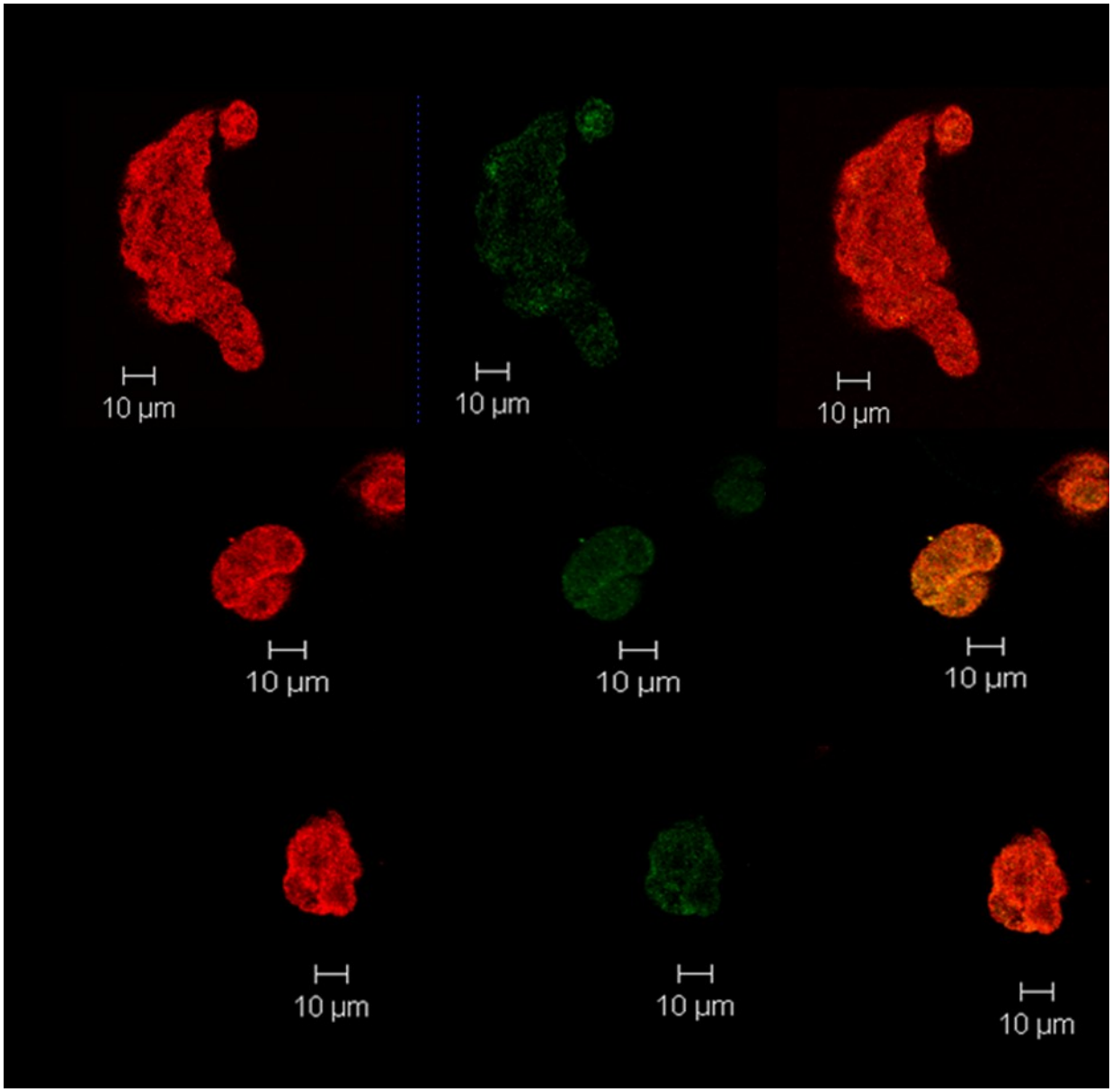
10 µm
10 µm
10 µm
10 µm
10 µm
10 µm
10 µm
10 µm
10 µm

Figure 3.15 Down-regulating NHERF1 by siRNA Transfection Prevented VIP-Dependent Increase of CFTR Membrane Localization. 48 h after NHERF1-siRNA transfection, Calu-3 cells maintained at 37°C were labeled with the membrane dye CM-Dil (red signal) followed by immuno-labeling for CFTR (green signal). Overlapping signals (yellow) indicate membrane localization. The different stimulation conditions are indicated on the figure.

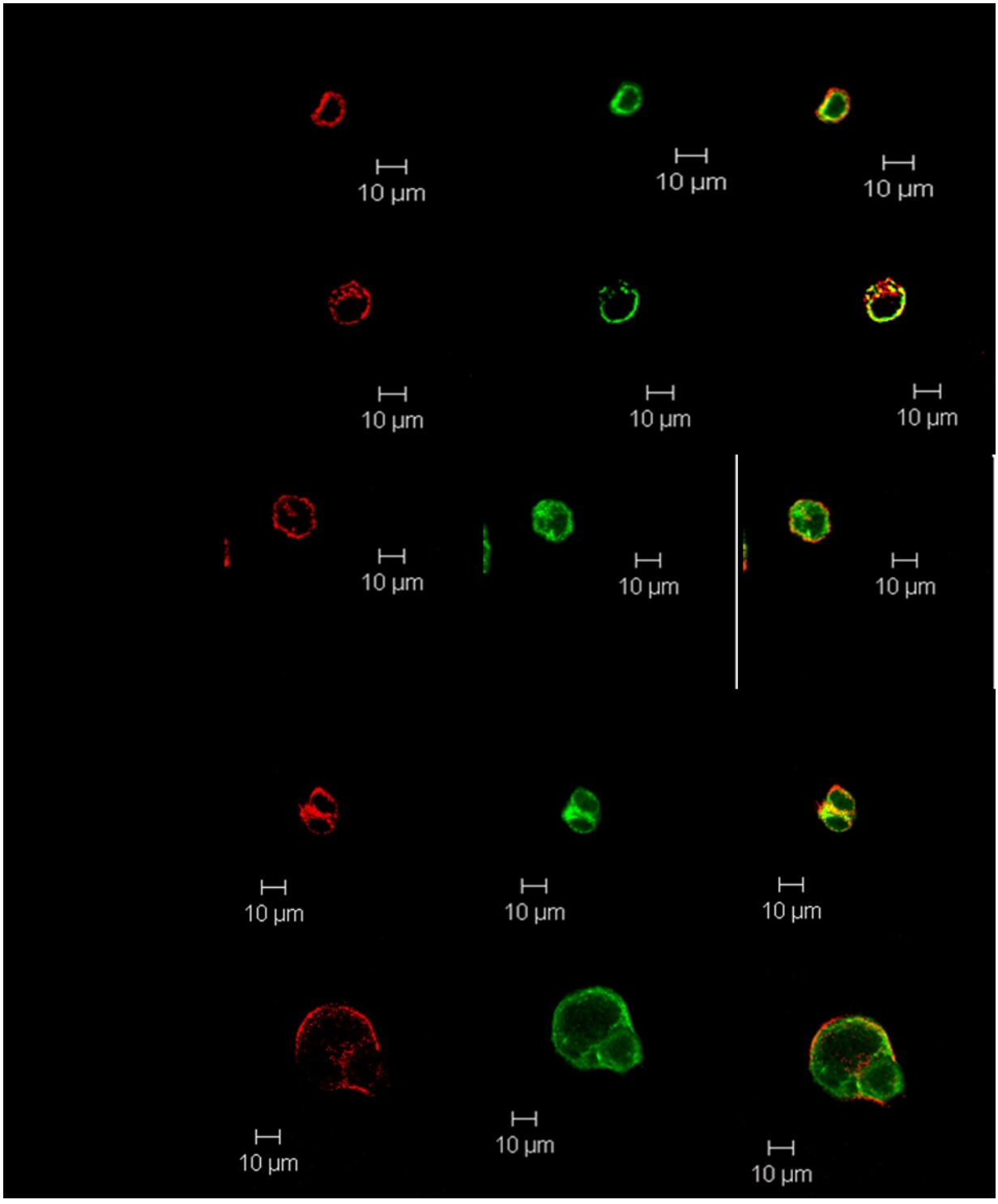
10 µm
10 µm
10 µm
10 µm
10 µm
10 µm
10 µm
10 µm
10 µm
10 µm
10 µm
10 µm
10 µm
10 µm
10 µm

VIII. The Increase in CFTR-NHERF1 Interaction is Mediated by PKC Activation

To test whether PKC activation can increase NHERF1-CFTR interaction, a disuccinimidyl suberate (DSS) cross-linker was used. Calu-3 cells were treated with 4 mM DSS alone or with 20 nM PMA for 30 min.

We observed an increase in CFTR density and molecular weight on immunoblots of samples from cells cross-linked and PMA stimulated compared to control cross-linked samples indicating that other proteins interact with CFTR upon PKC stimulation (figure 3.16 A). After CFTR antibody was stripped and the membrane was re-probed for NHERF1, we detected a minimal amount of NHERF1 at the level of CFTR under control cross-linked conditions which indicates a basal level of CFTR-NHERF1 interaction. In PMA stimulated cross-linked samples, the amount of NHERF1 observed at CFTR level was higher compared to control cross-linked sample indicating an increased CFTR-NHERF1 interaction after PKC activation (figure 3.16 B). This experiment suggests that PKC activation increases CFTR-NHERF1 interaction.

Figure 3.16 PKC Activation Increased NHERF1-CFTR Interaction.

A: Representative immunoblots of cross-linked Calu-3 cell lysate. Cells maintained at 37°C were treated with 4 mM DSS under control condition or after 20 nM PMA treatment for 30 min. 20 μg of cell lysate were separated by SDS PAGE (6% resolving gel) and detected by the monoclonal anti-CFTR antibody M3A7 followed by peroxidase conjugated secondary antibody and visualized by chemiluminescence. **B**: Blotting membranes were stripped and re-probed for NHERF1. Expected sizes (kDa) for NHERF1:50, CFTR: 180; N=3 experiments.

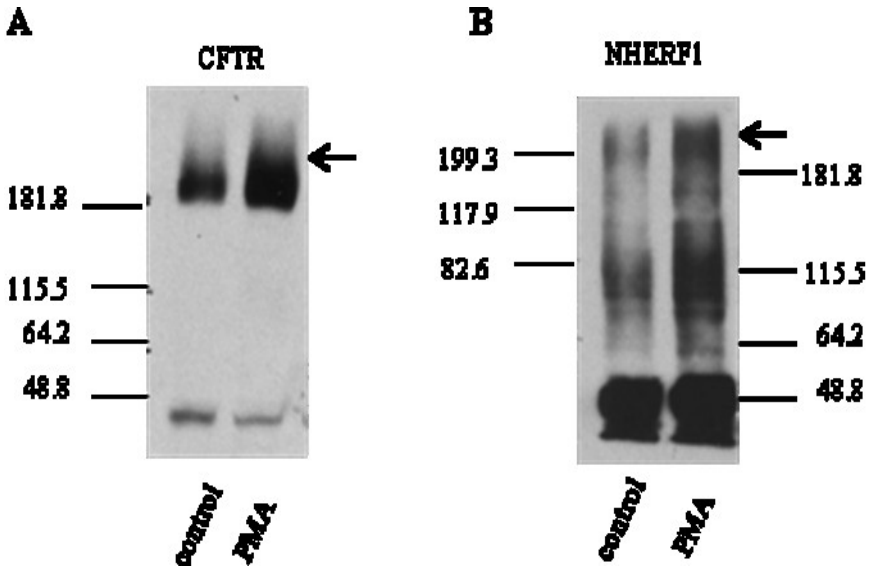

IX. VIP Stimulation has No Effect on CAL Cellular Localization

We next examined the effect of VIP stimulation on CFTR-CAL interaction. CAL is an adaptor protein known as a competitor of NHERF1 for CFTR interaction (Cushing *et al*., 2008). It is mainly localized to the Golgi network and its associated vesicles. We used RT-PCR to detect CAL mRNA using primers designed against the human CAL as described in the method section. Our results show that CAL mRNA is present in Calu-3 lysates (figure 3.17 A). Using immunoblotting experiments we determined the amount of endogenous CAL protein expression in Calu-3 cells (figure 3.17 B and figure 2.3 in the method section).

We next examined CAL cellular localization using immuno-labeling and confocal microscopy. As expected, we found that CAL is localized around the nucleus. We found that VIP stimulation (300 nM) for 1 h had no noticeable effect on CAL cellular localization (figure 3.18 A and B). Negative control where the primary anti-CAL antibody was omitted from the immuno-labeling experiment is shown in figure (3.18 C).

Figure 3.17 CAL mRNA and Protein Expression in Calu-3 Cells.

A: CAL mRNA was detected by RT-PCR after RNA extraction from Calu-3 cells. PCR products were subjected to 1.5% agarose gel electrophoresis for analysis. Lane 1: DNA ladder Ø, Lane 2: PKCα (positive control), Lane 3: CAL. Lane 4: negative control where primers are omitted from the RT-PCR reaction. Specific primers of human CAL were used, see materials and methods. Expected sizes (bp) of amplified products are indicated under the figure. **B**: Representative immunoblot showing endogenous CAL expression in CAlu-3 cells. Expected sizes for CAL (kDa) 60/35).

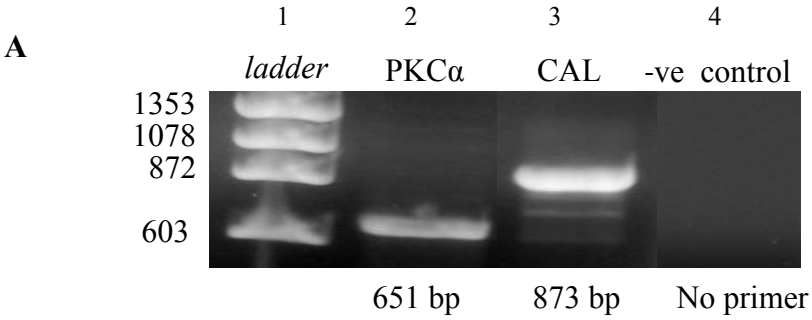

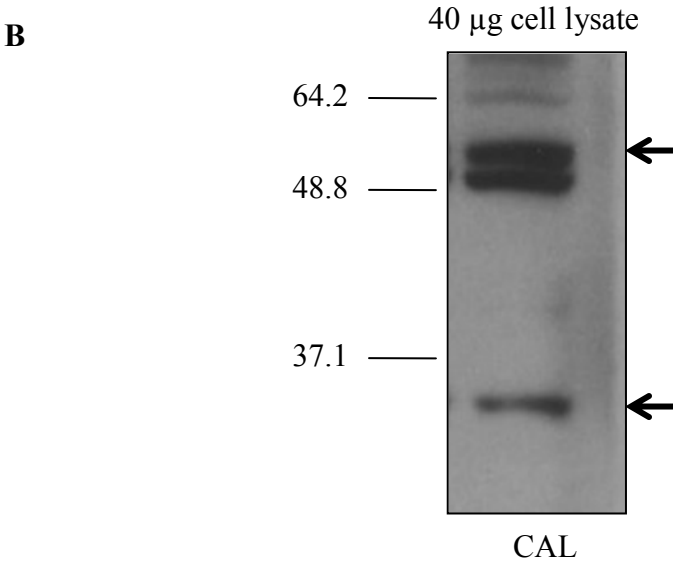

Figure 3.18 Immuno-localization and Confocal Microscopy Pictures of CAL in Calu-3 Cells. Calu-3 cells maintained at 37°C were labeled with anti-CAL antibodies followed by secondary antibody conjugated to Dylight 650 (blue signal). Images were visualized using the LSM 650 confocal microscope. **A**: Control untreated cells, **B**: Cells treated for 1 h with 300 nM of VIP before immuno-labeling. **C**: Negative control where the CAL antibody was omitted.

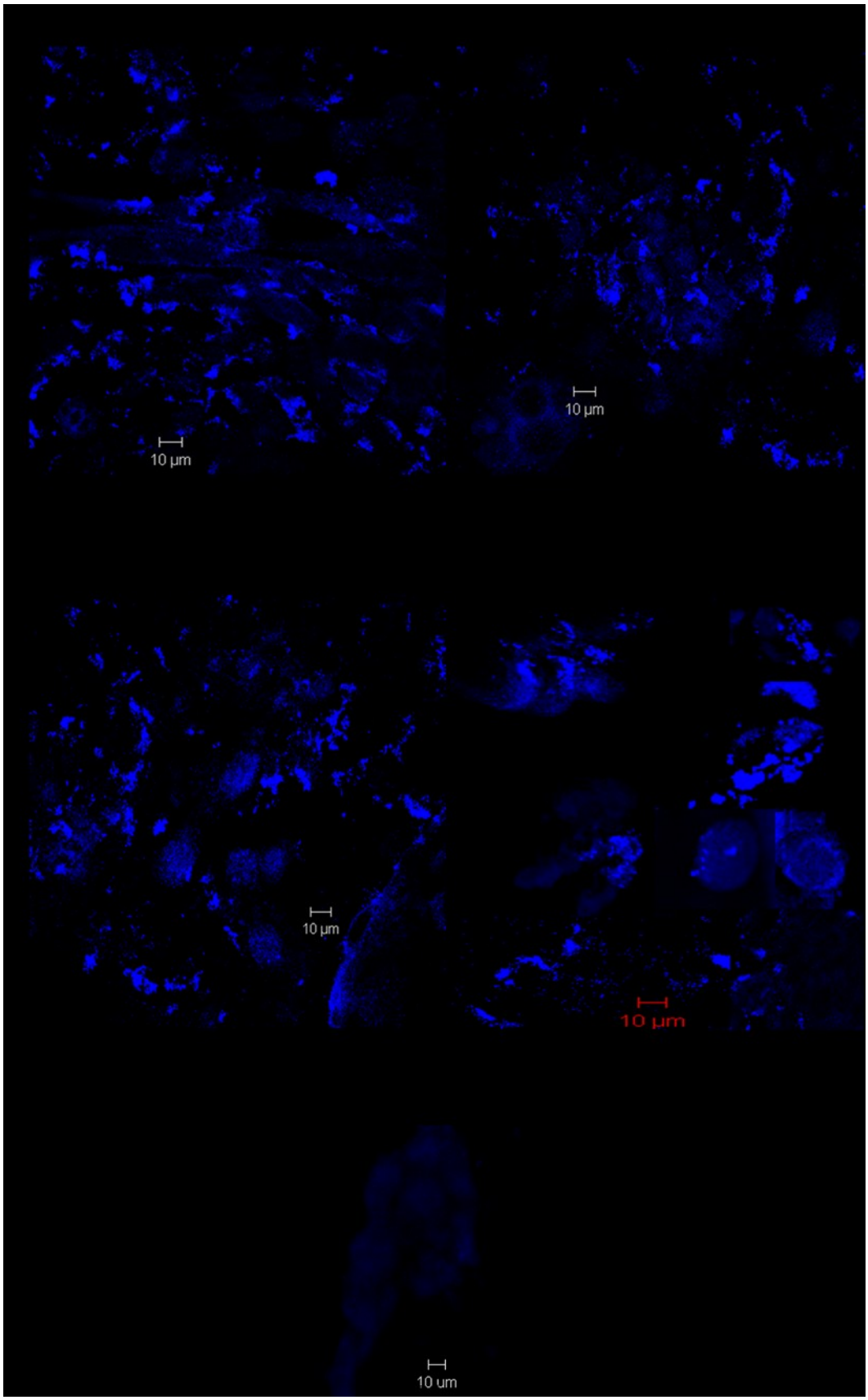
10 µm
10 µm
10 µm
10 µm
10 um

X. VIP Stimulation Decreases CAL-CFTR Co-localization

Taking into account the VIP-dependent modification of CFTR cellular localization from the cytoplasm to the plasma membrane, and the VIP-dependent increase in CFTR-NHER1 interaction at the membrane, we tested the possibility of a disruption of CFTR interaction with CAL after VIP stimulation. We labeled Calu-3 cells for both CFTR and CAL using the anti-CFTR antibody M3A7 and a polyclonal anti-CAL antibody, and we examined their cellular localization using confocal microscopy. As expected, we were able to detect the co-localization between CFTR and CAL around the nucleus in control unstimulated cells (figure 3.19 A). Interestingly, 1 h VIP treatment (300 nM) of Calu-3 cells induced a significant reduction in CFTR-CAL co-localization signal in the cytoplasm (figure 3.19 B) compared to unstimulated cells (figure 3.19 A). This is consistent with the ability of VIP to increase CFTR membrane density by redistribution from the cytoplasm to the membrane (Ameen *et al*., 1999; Chappe *et al*., 2008; Qu *et al*., 2011).

Transfecting the cells with NHERF1-siRNA did not change the co-localization between CFTR and CAL in the cytoplasm (figure 3.19 C). However, the reduction in cytoplasmic CFTR-CAL co-localization induced by VIP in control cells was lost in cells transfected with NHERF1-siRNA (figure 3.19 D) consistent with the balanced competition model between NHERF1 and CAL for CFTR interaction.

Figure 3.19 VIP Stimulation Decreased CFTR-CAL Co-localization in the Cytoplasm, the Effect that was Lost in NHERF1-siRNA Transfected Cells.

Immuno-localization and confocal microscopy pictures of CFTR and CAL in Calu-3 cells. Calu-3 cells maintained at 37°C were transfected with NHERF1-siRNA or with Scrambled-siRNA. 48 h after transfection, the cells were labeled with anti-CFTR antibody M3A7 (1:1,000) followed by a secondary antibody conjugated to CY3 (1-100) (red signal) and with anti-CAL antibody (1-600) followed by a secondary antibody conjugated to Dylight (1:200) (green signal) **A**: Control cells transfected with scrambled-siRNA. **B**: Cells transfected with scrambled-siRNA and treated with 300 nM VIP for 60 min before immuno-labeling. **C**: Control cells transfected with NHERF1-siRNA **D**: Cells transfected with NHERF1-siRNA treated with 300 nM VIP for 60 min before immuno-labeling. Images were visualized using the LSM 650 confocal microscope. N = 3 experiments.

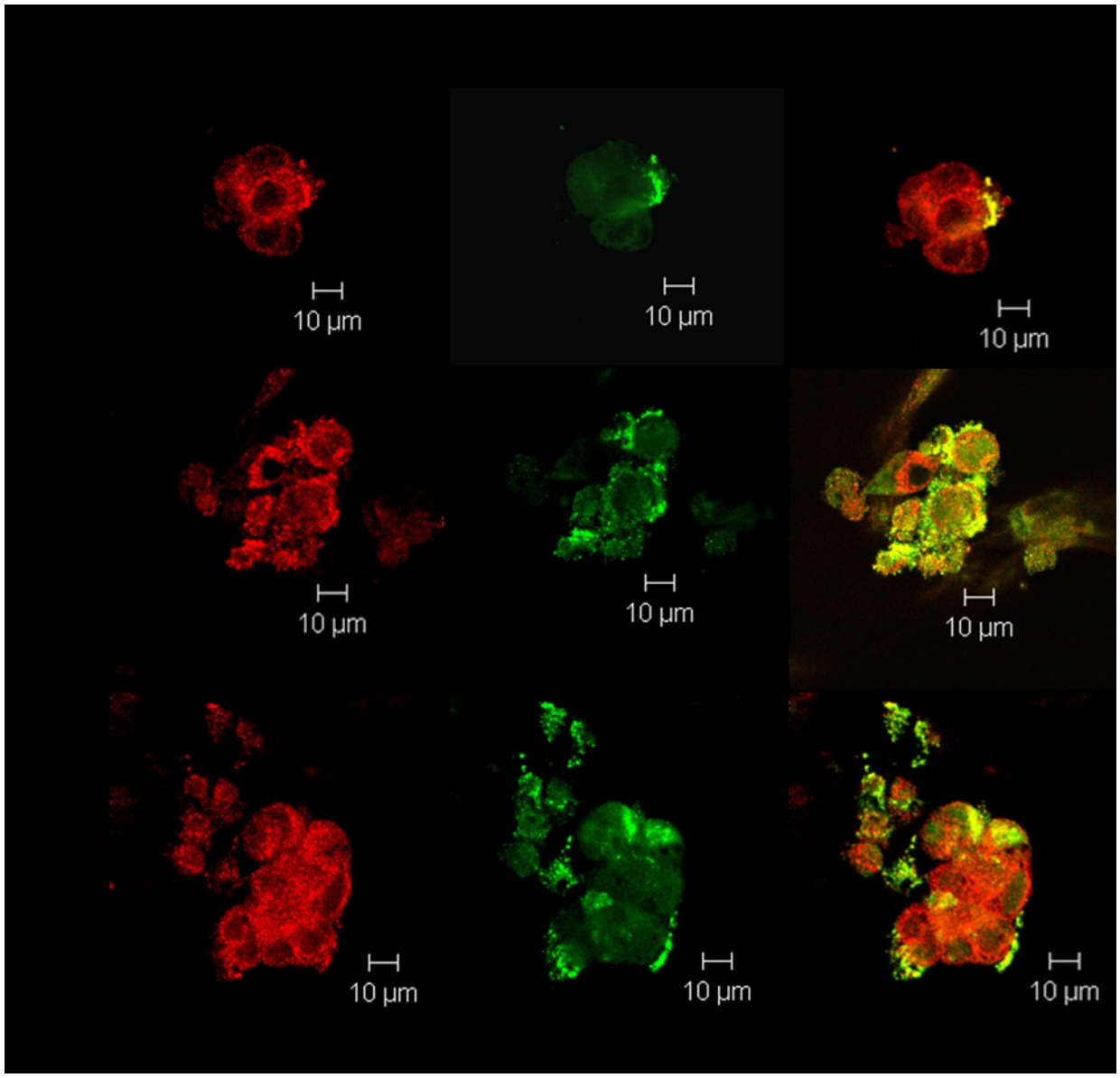
10 µm
10 µm
10 µm
10 µm
10 µm
10 µm
10 µm
10 µm
10 µm

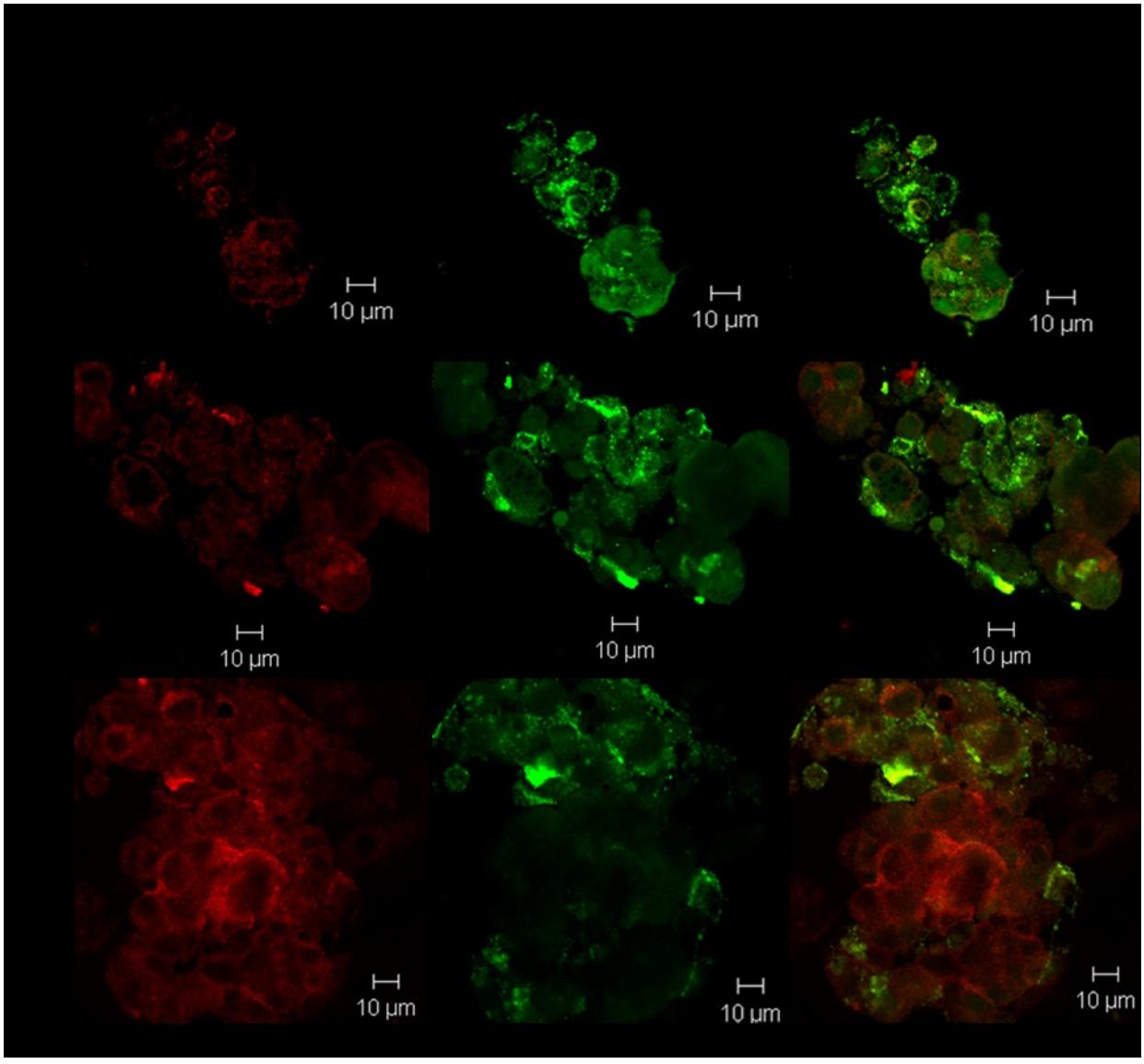
10 µm
10 µm
10 µm
10 µm
10 µm
10 µm
10 µm
10 µm
10 µm

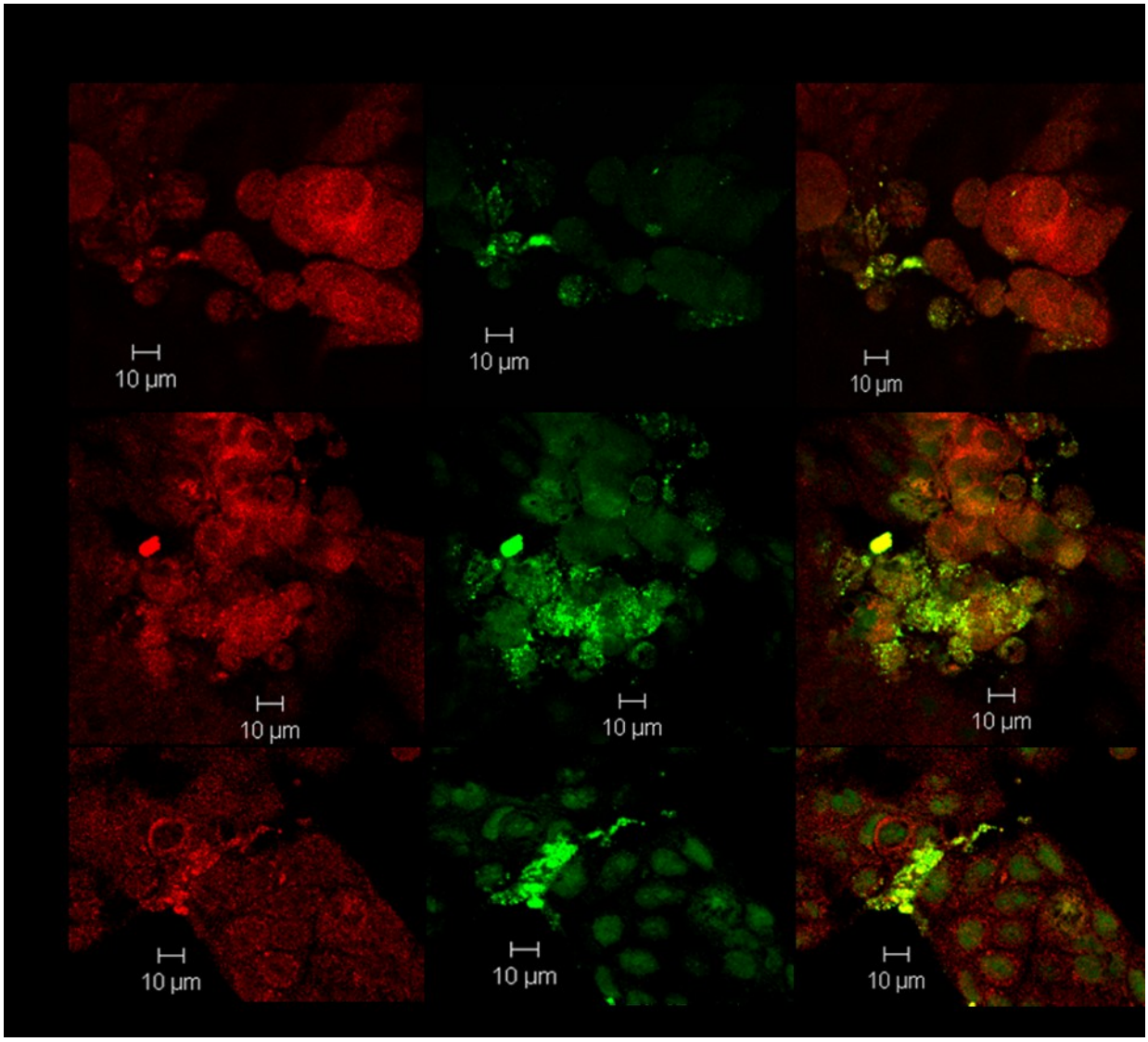
10 µm
10 µm
10 µm
10 µm
10 µm
10 µm
10 µm
10 µm
10 µm

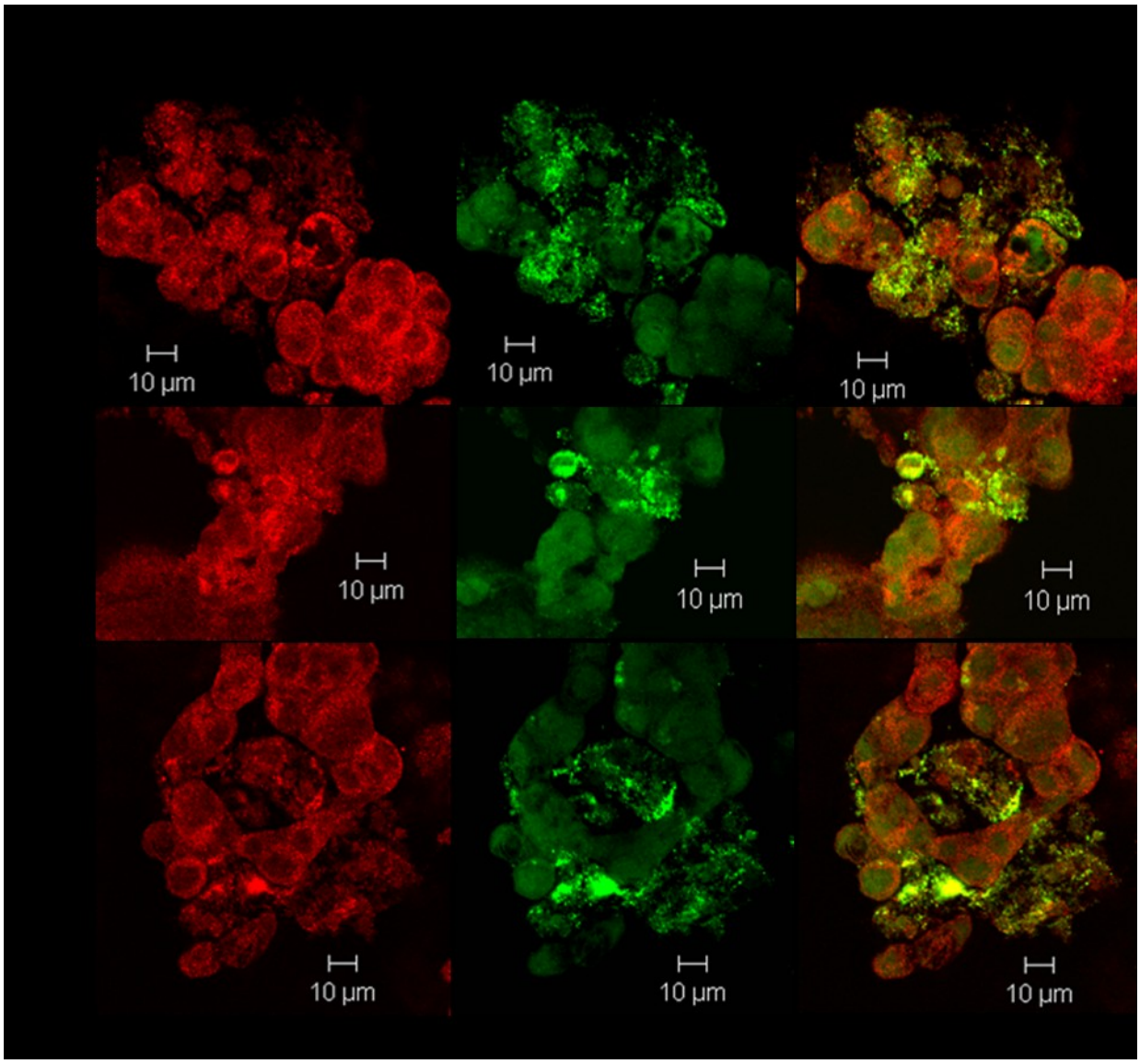
10 µm
10 µm
10 µm
10 µm
10 µm
10 µm
10 µm
10 µm
10 µm

XI. VIP Increased CFTR-NHERF1-P-ERMs Interaction While Decreasing CFTR-CAL Interaction.

Immunopreciptation assays to measure the interaction between CFTR and NHERF1 or CAL after VIP stimulation showed some inconsistencies and low success rate. We could observe less CAL pulled-down with CFTR after VIP stimulation, however, our results showed no significant difference between the amount of NHERF1 immunopreciptated with CFTR after VIP stimulation compared to control unstimulated samples (figure 3.20).

We then used the *in situ* proximity ligation assay, to detect changes in NHERF1-P-ERMs interaction as well as CAL interaction with CFTR after VIP stimulation. With this assay we were able to detect the direct endogenous interaction between CFTR and CAL (figure 3.22 A) and between CFTR and NHERF1 (figure 3.21 A). Importantly, and consistent with our previous immuno-labeling results, we were able to see a strong increase in CFTR-NHERF1 interaction upon VIP stimulation (figure 3.21 B). Moreover, significant decrease in CFTR-CAL interaction was observed after VIP stimulation (figure 3.22 B). Additionally, in control untreated cells, the interaction between either NHERF1 (figure 3.23 A) or CFTR (figure 3.24 A) with P-ERMs was very minimal to absent, as represented by only a few red dots to no dots. Interestingly, the red dots fluorescence signal increased significantly after VIP stimulation in both cases, indicating an increase in NHERF1 / P-ERMs (figure 3.23 B) and CFTR / P-ERMs (figure 3.24 B) interaction following VIP stimulation. Negative controls were done by either omitting the primary antibodies (figure 25 A) or by selecting non interacting proteins such as CAL and NHERF1 (figure 25 B).

Figure 3.20 VIP Stimulation Reduces CAL-CFTR Interaction.

Representative immunoblots of co-immunopreciptated CFTR with NHERF1 and CAL. Calu-3 cells maintained at 37°C were treated with 300 nM VIP for 30 min. The immunopreciptate was separated by SDS-PAGE and detected by monoclonal anti-CFTR antibodies followed by a peroxidase conjugated secondary antibody and revealed by chemiluminescence. Blotting membranes were stripped and re-probed for NHERF1 and CAL. Expected sizes (kDa) for NHERF1:50, CFTR: 180; CAL: 60/35. N=3 independent experiments.

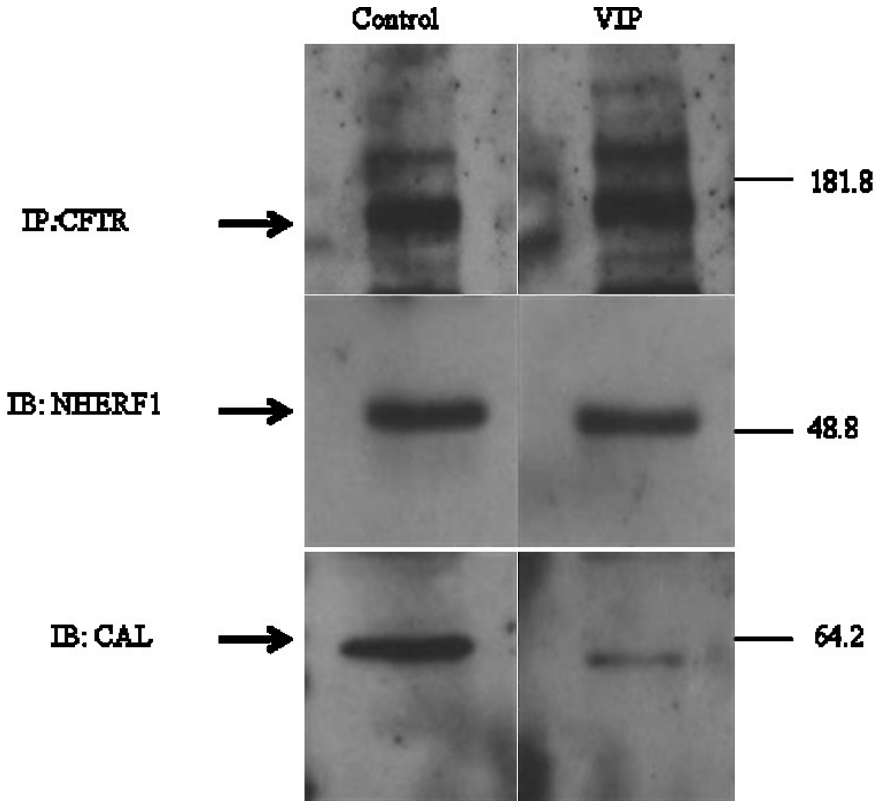

Figure 3.21 *In situ* proximity Ligation Assay Results Showing VIP Ability to Increase CFTR-NHERF1 Interaction. Calu-3 cells maintained at 37°C were treated or not with 300 nM VIP for 1 h before fixation, permeabilization and incubation with Mouse anti-CFTR and Rabbit anti-NHERF1 antibodies overnight at 4°C. The cells were then incubated with the secondary antibodies conjugated to Plus and Minus PLA probes for 60 min at 37°C. The two PLA probes were allowed to bind for 30 min at 37°C with ligase. The ligated PLA probes were amplified and fluorescently labeled. The signal was recorded using Zeiss Axiovert 200 fluorescence microscope. Each red dot represents an interacting CFTR and NHERF1. **A**: Control cells, **B**: Cells treated with VIP (300 nM, 1 h) before the assay.

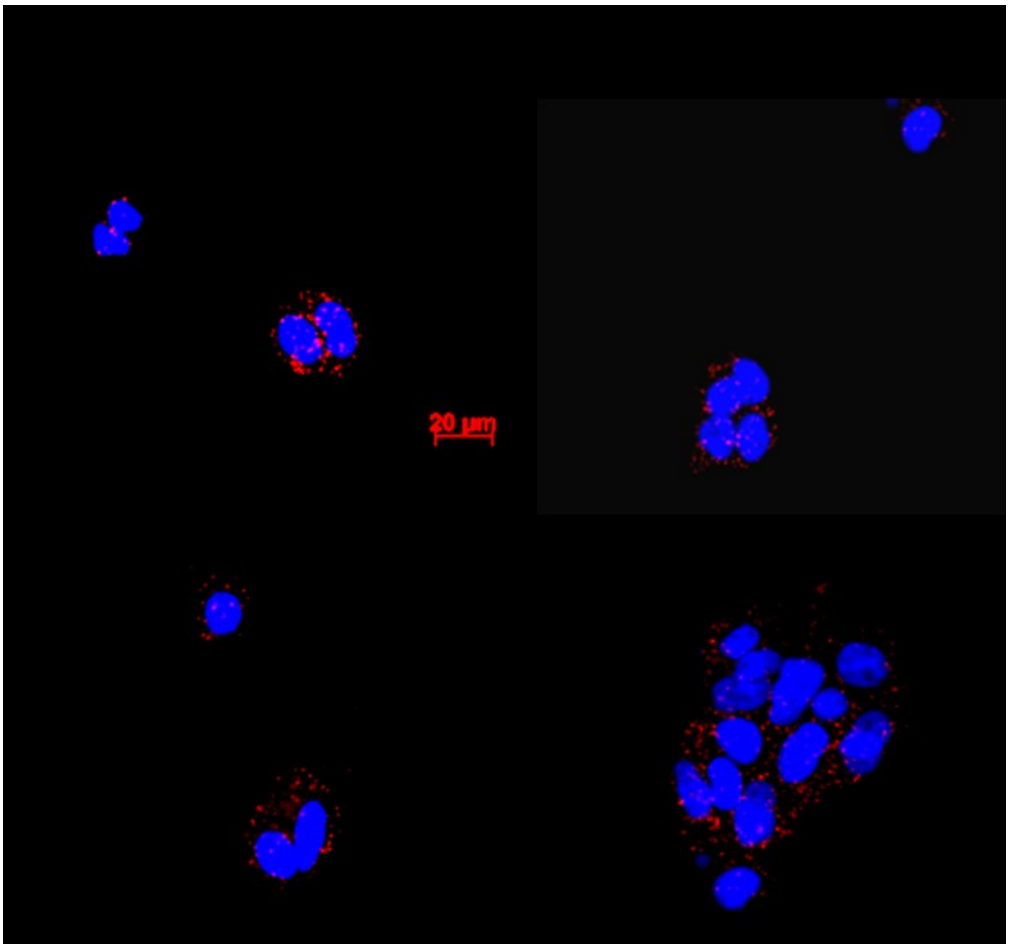
20 µm

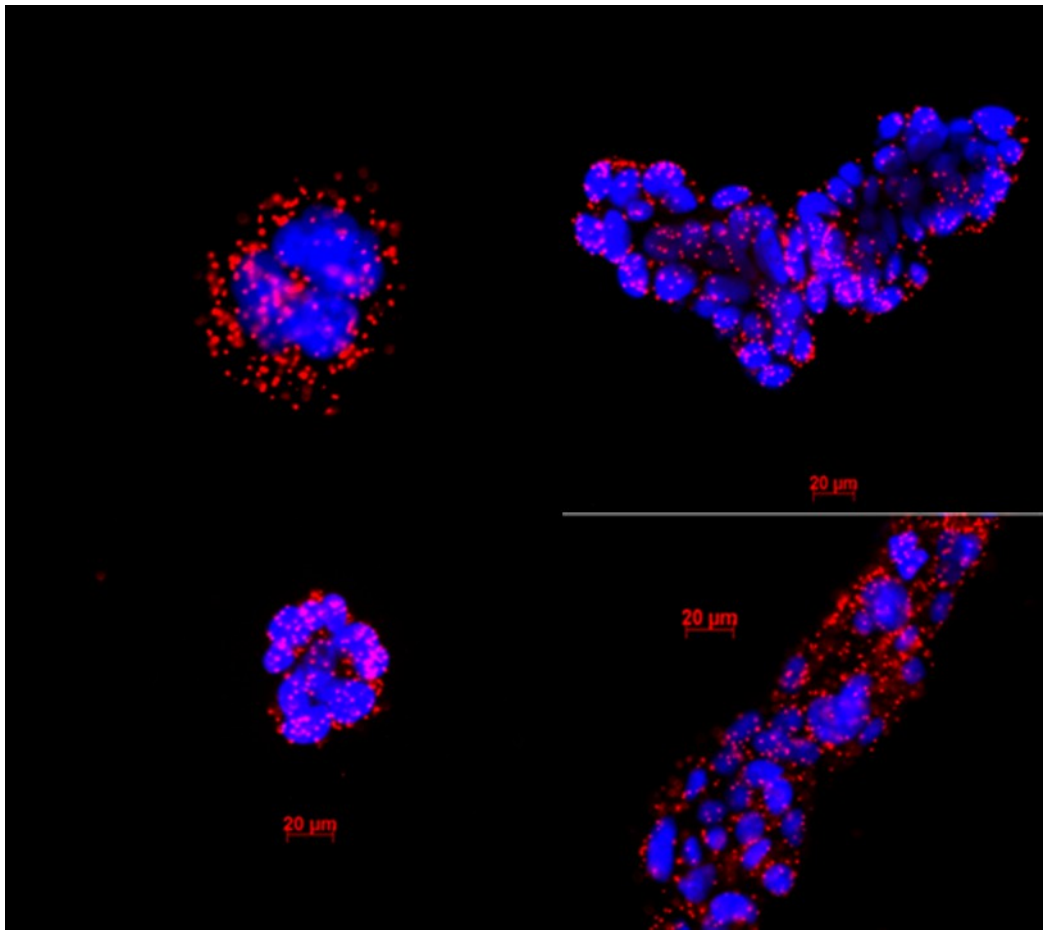
20 µm
20 µm
20 µm

Figure 3.22 *In Situ* proximity ligation Assay Showing VIP Effect on CFTR-CAL Interaction. Calu-3 cells maintained at 37°C were treated or not with 300 nM VIP for 1 h before fixation, permeabilization and incubation with Mouse anti-CFTR and Rabbit anti-CAL antibodies over night at 4°C. The cells were then incubated with the secondary antibodies conjugated to Plus and Minus PLA probes for 60 min at 37°C. The two PLA probes were allowed to bind, amplified and fluorescently labeled. The signal was recorded using Zeiss Axiovert 200 fluorescence microscope. Each red dot represents an interacting CFTR and CAL. **A**: Control cells, **B**: Cells recieved VIP stimulation (300 nM, 1 h) before the assay.

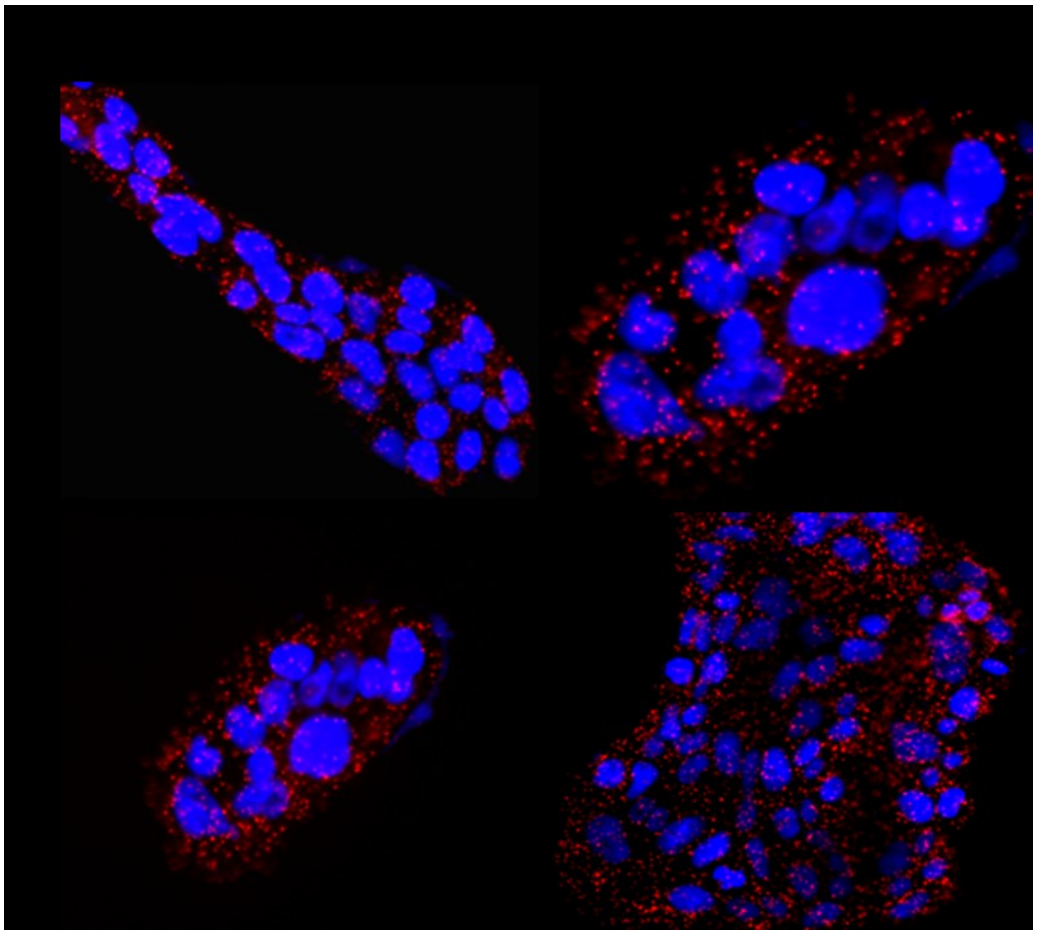

B

VIP treated cells
CAL-CFTR *in situ* interaction

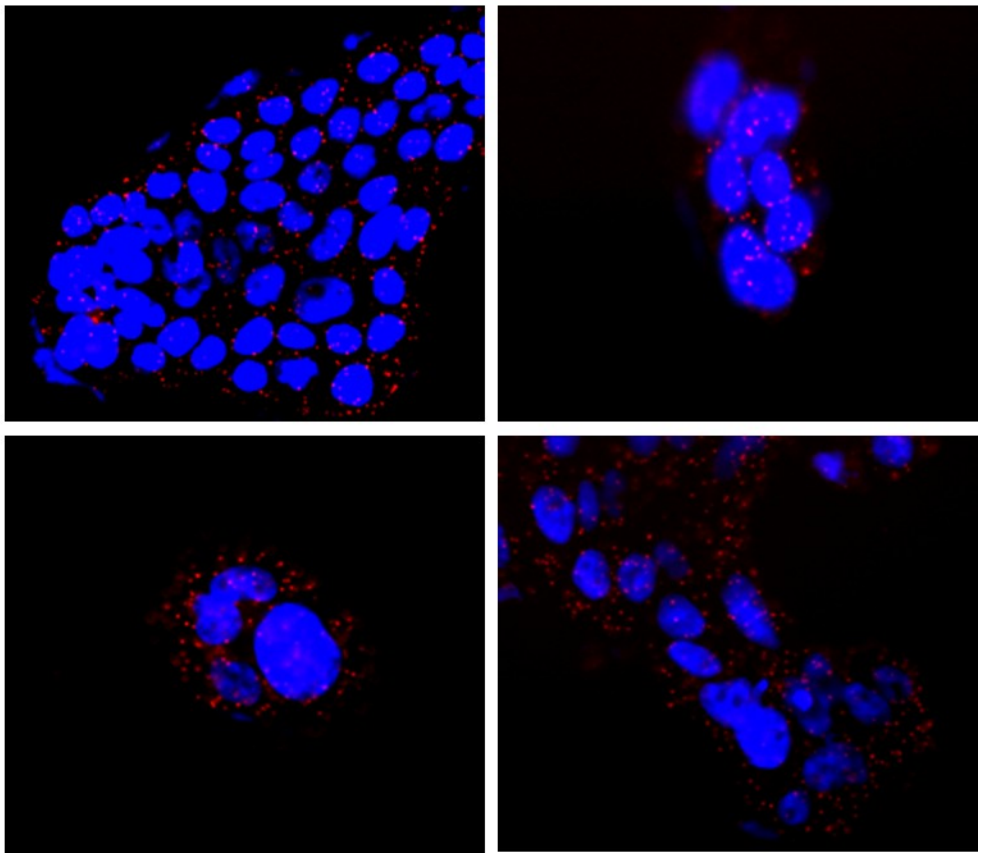

Figure 3.23 *In Situ* Proximity Ligation Assay Showing VIP Effect on NHERF1 / P-ERMs Interaction. Calu-3 cells maintained at 37°C were treated or not with 300 nM VIP for 1 h before fixation, permeabilization and incubation with Mouse anti-NHERF1 and Rabbit anti-P-ERM antibodies overnight at 4°C. The cells were then incubated with the secondary antibodies conjugated to Plus and Minus PLA probes for 60 min at 37°C. The two PLA probes were allowed to bind, then amplified and fluorescently labeled. Signals were recorded using Zeiss Axiovert 200 fluorescence microscope. Each red dot represents an interacting NHERF1 and P-ERMs. **A**: Control cells, **B**: Cells received VIP stimulation (300 nM, 1 h) before the assay.

A

Control

P-ERM / NHERF1 *in situ* interaction

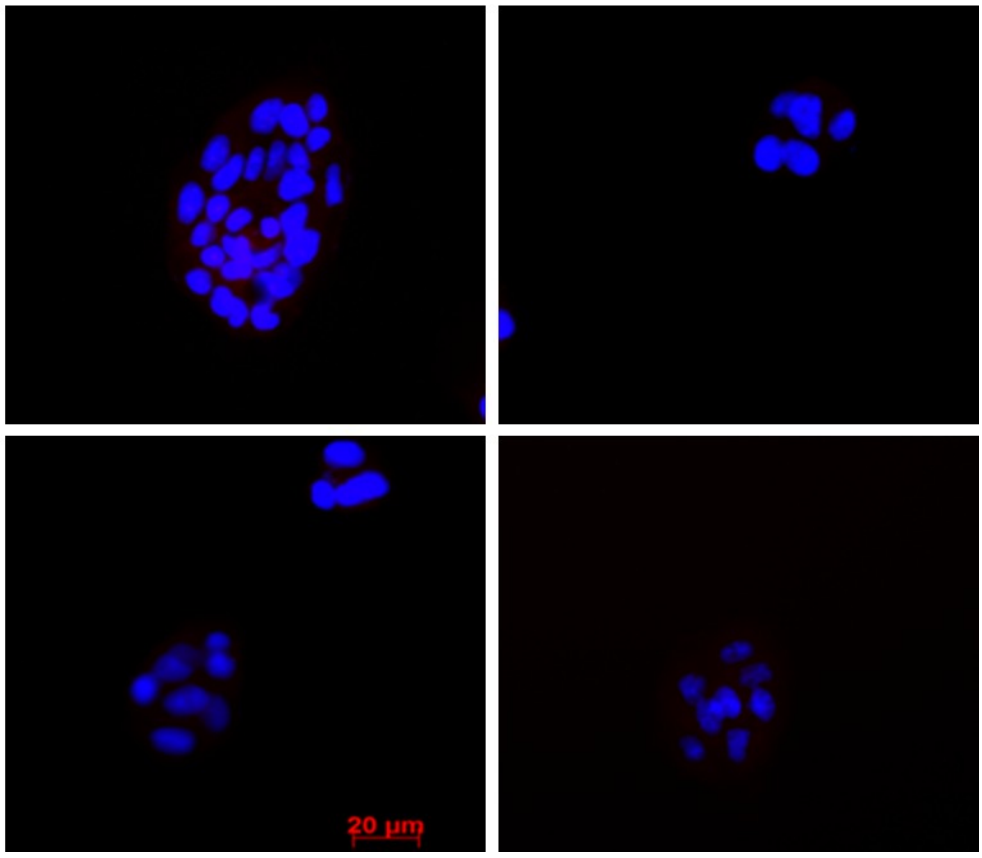

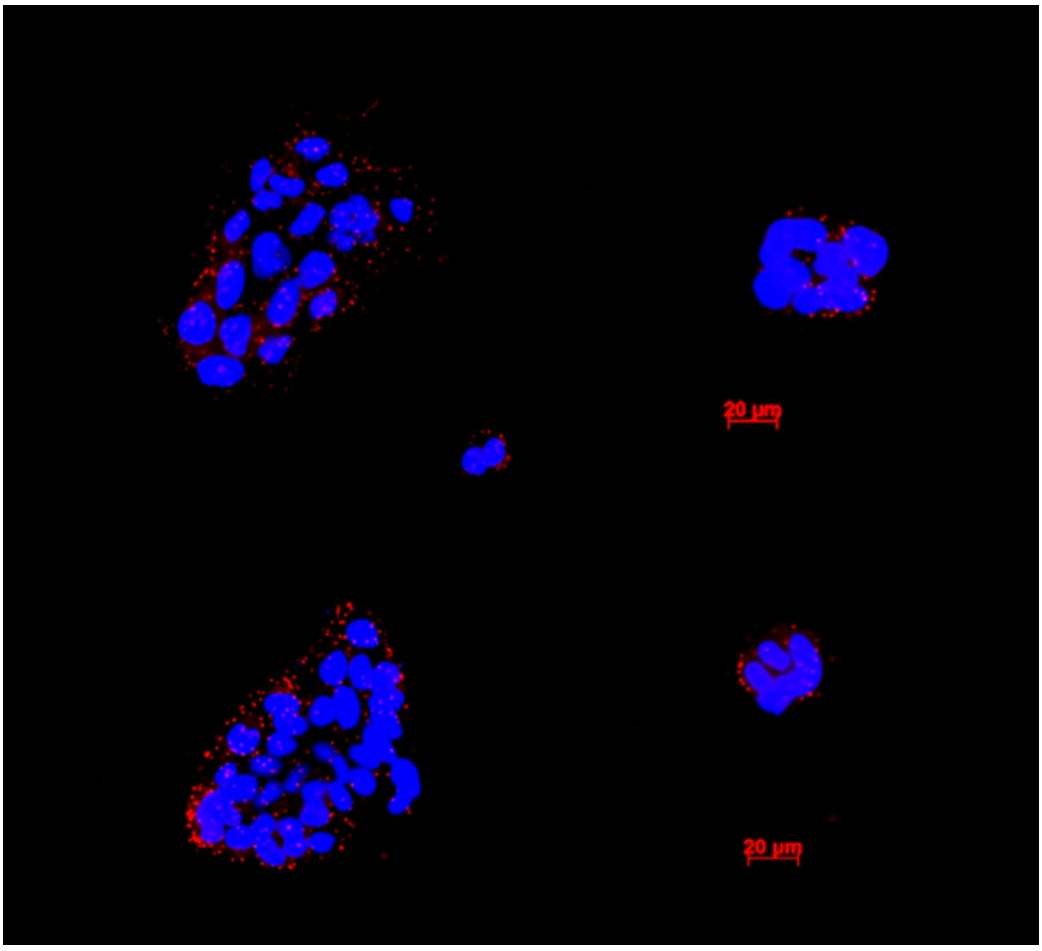
20 µm
20 µm

Figure 3.24 *In Situ* Proximity Ligation Assay Showing VIP Effect on CFTR / P-ERMs Interaction. Calu-3 maintained at 37°C were treated or not with 300nM VIP for 1 h before fixation, permeabilization and incubation with Mouse anti-CFTR and Rabbit anti-P-ERM antibodies overnight at 4°C. The cells were then incubated with the secondary antibodies conjugated to Plus and Minus PLA probes for 60 min at 37°C. The two PLA probes were allowed to bind, then amplified and fluorescently labeled. The signals were recorded using the Zeiss Axiovert 200 fluorescence microscope. Each red dot represents an interacting CFTR and P-ERM. **A**: Control, **B**: Cells received VIP stimulation (1 h, 300 nM) before the assay.

A

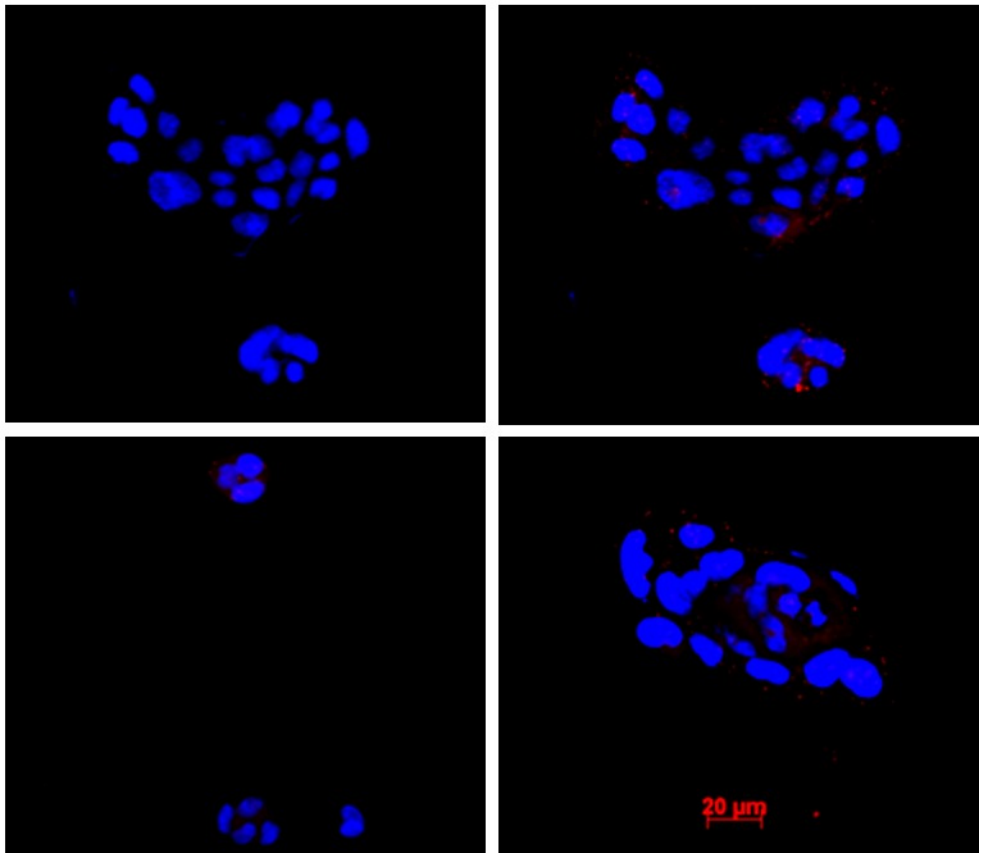

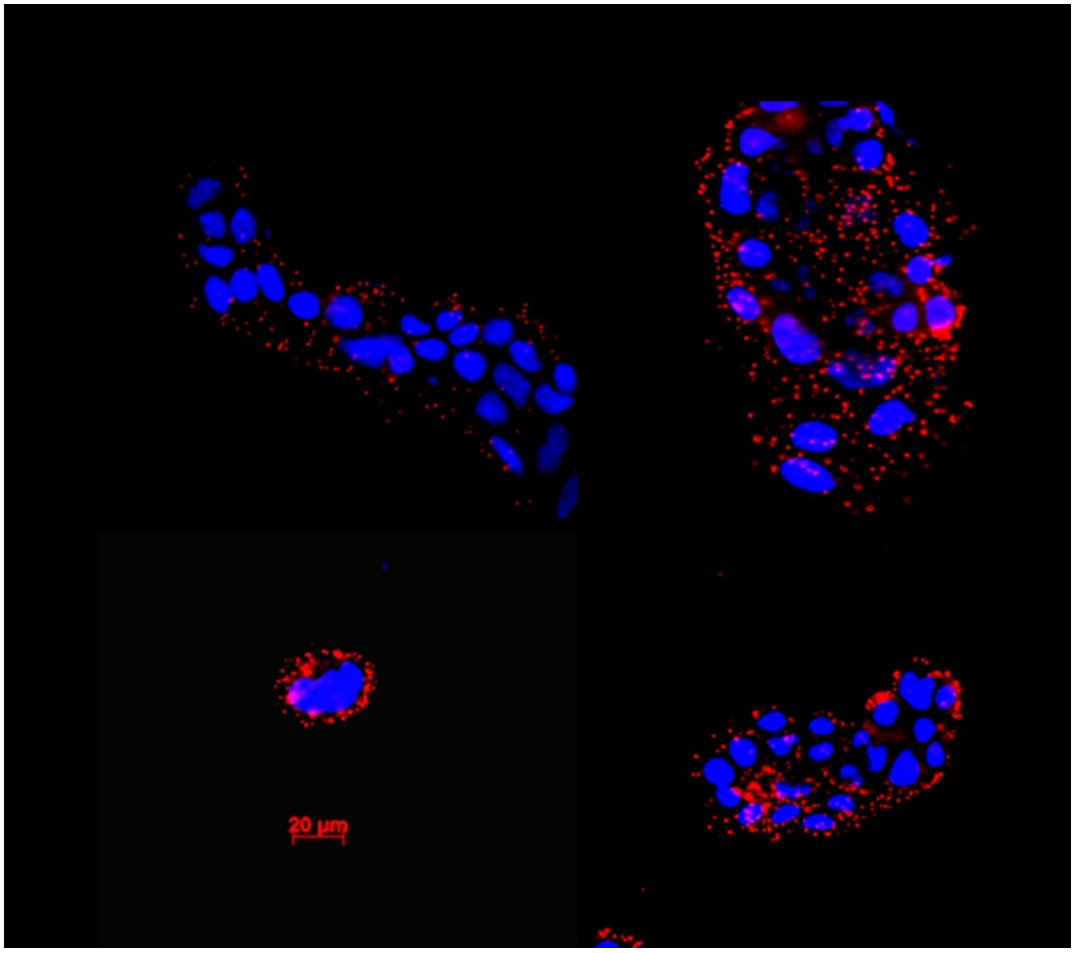
20 µm

Figure 3.25 *In Situ* Proximity Ligation Assay Negative Controls.

Calu-3 maintained at 37°C were fixed, permeabilized and incubated with antibody buffer with no primary antibodies as in (**A**) or with Rabbit anti-CAL and Mouse anti-NHERF1 antibodies as in (**B**) overnight at 4°C. The cells were then incubated with the secondary antibodies conjugated to Plus and minus PLA probes for 60 min at 37°C. The two PLA probes were allowed to bind, then amplified and fluorescently labeled as before. The signals were recorded using the Zeiss Axiovert 200 fluorescence microscope.

Negative control

A No primary antibodies

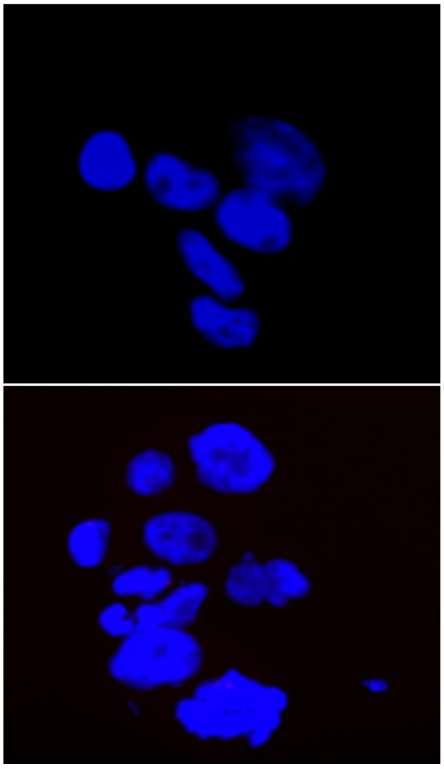

B NHERF1-CAL *in situ* interaction

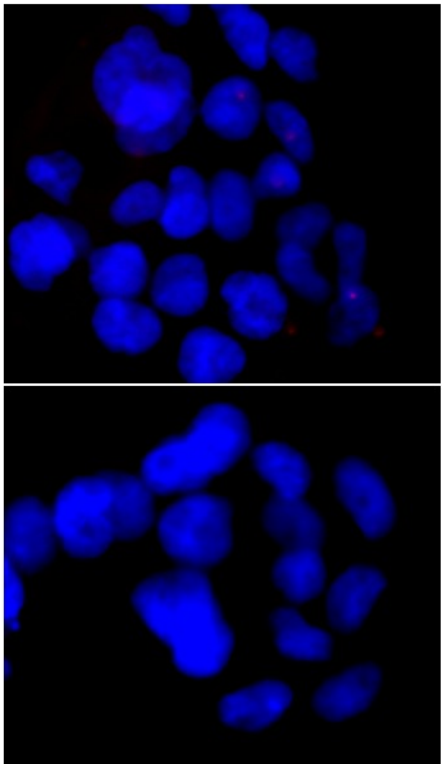

Chapter 4: Discussion

I. CFTR Regulation by Agonist-Induced PKA and PKC Signaling Cascades

The ability of VIP to stimulate fluid secretion, which is needed for the airway defense mechanism, is related to its direct regulation of CFTR trafficking and function (Wine, 2007). Deficiency in VIP release from sparse VIP innervations of CF tissues (Heinz-Erian *et al*., 1985; Savage *et al*., 1990) strongly suggests an important role of VIP deficiency in CF patho-physiology. In the human airways, after binding to VPAC1 receptors on the basolateral membrane of serous cells, VIP activates Gαs-PKA and/or Gαq / i-PKC signaling pathways (Chappe & Said, 2012). Activation of PKA was shown to activate CFTR function through direct channel phosphorylation, and in some cell lines by promoting CFTR recycling to the membrane (N. A. Ameen *et al*., 2003). Activation of PKC alone through Gαq/i plays little role in CFTR-dependent chloride secretion, but is required for potent PKA-dependent activation of the channel (Dechecchi *et al*., 1992; Bajnath *et al*., 1993; Jia *et al*., 1997; Liedtke & Cole, 1998; Chappe *et al*., 2004; Seavilleklein *et al.*, 2008). Not only activated PKC increases CFTR responsiveness to PKA activation but also it seems to play an important role in the regulation of CFTR membrane density (Chappe *et al*., 2008; Alcolado *et al*., 2011; Chappe & Said, 2012). The role of VIP and PKC in regulating CFTR surface density is attributed to the increase in CFTR stability at the cell membrane by preventing its premature endocytosis (Chappe *et al*., 2008). We postulate that the VIP-dependent accumulation of CFTR at the membrane of airway epithelial cells results from the potentiation of CFTR exocytosis to the membrane from the submembranous endosomal pool (Ameen *et al*., 1999; Ameen *et al*., 2003) and by a PKC-dependent reduction in CFTR endocytosis rate (Chappe *et al*., 2008; Alshafie *et al*., 2013).

The agonist-dependent up-regulation of surface expression of membrane transporters was long thought to be dependent on recruitment from a vesicular storage pool to the plasma membrane (exocytosis or membrane insertion) while the role of regulated endocytosis was underestimated. The importance of regulated endocytosis in the membrane accumulation of membrane transporters was discovered by simple

observation when blocking endocytosis in cultured cells resulted in membrane accumulation of apical membrane proteins such as CFTR (Lukacs *et al*., 1997), water channels (Sun *et al*., 2002, Brown *et al*., 2012), glucose transporter (Leto & Saltiel, 2012), in the absence of any hormonal stimulus. Additionally, the role of endocytosis inhibition in agonist-dependent surface accumulation of membrane proteins has been also described. For example, the role of endocytosis reduction (surface stability) in membrane accumulation of aquaporin 2 water channel (AQP2) in response to vasopressin stimulation was described by Brown D. and others (Brown *et al*., 2012). The discovery of the involvement of the endocytosis pathway in agonist-dependent increase in membrane protein density might open new therapeutic windows for treating diseases where reduction in membrane protein localization is the underlying cause.

In the present study, we chose Calu-3 cells, the most widely used cell model for airway submucosal serous cells, because they endogenously express VPAC1 receptors for VIP on their basolateral membrane and CFTR on their apical membrane (figure 1.6). Also, previous studies from the Chappe lab demonstrated VIP-dependent increase in membrane CFTR stability in these cells. In agreement with previous publications, we confirmed the VIP positive effect on CFTR membrane density and showed that it depends on PKCε (figure 3.1). Contradictory to our results, Ameen N. *et al*., reported that the increase in CFTR membrane density after VIP stimulation was dependent on PKA activation in CFTR high expressor duodenal cells (Ameen *et al*., 1999). Even though their study did not delineate the mechanism involved (exocytosis vs endocytosis) and did not examine the possible role of PKC in their cell model, we propose that VIP-dependent regulation of CFTR trafficking is cell-type specific. Conflicting reports on whether PKC and/or PKA activation modulate CFTR trafficking support the differential regulation mechanism based on the cell model. No clear agreement was reached among the various studies describing the regulation of CFTR recycling by PKA or PKC signaling cascades, in support to our conclusion. Activation of the PKA signaling pathway was mostly shown to increase CFTR membrane density in heterogeneous systems and in intestinal cell systems (Bradbury, 1999). Elevation of cAMP by forskolin to activate PKA in human colonic carcinoma cells (T84) was shown to inhibit the rate of CFTR internalization from

the membrane (Bradbury *et al*., 1992). Increased CFTR membrane density through increased CFTR insertion to the membrane was also reported to depend on PKA activation in intestinal epithelium (Ameen *et al*., 2003; Collaco *et al*., 2013). Both PKA and PKC activation were described to inhibit CFTR endocytosis in Chinese Hamster Ovary (CHO) cells (Lukacs *et al*., 1997). Another study also reported the ability of PKA activation to inhibit tagged-CFTR surface endocytosis resulting in an increase in CFTR plasma membrane density in Hela cells (Howard *et al*., 1996). However, the involvement of cAMP activated PKA in the regulation of CFTR trafficking was challenged by several other studies. The role of PKA in stimulating CFTR-mediated Cl^- secretion was shown to be limited to the activation of CFTR channels present in the apical plasma membrane and not to modulate its trafficking both in Calu-3 and T84 cell lines. (Prince *et al*., 1993; Loffing *et al*., 1998). Santos G (Santos & Reenstra, 1994) showed that the concentration of forskolin that inhibit CFTR endocytosis did not correlate with the dose needed to activate CFTR function in two cells lines (T84 human colonic cell line, and HTEo-tracheal cell line). They described the ability of PKA to reduce CFTR endocytosis as insignificant to contribute to CFTR function. Additionally, in T84 cells, PKA activation was reported to have no effect on CFTR endocytosis as measured by biotin-avidin based endocytosis assay (Prince *et al*., 1993) which is an opposing report from earlier study in the same cell line (Bradbury *et al*., 1992). On the other side, many studies described the role of PKC activation in the regulation of CFTR membrane insertion and surface stability (Dechecchi *et al*., 1992; Bajnath *et al*., 1993; Dechecchi *et al*., 1993; Bajnath, *et al*., 1995; Winpenny *et al*., 1995; Chappe *et al*., 2008; Alcolado *et al*., 2011). In particular, several studies support the role of PKC in CFTR trafficking regulation in Calu-3 cell line. No major effect of PKA activation on CFTR membrane density was detected in Calu-3 cell, as assayed using both confocal microscopy after immunolabeling and cell surface biotinylation assay (Loffing *et al*., 1998; Chappe *et al* 2008).

Among the 11 known PKC isoforms, the calcium-independent novel isoform epsilon (PKCε) was shown to associate with CFTR to regulate its activity in Calu-3 cells (Liedtke *et al*., 2002). PKCε was also identified as the exclusive isoform involved in relaying the VIP-dependent increase in ΔF508-CFTR membrane density in JME/CF15

cells and in recombinant BHK cells (Rafferty *et al*., 2009; Alcolado *et al*., 2011). Some of the downstream events after PKCε activation were elucidated during the present study.

II VIP Activates ERMs to Link CFTR to the Actin Cytoskeleton

We examined the effect of VIP on ERMs phosphorylation because the role of the actin network and its associated proteins ERMs have been widely recognized to regulate CFTR surface stability (Cantiello, 1996; Prat *et al*., 1999; Bretscher, 1999; Bretscher *et al*., 2000; - , 2000; Bretscher *et al*., 2002; Ganeshan *et al*., 2007). An organized actin cytoskeleton was shown to be required for cAMP-dependent activation of CFTR. Disruption of the actin cytoskeleton with cytochalasin D in the mouse mammary adenomelanoma cells expressing human CFTR completely prevented cAMP activation of CFTR. CFTR function was restored by addition of exogenous actin to the cytosolic side of quiescent excised inside-out patches of CFTR (Prat *et al*., 1995). Similarly disruption of the actin polymerization negatively impacted CFTR function (Ganeshan *et al*., 2007). Modifying the structural arrangement of three dimensional actin networks by applying actin cytoskeleton-modifying agents partially reduced cAMP dependent Cl^- current suggesting that the actin cytoskeleton conformation is important for CFTR function. In agreement with the later observation, Monterisi S. *et al*. showed that actin cytoskeleton organization is necessary for cAMP apical compartmentalization with CFTR (Monterisi *et al*., 2012).

In the present study, we found that stimulation of Calu3 cells with VIP (300 nM), or direct activation of PKC by PMA (20 nM), increased the phosphorylation level of ERM proteins significantly. It has been shown that phosphorylation of ERMs leads to their activation and recruitment from the cytoplasm to the membrane where they link the actin cytoskeleton to membrane proteins (Simons *et al*., 1998; Lopez *et al*., 2010). This linker activity regulates membrane proteins by controlling their surface density and preventing their endocytosis to modulate their function (Bretscher *et al* - , 2000; Bretscher *et al*., 2002; Neisch & Fehon, 2011).

Previous experiments showed that the time-course of VIP-dependent increase in CFTR membrane density was maximum after 30 minutes of stimulation and the effect could be sustained for up to two hours (Chappe *et al*., 2008). We thus hypothesized that if ERMs phosphorylation is part of the VIP signaling cascade, it should follow a similar time course. Interestingly, we found that VIP ability to phosphorylate ERMs followed a time order consistent with its ability to increase CFTR membrane stability. Moreover, VIP effect on CFTR, as well as ERMs phosphorylation, was almost lost in cells pre-treated with the PKCε inhibitor peptide EAVSLKPT, confirming the role of PKCε and ERMs in the VIP signaling cascade.

Phosphorylation of inactive ERMs by PKC on critical threonine residues is a prerequisite mechanism for their activation (Simons *et al*., 1998; Bretscher *et al*., 2002; Larsson, 2006; Hong *et al*., 2011). In the cytoplasm, ERMs exist in a dormant monomeric form by virtue of intra-molecular interactions between the amino- and carboxyl-terminal domains; masking both membrane and cytoskeletal association sites (Gary & Bretscher, 1995; Bretscher *et al*., 1997; Simons *et al*., 1998; Pearson *et al*., 2000). Phosphorylation disrupts the intra-molecular interaction unmasking both the F-actin and membrane protein binding sites.

The interaction between CFTR and P-ERMs was measured using the *in situ* proximity ligation assay. Unlike ordinary co-immunopreciptation experiments, this assay allows direct measurement of endogenous protein-protein interactions in a physiological context. Our results showed minimal to no interaction between CFTR and P-ERM proteins under control condition, which was expected since under control condition ERMs are mainly in the inactive dormant unphosphorylated state. Importantly, after VIP stimulation a significant increase in CFTR-P-ERMs interaction was observed, consistent with our proposed model on the ability of VIP to phosphorylate ERM proteins leading to their activation, recruitment to the membrane and interaction with CFTR.

III VIP Increases CFTR-NHERF1 Interaction at the Membrane of Calu-3 Cells

Because the interaction of CFTR and P-ERMs is thought to be mediated through NHERF1 (Bretscher *et al*., 2000), we next investigated the involvement of NHERF1 in VIP signaling cascade. The role of NHERF1 in regulating CFTR membrane turnover has been studied in details (Short *et al*., 1998; Guerra *et al*., 2005; Kwon *et al*., 2007; Favia *et al*., 2010). In the present study, we found that VIP increased CFTR-NHERF1 co-localization at the membrane of Calu-3 cells in immuno-labeling experiments.

NHERF1 is well known as a positive regulator of CFTR surface stability. Down-regulating NHERF1 reversibly reduces the surface expression of WT-CFTR without altering its total expression level. On the other hand, over-expression of NHERF1 increases the membrane density of both WT-CFTR and ΔF508-CFTR by redistributing CFTR from the cytoplasm to the membrane with subsequent increase in CFTR-dependent chloride secretion (Guerra *et al.,* 2005). NHERF1 down-regulation was also shown to reduce both surface and total expression of ΔF508-CFTR (Kwon *et al.,* 2007). Also, Favia *et al*. identified the correction of F-actin disassembly seen in the CF airway cell line CFBE41o and the formation of the NHERF1-ezrin-actin complex as the mechanism responsible for the ability of NHERF1 to rescue ΔF508-CFTR membrane localization (Favia *et al.,* 2010). Moreover, disrupting CFTR-NHERF1 interaction by either deleting the PDZ-binding motif DTRL on CFTR C-terminal or by expressing an exogenous peptide to compete with CFTR for NHERF1 interaction resulted in enhanced endocytosis by reduced surface stability of wild-type and ΔF508-CFTR as monitored by single particle tracking (SPT) in live cells (Valentine *et al.,* 2012). The ability of NHERF1 to positively regulate membrane proteins other than CFTR such as β2AR and parathyroid hormone receptors was also described (Ritter and Hall, 2009).

It seems that NHERF1 exerts its positive effect on CFTR membrane localization through several mechanisms. Other than bridging CFTR to the actin cytoskeleton to mediate its surface stability, NHERF1 was also shown to tether several activated kinases in close vicinity to CFTR. A series of studies by Liedtke *et al*., showed that the receptor

for the active C kinase (RACK1), which shuttles active PKC to where their action is needed, interacts directly with NHERF1(Liedtke *et al.,* 2002; Liedtke *et al.,* 2004; Liedtke & Wang, 2006). Such interaction allows the compartmentalized localization of PKCε in close proximity to CFTR and other apical membrane proteins for efficient and specific signaling. Silencing endogenous RACK1 with siRNA, drastically reduced CFTR surface expression in Calu-3 cells, in agreement with our finding that inhibiting PKCε decreases CFTR surface expression. In their most recent study, Smith *et al*., (2013) identified another protein, FlnA that interacts with CFTR N-terminal domain, to localize RACK1 and PKCε to CFTR micro domains. Thus RACK1-PKCε can be positioned near both the N- and C- termini of CFTR by either FlnA or NHERF1 interaction respectively, perhaps to phosphorylate different sites on CFTR or other proteins.

Using the immunopreciptation method (IP), we found a similar amount of NHERF1 pulled-down with CFTR under the control condition and after VIP stimulation. Failure to detect an increase in CFTR-NHERF1 interaction after VIP stimulation was most probably due to the transient nature of this interaction. Also, phosphorylation forms weak liable interactions which are technically challenging to identify and can be lost during the lengthy co-immunoprecipitation experimental procedure. Although we applied the amine cross-linker DSS before the IP experiment, we failed to co-immunopreciptate CFTR and NHERF1. Co-immunopreciptations might be efficient in the case of over-expressed proteins but not with endogenous proteins with low expression level; however, we decided to study the interaction of CFTR and other proteins endogenously expressed in Calu-3 cells in order to obtain physiologically relevant data.

To overcome the IP technical challenges, we have implemented the new PLA technology to measure the *in situ* interaction between CFTR and NHERF1 directly in fixed Calu3 cells. The interaction at the molecular level appears as fluorescent dots which allow detection of changes in protein-protein interaction under different conditions. With this method, we were able to detect a significant increase in CFTR-NHERF1 interaction upon VIP stimulation compared to control unstimulated condition.

We also used siRNA transfections to reduce the expression levels of both NHERF1 and ERMs as another way to characterize their role in the VIP signaling cascade. Calu-3 are epithelial cells and as such they are highly resistant to conventional transfection methods. Electroporation has been reported to be an efficient method to transfect DNA vectors in epithelial cells for the expression of recombinant proteins (Deora *et al.,* 2007). Using siRNA electroporation in control experiments with fluorescently labeled scrambled-siRNAs, we observed that 40-50 % of all cells could be effectively transfected with this method. This resulted in ~ 40-50% reduction of the targeted protein expression when measured by immunobloting of total cell lysates. Although this seemed to be a low efficiency, this average value reflected a mixed population of transfected and untransfected cells. To overcome this variability in transfection efficiency, we selected immuno-labeled cells which displayed efficient siRNA transfection as indicated by very low to no fluorescence signal in confocal microscopy images for NHERF1 or P-ERMs. This method provided reliable and significant results. We showed that the absence of NHERF1or ERMs prevented VIP ability to increase CFTR membrane density, confirming the involvement of both proteins in the VIP signaling cascade.

In cross-linking experiments, we observed that activating PKC by PMA increased the association between NHERF1 and CFTR, suggesting that PKC phosphorylation promotes CFTR and NHERF1 interaction. We provided no direct evidence for the mechanism by which PKCε activates NHERF1 to interact with CFTR at the membrane. However, two possible mechanisms can be proposed. The first possibility is the direct phosphorylation of NHERF1 by PKCε and the second is a cooperative activation model where ERMs activation by phosphorylation induces NHERF1 activation. In support of the first hypothesis, a study by Zimei Bu (Li *et al.,* 2007) provided evidence for the ability of PKC to phoshorylate NHERF1, on two amino acid residues, Ser-339 and Ser-340, in the C-terminal domain, which disrupted NHERF intra-molecular auto-inhibition and enabled the interaction of NHERF1 with its ligands. Also, in Calu3 cells, it is known that activated PKCε binds to RACK1 that shuttles and holds the active kinase to apical cellular microdomains where it interacts with NHERF1 which serve as a scaffolding

protein to anchor the enzyme in proximity to CFTR (Liedtke *et al*., 2002). The confinement of active PKCε in the same microdoamin of NHERF1 that harbors phosphorytion sites for PKC could enable direct phosphorylation of NHERF1 by PKCε. In support to the second hypothesis, one study showed that Ezrin activation can stimulate NHERF1 to increase its capacity to assemble macromolecular complexes including CFTR (Li *et al*., 2005). Moreover, the cooperative activation of NHERF1 and ERMs was best demonstrated in NHERF1-deficient mice or Ezrin-deficient mice. These mice showed evidence that these proteins are needed to stabilize each other activation at the apical membrane of polarized epithelial cells. In NHERF1-KO mice, ERMs cytoplasmic localization correlates with structural defects in the epithelium (Morales *et al*., 2004). In the present study, we provide evidence that PKCε activation after VIP stimulation increases the phosphorylation level of ERM proteins. Activation of ERMs might in turn activate NHERF1, increasing its interaction with CFTR.

IV. VIP Reduces CAL-CFTR Interaction

We showed that VIP treatment reduced both the co-localization and the *in situ* interaction between CFTR and CAL. CAL is a Golgi localized PDZ adaptor protein that is known as a negative regulator for WT-CFTR as well as ΔF508-CFTR total and surface expression by promoting cytoplasmic retention and lysosomal degradation after endocytosis (Cheng *et al*., 2002; Cheng *et al*., 2004; Wolde *et al.,* 2007; Cushing *et al.,* 2010). The reduction of CFTR-CAL intracellular localization, observed in this study, is consistent with the ability of VIP to redistribute CFTR from the cytoplasm to the membrane. We found no changes in CAL localization after VIP stimulation, confirming that only CFTR cellular localization was changed after VIP stimulation.

It is well established that CAL competes with NHERF1 for the same PDZ binding motif in the C-terminal domain of CFTR to regulate its surface expression in an opposite manner (Cheng *et al*., 2002; Ameen *et al*., 2007; Cushing *et al*., 2008; Lee & Zheng, 2010). While NHERF1 favors surface stability of CFTR, CAL favors its cytoplasmic retention and lysosomal degradation. In agreement with the balanced competition model, we showed that VIP treatment failed to reduce the intracellular co-localization of CAL and CFTR in cells pretreated with NHERF1-siRNA.

To examine the functional significance of disrupting CFTR-NHERF1-P-ERMs complex on VIP-dependent increase in CFTR function by down regulating NHERF1 or ERMs, we measured changes in iodide efflux rates. Acute stimulation of CFTR with cAMP produced a large but transient stimulation of the iodide efflux rate, reflecting CFTR direct phosphorylation of its regulatory domain by PKA *(Gadsby & Nairn, 1999a; Gadsby & Nairn, 1999b; Seavilleklein et al*., 2008). However, prolonged stimulation by VIP (30 min to 1 h) produced a sustained activation of CFTR-dependent iodide efflux rate, which is consistent with both CFTR activation by phosphorylation and an increase in the density of active channels at the cell membrane (Chappe *et al.*, 2008). We observed that after down-regulating NHERF1 or ERMs by siRNAs transfection, cAMP-stimulation still produced a rapid transient increase in the iodide efflux rate. However, the sustained VIP effect was lost, confirming that NHERF1 and ERMs are necessary for the regulation

of CFTR activity by VIP. The functional significance of promoting CFTR interaction with NHERF1/ P-ERMs complex after VIP stimulation correlates with data obtained in a series of studies by Casavola et al. (Guerra *et al*., 2005; Favia *et al*., 2010; Monterisi S. *et al*., 2012). They showed that promoting CFTR-NHERF1-Ezrin-actin complex formation was necessary for NHERF1-overexpression-dependent rescue of ΔF508-CFTR-dependent chloride

V. Conclusion

Regulation of chloride secretion by changes in the number of membrane CFTR through modulation of its recycling and surface stability by physiological agonists has been largely underestimated. Certainly, the finding of the involvement of the endocytosis pathway in VIP-dependent increase in CFTR density might open a new therapeutic window for modulating CFTR surface density and treating several CF-causing mutations with surface stability problems including the most common CF mutation, ΔF508. Here we identified a molecular mechanism responsible for the VIP-PKCε induced CFTR surface stability. This involves the dissociation of CFTR from CAL in the cytoplasm while potentiating NHERF1-P-ERMs interaction with membrane CFTR in Calu-3 cells.

In agreement with previous lab reports, we showed that VIP stimulation increased CFTR membrane density. PKCε inhibition affected VIP ability to increase CFTR membrane density confirming the direct involvement of PKCε in the VIP signaling cascade. With immuno-labeling experiments we showed that VIP stimulation increased the co-localization of CFTR and NHERF1 at the membrane of Calu-3 cells and reduced CAL-CFTR co-localization in the cytoplasm. Additionally, we showed that both VIP stimulation and direct activation by PMA increased the phosphorylation level of ERM proteins by PKCε. Importantly, we confirmed the endogenous complex assembly after VIP stimulation with the new *in situ* PLA technology. Down-regulating ERMs and NHERF1 expression provided further confirmation of the functional role of these proteins in VIP signaling cascade. Accordingly, we provided a two steps model where VIP ability to stabilize CFTR at the membrane is mediated through potentiating CFTR-NHERF1-P-ERMs complex formation at the membrane that confer CFTR surface stability while dissociating CFTR from CAL interaction in the cytoplasm leading to its membrane insesion (figure 4.1).

Figure 4.1 Regulation of CFTR Membrane Expression by VIP in Calu-3 Cells.
After binding to VPAC1 receptors on the basolateral membrane, VIP activates both Gαs and Gαi/q signaling cascades. Activation of Gαi/q activates PKCε and its interaction with RACK1. In the apical domain the PKCε-RACK1 complex binds to NHERF1. Such interaction help tether the activated PKCε in the apical cellular microdomain in close proximity to CFTR. The active PKCε in turn phosphorylates ERMs and activates NHERF1 leading to their interaction with CFTR. Such CFTR/NHERF1/P-ERMs interaction bridges CFTR to the actin cytoskeleton. VIP stimulation also results in enhanced exocytotic insertion of CFTR to the membrane by uncoupling CFTR from CAL interaction, an adaptor protein that mediates CFTR cytoplasmic retention and eventual degradation. Both PKA and/or PKCε are proposed to mediate the later mechanism.

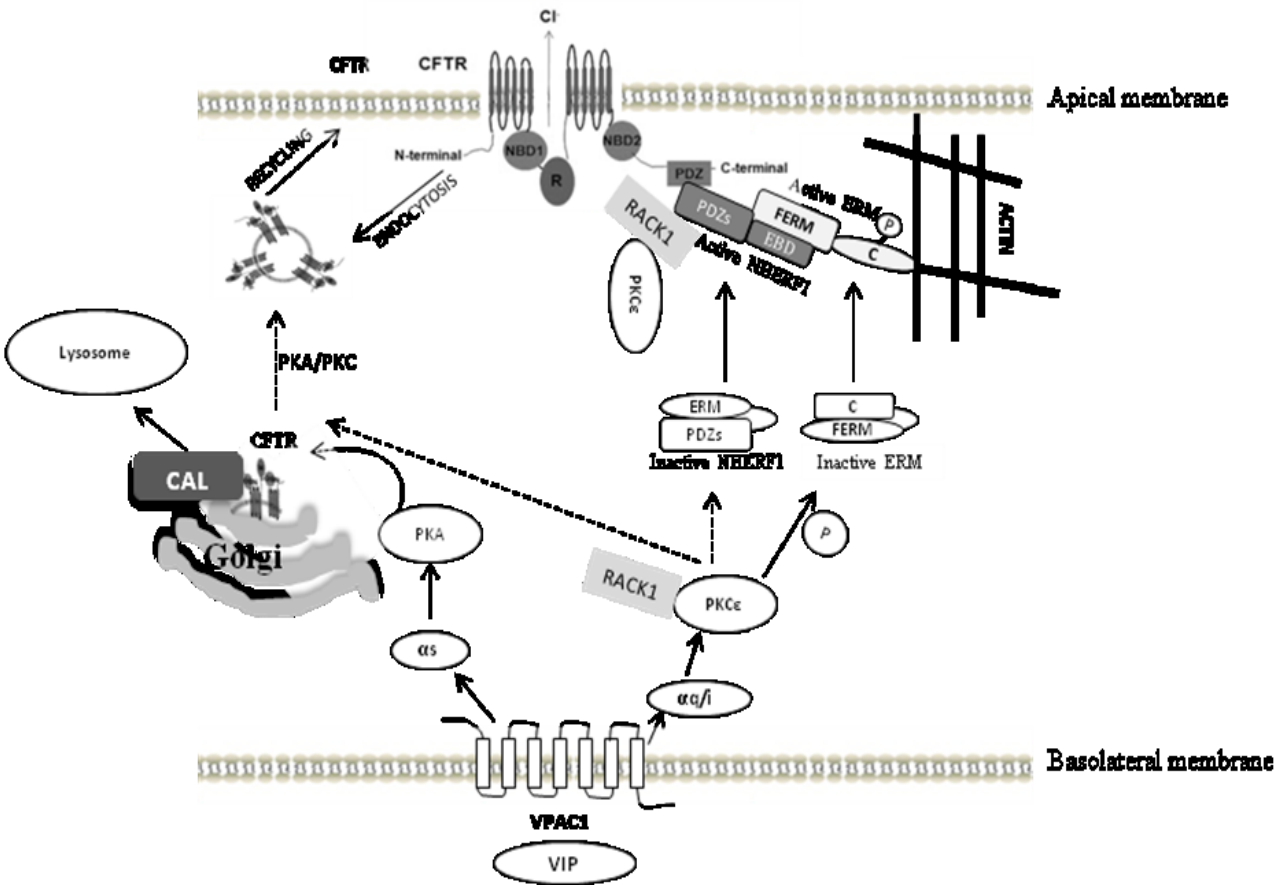

VI. Significance

The amount of CFTR at the membrane can be reduced due to genetic defects like in CF or due to post transcriptional damages as in oxidative stress (Cantin *et al*., 2006; Cantin *et al.,* 2006; Rab *et al*., 2013). The reduced membrane expression of CFTR was described in relation to chronic environmental stresses resulting from oxidative insults such as cigarette smoke, pollution and chronic viral-induced inflammation. Since depletion of the ASL, accumulation of viscous mucus, inflammation, chronic infection and reduced CFTR function are shared features in obstructive lung disease; effective therapeutic approaches that targets the basic molecular defect might be helpful in multiple respiratory disease conditions. The role of VIP in increasing CFTR surface expression and thus function provides a great potential to counteract the effect of CFTR dysfunction in multiple respiratory conditions.

Recently, attention has been drawn to the therapeutic potential of VIP for the treatment of respiratory diseases including asthma, sarcoidosis, pulmonary arterial hypertension and chronic bronchitis based on its anti-inflammatory, immunomodulatory, potent vasodilatory and bronchodilatory effects (Wu *et al*., 2011). Noteworthy, external VIP administration was shown to improve the cardio-pulmonary function in patients suffering from pulmonary arterial hypertension where VIP nerves are deficient (Hamidi *et al*., 2011). We speculate that VIP could have therapeutic benefit for CF patients owing to its positive regulation of CFTR trafficking and function.

Despite the therapeutic potential of VIP in treating many respiratory diseases, it is still not in clinical use. The initial obstacle associated with VIP therapy was related to its poor metabolic stability due to rapid degradation by peptidases (Groneberg *et al*., 2006). Thus the initial efforts were focused on the creation of more stable VIP analogues. Because systemic administration caused cardiovascular side effects by decreasing the blood pressure, the drug delivery by inhalation was necessary. The creation of either VPAC1 or VPAC2 selective agonists was also proposed. The identification of major

cleavage sites for VIP led to the synthesis of metabolically more stable synthetic analogues like Ro 25-1553 and Ro 25-1392 (highly selective agonists of the VPAC2 Receptor) which are proven to be very potent anti-inflammatory and broncho-relaxant agents (Groneberg *et al*., 2006). The aerosolic administration of Ro 25- 1553 was tested in a clinical trial to 24 patients with moderate stable asthma. A rapid-onset, but short-duration potent bronchodilatory effect was achieved without adverse effects. The study concluded that more stable VPAC2 agonists could be used for the treatment of moderate stable asthma (Linden *et al*., 2003). Another study reported a temporary vasodilation and improvement of the cardio-pulmonary function for 20 patients with primary pulmonary hypertension after administration of Aviptadil, which is another inhaled VIP analogue with no side effects reported (Leuchte *et al*., 2008). Additionally, following Aviptadil aerosolic administration to patients with sarcoidosis (a non-infectious inflammatory condition), a suppression of inflammation without any obvious side effects or systemic immunosuppression was achieved (Prasse *et al*., 2010). Owing to the therapeutic potential of VIP, efforts are directed toward the development of more stable, long lasting synthetic VIP analogues. A wider and longer clinical trial will be necessary before establishment of the VIP analogues in human therapy.

In the present study, we unrevealed the mechanism by which VIP increases CFTR surface expression. Targeting this mechanism might be of great therapeutic value to treat ΔF505-CFTR and other CF-causing mutations with surface stability defect. Beside the clinical benefits that could results by exploiting this mechanism, it provides fundamental information on VIP biology. Understanding VIP mechanism of action is essential for the development of specific and safe therapies.

Many CFTR mutations result in more than one single defect in CFTR. This includes ΔF508-CFTR which shows defects in trafficking, surface stability and gating. The recent focus in CFTR associated therapy is the development of drugs that can target more than one defect. Several CFTR modulators with activator, potentiator or corrector effect are being developed. CFTR activators are molecules that increase CFTR function. CFTR potentiators are molecules that can directly increase the gating of cell-surface

localized CFTR to augment ion transport. CFTR correctors are molecules that increase the amount of functional CFTR at the cell surface from modulating its trafficking (Zhang *et al.*, 2012). Because each of these modulators target CFTR at one level, the co-administration of CFTR corrector and potentiator might be necessary to treat CF patients with CFTR mutations inducing more than one defect. Since the single-drug therapy is favorable over multiple drugs, efforts are directed toward the identification of compounds with independent correcting and potentiating abilities or synthesizing 'hybrid' molecules that can increase CFTR function through different mechanisms. As a natural neuropeptide that can regulate many aspects of CFTR including its trafficking, surface stability and gating, VIP might be of great value to treat many CF-causing mutations including those presenting multiple defects. The use of VIP or long acting agonists as a CF drug should be thoroughly investigated.

VII. Future directions

The importance of NHERF1-P-ERMs interaction with CFTR after VIP stimulation could be confirmed *in vivo* by applying the *in situ* PLA technology to tissue sections. Previously, our group has shown that the absence of VIP in VIP-KO mice resulted in reduced CFTR membrane localization that was associated with a CF-like pathology. CFTR membrane localization was restored and the tissue inflammation was corrected by external intra-peritoneal VIP administration every other day for 3 weeks. By comparing NHERF1-P-ERMs interaction with CFTR in tissues from mice lacking VIP (VIP-KO) to the tissues sections from VIP-treated mice, we could confirm the importance of VIP stimulation in the association of this multi-protein complex *in vivo*.

One more question that could be answer, as an extension to my project is what signaling pathway (PKA and/or PKC) is involved in the VIP-dependent increase in CFTR membrane insertion from the intracellular pool. As we observed reduced interaction between CFTR and CAL in the cytoplasm after VIP stimulation, CAL-CFTR interaction can be used as a marker. In this case an inhibitor for either PKA or PKC or both could be applied along with VIP treatment. The inhibitor that prevents the VIP-dependent reduction in CAL-CFTR interaction will tell us which kinase is involved in this mechanism. Specific CAL siRNA could be used to confirm the importance of CFTR membrane insertion in the VIP mechanism.

The multi-protein complex CFTR-NHERF1-Ezrin-actin was shown to play an important role in maintaining the epithelium integrity by controlling tight junction organization and therefore the barrier function (Castellani *et al*., 2012). Absence of CFTR membrane localization (ΔF508-CFTR) was shown to disrupt the tight junction organization (Castellani *et al*., 2012). This permits defective transport through the paracellular pathway as well as allowing the bacteria to interact with critical basolateral receptors. The natural extension of our proteome will be the study of tight junction proteins like zonula occludens , occludins, and E-Cadherin. To understand the role of CFTR membrane localization and complex formation with NHERF1 and P-ERMs in tight junctions formation and organization, we could compare VIP-KO mice where CFTR

is absent from the membrane, and VIP treated VIP-KO mice, where CFTR is present at the membrane. If CFTR membrane localization is necessary, we should see a disruption of the tight junction proteins organization as well as the actin cytoskeleton in tissues obtained from VIP-KO mice which should be corrected in VIP treated VIP-KO mice. Results from this study will also provide an insight about whether chronic VIP stimulation is necessary for this multi-protein complex association to maintain epithelial integrity.

Bibliography

Adams, D. R., Ron, D., & Kiely, P. A. (2011). RACK1, A multifaceted scaffolding protein: Structure and function. *Cell Communication and Signaling: CCS, 9*, 22-811X-9-22.

Agnese, M., Rosati, L., Muriano, F., Valiante, S., Laforgia, V., Andreuccetti, P., *et al*. (2012). Expression of VIP and its receptors in the testis of the spotted ray torpedo marmorata (risso 1880). *Journal of Molecular Neuroscience: MN, 48*(3), 638-646.

Alcolado, N., Conrad, D. J., Rafferty, S., Chappe, F. G., & Chappe, V. M. (2011). VIP-dependent increase in F508del-CFTR membrane localization is mediated by PKCepsilon. *American Journal of Physiology.Cell Physiology, 301*(1), C53-65.

Alcolado, N. (2010). Masters Thesis: Regulation of CFTR membrane localization by the Vasoactive Intestinal Peptide (VIP).

Alshafie Walaa, Chappe Frederic G, Li Mansong, Anini Younes and Chappe Valerie M (2013). VIP regulates CFTR membrane expression and function in Calu-3 cells by increasing its interaction with NHERF1 and P-ERM in a VPAC1 and PKCε -dependent manner. Submitted to American journal of Physiology.

Aliakbari, J., Sreedharan, S. P., Turck, C. W., & Goetzl, E. J. (1987). Selective localization of vasoactive intestinal peptide and substance P in human eosinophils. *Biochemical and Biophysical Research Communications, 148*(3), 1440-1445.

Ameen NA, Martensson B, Bourguinon L, Marino C, Isenberg J, & McLaughlin GE. (1999). CFTR channel insertion to the apical surface in rat duodenal villus epithelial cells is upregulated by VIP in vivo. *Journal of Cell Science, 112*, 887-94.

Ameen, N., Silvis, M., & Bradbury, N. A. (2007). Endocytic trafficking of CFTR in health and disease. *Journal of Cystic Fibrosis, 6*(1), 1-14.

Ameen, N. A., Marino, C., & Salas, P. J. (2003). cAMP-dependent exocytosis and vesicle traffic regulate CFTR and fluid transport in rat jejunum in vivo. *American Journal of Physiology.Cell Physiology, 284*(2), C429-38.

Amieva, M. R., & Furthmayr, H. (1995). Subcellular localization of moesin in dynamic filopodia, retraction fibers, and other structures involved in substrate exploration, attachment, and cell-cell contacts. *Experimental Cell Research, 219*(1), 180-196.

Amieva, M. R., Wilgenbus, K. K., & Furthmayr, H. (1994). Radixin is a component of hepatocyte microvilli *in situ*. *Experimental Cell Research, 210*(1), 140-144.

Ardura, J. A., & Friedman, P. A. (2011). Regulation of G protein-coupled receptor function by Na+/H+ exchange regulatory factors. *Pharmacological Reviews, 63*(4), 882-900.

Antunes, M. B., & Cohen, N. A. (2007). Mucociliary clearance--a critical upper airway host defense mechanism and methods of assessment. *Current Opinion in Allergy and Clinical Immunology, 7*(1), 5-10.

Bajnath, R. B., Dekker, K., De Jonge, H. R., & Groot, J. A. (1995). Chloride secretion induced by phorbol dibutyrate and forskolin in the human colonic carcinoma cell line HT-29Cl.19A is regulated by different mechanisms. *Pflugers Archiv: European Journal of Physiology, 430*(5), 705-712.

Bajnath, R. B., Groot, J. A., De Jonge, H. R., Kansen, M., & Bijman, J. (1993). Synergistic activation of non-rectifying small-conductance chloride channels by forskolin and phorbol esters in cell-attached patches of the human colon carcinoma cell line HT-29cl.19A. *Pflugers Archiv: European Journal of Physiology, 425*(1-2), 100-108.

Baker, D. G. (1986). Parasympathetic motor pathways to the trachea: Recent morphologic and electrophysiologic studies. *Clinics in Chest Medicine, 7*(2), 223-229.

Ballard ST, & Inglis SK. (2004). Liquid secretion properties of airway submucosal glands. *The Journal of Physiology, 556*(Pt), 1-10.

Ballard, S. T., & Spadafora, D. (2007). Fluid secretion by submucosal glands of the tracheobronchial airways. *Respiratory Physiology & Neurobiology, 159*(3), 271-277.

Ballard, S. T., Trout, L., Garrison, J., & Inglis, S. K. (2006). Ionic mechanism of forskolin-induced liquid secretion by porcine bronchi. *American Journal of Physiology.Lung Cellular and Molecular Physiology, 290*(1), L97-104.

Ballard, S. T., Trout, L., Mehta, A., & Inglis, S. K. (2002). Liquid secretion inhibitors reduce mucociliary transport in glandular airways. *American Journal of Physiology. Lung Cellular and Molecular Physiology, 283*(2), L329-35.

Basbaum, C. B., Jany, B., & Finkbeiner, W. E. (1990). The serous cell. *Annual Review of Physiology, 52*, 97-113.

Bayliss, W. M., & Starling, E. H. (1902). The mechanism of pancreatic secretion. *The Journal of Physiology, 28*(5), 325-353.

Benharouga, M., Sharma, M., So, J., Haardt, M., Drzymala, L., Popov, M., *et al*. (2003). The role of the C terminus and Na+/H+ exchanger regulatory factor in the functional expression of cystic fibrosis transmembrane conductance regulator in nonpolarized cells and epithelia. *The Journal of Biological Chemistry, 278*(24), 22079-22089.

Bewley, M. S., Pena, J. T. G., Plesch, F. N., Decker, S. E., Weber, G. J., & Forrest, J. N. (2006). Shark rectal gland vasoactive intestinal peptide receptor: Cloning, functional expression, and regulation of CFTR chloride channels. *American Journal of Physiology., 291*(4), R1157-R1164.

Bhattacharya S., Cowburn D., Dai Z., Li J., Baxter S., Bu Z., *et al*. (2010). A conformational switch in the scaffolding protein NHERF1 controls autoinhibition and complex formation. *J.Biol.Chem.Journal of Biological Chemistry, 285*(13), 9981-9994.

Boucher, R. C. (2007). Cystic fibrosis: A disease of vulnerability to airway surface dehydration. *Trends in Molecular Medicine, 13*(6), 231-240.

Bradbury NA. (1999). Intracellular CFTR: Localization and function. *Physiological Reviews, 79*(1), 175-91.

Bradbury, N. A., Jilling, T., Kirk, K. L., & Bridges, R. J. (1992). Regulated endocytosis in a chloride secretory epithelial cell line. *The American Journal of Physiology, 262*(3 Pt 1), C752-9.

Bretscher A. (1999). Regulation of cortical structure by the ezrin-radixin-moesin protein family. *Current Opinion in Cell Biology, 11*(1), 109-16.

Bretscher A, Edwards K, & Fehon RG. (2002). ERM proteins and merlin: Integrators at the cell cortex. *Nature Reviews.Molecular Cell Biology, 3*(8), 586-99.

Bretscher A, Reczek D, & Berryman M. (1997). Ezrin: A protein requiring conformational activation to link microfilaments to the plasma membrane in the assembly of cell surface structures. *Journal of Cell Science, 110*, 3011-8.

Bretscher, A. (1983). Purification of an 80,000-dalton protein that is a component of the isolated microvillus cytoskeleton, and its localization in nonmuscle cells. *The Journal of Cell Biology, 97*(2), 425-432.

Bretscher, A., Chambers, D., Nguyen, R., & Reczek, D. (2000). ERM-merlin and EBP50 protein families in plasma membrane organization and function. *Annual Review of Cell and Developmental Biology, 16*, 113-143.

Broere, N., Hillesheim, J., Tuo, B., Jorna, H., Houtsmuller, A. B., Shenolikar, S., *et al*. (2007). Cystic fibrosis transmembrane conductance regulator activation is reduced in the small intestine of Na+/H+ exchanger 3 regulatory factor 1 (NHERF-1)- but not NHERF-2-deficient mice. *The Journal of Biological Chemistry, 282*(52), 37575-37584.

Brone, B., & Eggermont, J. (2005). PDZ proteins retain and regulate membrane transporters in polarized epithelial cell membranes. *American Journal of Physiology., 288*(1), C20-C29.

Brown, D., Bouley, R., Paunescu, T. G., Breton, S., & Lu, H. A. (2012). New insights into the dynamic regulation of water and acid-base balance by renal epithelial cells. *American Journal of Physiology.Cell Physiology, 302*(10), C1421-33.

Cai Z.-W., Liu J., Li H.-Y., & Sheppard D.N. (2011). Targeting F508del-CFTR to develop rational new therapies for cystic fibrosis. *Acta Pharmacol.Sin.Acta Pharmacologica Sinica, 32*(6), 693-701. .

Cantiello, H. F. (1996). Role of the actin cytoskeleton in the regulation of the cystic fibrosis transmembrane conductance regulator. *Experimental Physiology, 81*(3), 505-514.

Cantin, A. M., Bilodeau, G., Ouellet, C., Liao, J., & Hanrahan, J. W. (2006). Oxidant stress suppresses CFTR expression. *American Journal of Physiology.Cell Physiology, 290*(1), C262-70.

Cantin, A. M., Hanrahan, J. W., Bilodeau, G., Ellis, L., Dupuis, A., Liao, J., *et al*. (2006). Cystic fibrosis transmembrane conductance regulator function is suppressed in cigarette smokers. *American Journal of Respiratory and Critical Care Medicine, 173*(10), 1139-1144.

Carstairs, J. R., & Barnes, P. J. (1986). Visualization of vasoactive intestinal peptide receptors in human and guinea pig lung. *The Journal of Pharmacology and Experimental Therapeutics, 239*(1), 249-255.

Castellani, S., Guerra, L., Favia, M., Di Gioia, S., Casavola, V., & Conese, M. (2012). NHERF1 and CFTR restore tight junction organisation and function in cystic fibrosis airway epithelial cells: Role of ezrin and the RhoA/ROCK pathway. *Laboratory Investigation; a Journal of Technical Methods and Pathology, 92*(11), 1527-1540.

Caughey, G. H., Leidig, F., Viro, N. F., & Nadel, J. A. (1988). Substance P and vasoactive intestinal peptide degradation by mast cell tryptase and chymase. *The Journal of Pharmacology and Experimental Therapeutics, 244*(1), 133-137.

Chambers, L. A., Rollins, B. M., & Tarran, R. (2007). Liquid movement across the surface epithelium of large airways. *Respiratory Physiology & Neurobiology, 159*(3), 256-270.

Chappe F, Loewen ME, Hanrahan JW, & Chappe V. (2008). Vasoactive intestinal peptide increases cystic fibrosis transmembrane conductance regulator levels in the apical membrane of calu-3 cells through a protein kinase C-dependent mechanism. *The Journal of Pharmacology and Experimental Therapeutics, 327*(1), 226-38.

Chappe V, Hinkson DA, Howell LD, Evagelidis A, Liao J, Chang XB, *et al*. (2004). Stimulatory and inhibitory protein kinase C consensus sequences regulate the cystic fibrosis transmembrane conductance regulator. *Proceedings of the National Academy of Sciences of the United States of America, 101*(1), 390-5.

Chappe V, Hinkson DA, Zhu T, Chang XB, Riordan JR, & Hanrahan JW. (2003). Phosphorylation of protein kinase C sites in NBD1 and the R domain control CFTR channel activation by PKA. *The Journal of Physiology, 548*(Pt), 39-52.

Charest, A., Lane, K., McMahon, K., & Housman, D. E. (2001). Association of a novel PDZ domain-containing peripheral golgi protein with the Q-SNARE (Q-soluble N-ethylmaleimide-sensitive fusion protein (NSF) attachment protein receptor) protein syntaxin 6. *The Journal of Biological Chemistry, 276*(31), 29456-29465.

Cheng J, Wang H, & Guggino WB. (2004). Modulation of mature cystic fibrosis transmembrane regulator protein by the PDZ domain protein CAL. *The Journal of Biological Chemistry, 279*(3), 1892-8.

Cheng SH, Gregory RJ, Marshall J, Paul S, Souza DW, White GA, et al. (1990). Defective intracellular transport and processing of CFTR is the molecular basis of most cystic fibrosis. *Cell, 63*(4), 827-34.

Cheng, H., Li, J., Fazlieva, R., Dai, Z., Bu, Z., & Roder, H. (2009). Autoinhibitory interactions between the PDZ2 and C-terminal domains in the scaffolding protein NHERF1. *Structure, 17*(5), 660-669.

Cheng, J., Moyer, B. D., Milewski, M., Loffing, J., Ikeda, M., Mickle, J. E., *et al*. (2002). A golgi-associated PDZ domain protein modulates cystic fibrosis transmembrane regulator plasma membrane expression. *The Journal of Biological Chemistry, 277*(5), 3520-3529.

Chishti, A. H., Kim, A. C., Marfatia, S. M., Lutchman, M., Hanspal, M., Jindal, H., *et al*. (1998). The FERM domain: A unique module involved in the linkage of cytoplasmic proteins to the membrane. *Trends in Biochemical Sciences, 23*(8), 281-282.

Choi, J. Y., Joo, N. S., Krouse, M. E., Wu, J. V., Robbins, R. C., Ianowski, J. P., *et al*. (2007). Synergistic airway gland mucus secretion in response to vasoactive intestinal peptide and carbachol is lost in cystic fibrosis. *The Journal of Clinical Investigation, 117*(10), 3118-3127.

Cohen, T. S., & Prince, A. (2012). Cystic fibrosis: A mucosal immunodeficiency syndrome. *Nature Medicine, 18*(4), 509-519.

Collaco, A. M., Jakab, R. L., Hoekstra, N. E., Mitchell, K. A., Brooks, A., & Ameen, N. A. (2013). Regulated traffic of anion transporters in mammalian brunner's glands: A role for water and fluid transport. *American Journal of Physiology.Gastrointestinal and Liver Physiology, 305*(3), G258-75.

Cushing P.R., Fellows A., Villone D., Madden D.R., & Boisguerin P. (2008). The relative binding affinities of PDZ partners for CFTR: A biochemical basis for efficient endocytic recycling. *Biochemistry Biochemistry, 47*(38), 10084-10098.

Cushing PR, Vouilleme L, Pellegrini M, Boisguerin P, & Madden DR. (2010). A stabilizing influence: CAL PDZ inhibition extends the half-life of ΔF508-CFTR. *Angewandte Chemie (International Ed.in English), 49*(51), 9907-11.

Cushing, P. R., Vouilleme, L., Pellegrini, M., Boisguerin, P., & Madden, D. R. (2010). A stabilizing influence: CAL PDZ inhibition extends the half-life of DeltaF508-CFTR. *Angewandte Chemie (International Ed.in English), 49*(51), 9907-9911.

Cutz, E., Chan, W., Track, N. S., Goth, A., & Said, S. I. (1978). Release of vasoactive intestinal polypeptide in mast cells by histamine liberators. *Nature, 275*(5681), 661-662.

Dajani, R., Zhang, Y., Taft, P. J., Travis, S. M., Starner, T. D., Olsen, A., *et al*. (2005). Lysozyme secretion by submucosal glands protects the airway from bacterial infection. *American Journal of Respiratory Cell and Molecular Biology, 32*(6), 548-552.

Dalemans, W., Barbry, P., Champigny, G., Jallat, S., Dott, K., Dreyer, D., *et al*. (1991). Altered chloride ion channel kinetics associated with the delta F508 cystic fibrosis mutation. *Nature, 354*(6354), 526-528.

Davis, B., Roberts, A. M., Coleridge, H. M., & Coleridge, J. C. (1982). Reflex tracheal gland secretion evoked by stimulation of bronchial C-fibers in dogs. *Journal of Applied Physiology: Respiratory, Environmental and Exercise Physiology, 53*(4), 985-991.

Dechecchi, M. C., Rolfini, R., Tamanini, A., Gamberi, C., Berton, G., & Cabrini, G. (1992). Effect of modulation of protein kinase C on the cAMP-dependent chloride conductance in T84 cells. *FEBS Letters, 311*(1), 25-28.

Dechecchi, M. C., Tamanini, A., Berton, G., & Cabrini, G. (1993). Protein kinase C activates chloride conductance in C127 cells stably expressing the cystic fibrosis gene. *The Journal of Biological Chemistry, 268*(15), 11321-11325.

Deliot, N., Hernando, N., Horst-Liu, Z., Gisler, S. M., Capuano, P., Wagner, C. A., *et al*. (2005). Parathyroid hormone treatment induces dissociation of type IIa na+-P(i) cotransporter-Na+/H+ exchanger regulatory factor-1 complexes. *American Journal of Physiology.Cell Physiology, 289*(1), C159-67.

Deora, A. A., Diaz, F., Schreiner, R., & Rodriguez-Boulan, E. (2007). Efficient electroporation of DNA and protein into confluent and differentiated epithelial cells in culture. *Traffic (Copenhagen, Denmark), 8*(10), 1304-1312.

, Montoni A, Bulteau-Pignoux L, Janet T, Moreau B, Muller JM, *et al*. (2004). Activation of VPAC1 receptors by VIP and PACAP-27 in human bronchial epithelial cells induces CFTR-dependent chloride secretion. *British Journal of Pharmacology, 141*(4), 698-708.

Dey RD, Altemus JB, & Michalkiewicz M. (1991). Distribution of vasoactive intestinal peptide- and substance P-containing nerves originating from neurons of airway ganglia in cat bronchi. *The Journal of Comparative Neurology, 304*(2), 330-40.

Dey RD, Shannon WA Jr, & Said SI. (1981). Localization of VIP-immunoreactive nerves in airways and pulmonary vessels of dogs, cat, and human subjects. *Cell and Tissue Research, 220*(2), 231-8.

Dickson, L., & Finlayson, K. (2009). VPAC and PAC receptors: From ligands to function. *Pharmacology & Therapeutics., 121*(3), 294-316.

Ding, X., Deng, H., Wang, D., Zhou, J., Huang, Y., Zhao, X., *et al*. (2010). Phospho-regulated ACAP4-ezrin interaction is essential for histamine-stimulated parietal cell secretion. *The Journal of Biological Chemistry, 285*(24), 18769-18780.

Dransfield, D. T., Bradford, A. J., Smith, J., Martin, M., Roy, C., Mangeat, P. H., *et al*. (1997). Ezrin is a cyclic AMP-dependent protein kinase anchoring protein. *The EMBO Journal, 16*(1), 35-43.

Farinha, C. M., Matos, P., & Amaral, M. D. (2013). Control of cystic fibrosis transmembrane conductance regulator membrane trafficking: Not just from the endoplasmic reticulum to the golgi. *The FEBS Journal, 280*(18), 4396-4406.

Favia, M., Guerra, L., Fanelli, T., Cardone, R. A., Monterisi, S., Di Sole, F., *et al*. (2010). Na+/H+ exchanger regulatory factor 1 overexpression-dependent increase of cytoskeleton organization is fundamental in the rescue of F508del cystic fibrosis transmembrane conductance regulator in human airway CFBE41o- cells. *Molecular Biology of the Cell, 21*(1), 73-86.

Franck, Z., Gary, R., & Bretscher, A. (1993). Moesin, like ezrin, colocalizes with actin in the cortical cytoskeleton in cultured cells, but its expression is more variable. *Journal of Cell Science, 105 (Pt 1)*(Pt 1), 219-231.

Frandsen, E. K., Krishna, G. A., & Said, S. I. (1978). Vasoactive intestinal polypeptide promotes cyclic adenosine 3',5'-monophosphate accumulation in guinea-pig trachea. *British Journal of Pharmacology, 62*(3), 367-369.

Frizzell, R. A., & Hanrahan, J. W. (2012). Physiology of epithelial chloride and fluid secretion. *Cold Spring Harbor Perspectives in Medicine, 2*(6), a009563.

Gadsby, D. C., & Nairn, A. C. (1999a). Control of CFTR channel gating by phosphorylation and nucleotide hydrolysis. *Physiological Reviews, 79*(1 Suppl), S77-S107.

Gadsby, D. C., & Nairn, A. C. (1999b). Regulation of CFTR cl- ion channels by phosphorylation and dephosphorylation. *Advances in Second Messenger and Phosphoprotein Research, 33*, 79-106.

Ganeshan, R., Nowotarski, K., Di, A., Nelson, D. J., & Kirk, K. L. (2007). CFTR surface expression and chloride currents are decreased by inhibitors of N-WASP and actin polymerization. *BBA - Molecular Cell Research, 1773*(2), 192-200.

Garbett, D., LaLonde, D. P., & Bretscher, A. (2010). The scaffolding protein EBP50 regulates microvillar assembly in a phosphorylation-dependent manner. *The Journal of General Physiology., 136*(5), i5.

Gary, R., & Bretscher, A. (1995). Ezrin self-association involves binding of an N-terminal domain to a normally masked C-terminal domain that includes the F-actin binding site. *Molecular Biology of the Cell, 6*(8), 1061-1075.

Ghatei, M. A., Sheppard, M. N., O'Shaughnessy, D. J., Adrian, T. E., McGregor, G. P., Polak, J. M., *et al*. (1982). Regulatory peptides in the mammalian respiratory tract. *Endocrinology, 111*(4), 1248-1254.

Goetzl, E. J., Sreedharan, S. P., Turck, C. W., Bridenbaugh, R., & Malfroy, B. (1989). Preferential cleavage of amino- and carboxyl-terminal oligopeptides from vasoactive intestinal polypeptide by human recombinant enkephalinase (neutral endopeptidase, EC 3.4.24.11). *Biochemical and Biophysical Research Communications, 158*(3), 850-854.

Groneberg, D. A., Hartmann, P., Dinh, Q. T., & Fischer, A. (2001). Expression and distribution of vasoactive intestinal polypeptide receptor VPAC(2) mRNA in human airways. *Laboratory Investigation; a Journal of Technical Methods and Pathology, 81*(5), 749-755.

Groneberg, D. A., Rabe, K. F., & Fischer, A. (2006). Novel concepts of neuropeptide-based drug therapy: Vasoactive intestinal polypeptide and its receptors. *European Journal of Pharmacology., 533*(1), 182.

Groneberg, D., Springer, J., & Fischer, A. (2001). Vasoactive intestinal polypeptide as mediator of asthma. *Pulmonary Pharmacology & Therapeutics, 14*(5), 391-401.

Guerra, L., Fanelli, T., Favia, M., Riccardi, S. M., Busco, G., Cardone, R. A., *et al*. (2005). Na+/H+ exchanger regulatory factor isoform 1 overexpression modulates cystic fibrosis transmembrane conductance regulator (CFTR) expression and activity in human airway 16HBE14o- cells and rescues DeltaF508 CFTR functional expression in cystic fibrosis cells. *The Journal of Biological Chemistry, 280*(49), 40925-40933.

Hall, R. A., Ostedgaard, L. S., Premont, R. T., Blitzer, J. T., Rahman, N., Welsh, M. J., *et al*. (1998). A C-terminal motif found in the beta2-adrenergic receptor, P2Y1 receptor and cystic fibrosis transmembrane conductance regulator determines binding to the Na+/H+ exchanger regulatory factor family of PDZ proteins. *Proceedings of the National Academy of Sciences of the United States of America, 95*(15), 8496-8501.

Hall, R. A., Premont, R. T., Chow, C. W., Blitzer, J. T., Pitcher, J. A., Claing, A., *et al*. (1998). The beta2-adrenergic receptor interacts with the Na+/H+-exchanger regulatory factor to control Na+/H+ exchange. *Nature, 392*(6676), 626-630.

Hall, R. A., Spurney, R. F., Premont, R. T., Rahman, N., Blitzer, J. T., Pitcher, J. A., *et al*. (1999). G protein-coupled receptor kinase 6A phosphorylates the na(+)/H(+) exchanger regulatory factor via a PDZ domain-mediated interaction. *The Journal of Biological Chemistry, 274*(34), 24328-24334.

Hamidi, S. A., Lin, R. Z., Szema, A. M., Lyubsky, S., Jiang, Y. P., & Said, S. I. (2011). VIP and endothelin receptor antagonist: An effective combination against experimental pulmonary arterial hypertension. *Respiratory Research, 12*, 141-9921-12-141.

Hayashi, K., Yonemura, S., Matsui, T., & Tsukita, S. (1999). Immunofluorescence detection of ezrin/radixin/moesin (ERM) proteins with their carboxyl-terminal threonine phosphorylated in cultured cells and tissues. *Journal of Cell Science, 112 (Pt 8)*(Pt 8), 1149-1158.

He, J., Lau, A. G., Yaffe, M. B., & Hall, R. A. (2001). Phosphorylation and cell cycle-dependent regulation of Na+/H+ exchanger regulatory factor-1 by Cdc2 kinase. *The Journal of Biological Chemistry, 276*(45), 41559-41565.

Heda, G. D., Tanwani, M., & Marino, C. R. (2001). The delta F508 mutation shortens the biochemical half-life of plasma membrane CFTR in polarized epithelial cells. *American Journal of Physiology.Cell Physiology, 280*(1), C166-74.

Heinz-Erian P, Dey RD, Flux M, & Said SI. (1985). Deficient vasoactive intestinal peptide innervation in the sweat glands of cystic fibrosis patients. *Science (New York, N.Y.), 229*(4720), 1407-8.

Heinz-Erian, P., Paul, S., & Said, S. I. (1986). Receptors for vasoactive intestinal peptide on isolated human sweat glands. *Peptides, 7 Suppl 1*, 151-154.

Heiska, L., Alfthan, K., Gronholm, M., Vilja, P., Vaheri, A., & Carpen, O. (1998). Association of ezrin with intercellular adhesion molecule-1 and -2 (ICAM-1 and ICAM-2). regulation by phosphatidylinositol 4, 5-bisphosphate. *The Journal of Biological Chemistry, 273*(34), 21893-21900.

Hollenhorst, M. I., Richter, K., & Fronius, M. (2011). Ion transport by pulmonary epithelia. *Journal of Biomedicine & Biotechnology, 2011*, 174306.

Hong, S. H., Osborne, T., Ren, L., Briggs, J., Mazcko, C., Burkett, S. S., *et al*. (2011). Protein kinase C regulates ezrin-radixin-moesin phosphorylation in canine osteosarcoma cells. *Veterinary and Comparative Oncology, 9*(3), 207-218.

Howard, M., Jilling, T., DuVall, M., & Frizzell, R. A. (1996). cAMP-regulated trafficking of epitope-tagged CFTR. *Kidney International, 49*(6), 1642-1648.

Hu W, Howard M, & Lukacs GL. (2001). Multiple endocytic signals in the C-terminal tail of the cystic fibrosis transmembrane conductance regulator. *The Biochemical Journal, 354*(Pt), 561-72.

Huang, P., Trotter, K., Boucher, R. C., Milgram, S. L., & Stutts, M. J. (2000). PKA holoenzyme is functionally coupled to CFTR by AKAPs. *American Journal of Physiology.Cell Physiology, 278*(2), C417-22.

Ianowski, J. P., Choi, J. Y., Wine, J. J., & Hanrahan, J. W. (2007). Mucus secretion by single tracheal submucosal glands from normal and cystic fibrosis transmembrane conductance regulator knockout mice. *The Journal of Physiology, 580*(Pt 1), 301-314.

Inglis, S. K., Corboz, M. R., Taylor, A. E., & Ballard, S. T. (1997). Effect of anion transport inhibition on mucus secretion by airway submucosal glands. *The American Journal of Physiology, 272*(2 Pt 1), L372-7.

Ishihara T, Shigemoto R, Mori K, Takahashi K, & Nagata S. (1992). Functional expression and tissue distribution of a novel receptor for vasoactive intestinal polypeptide. *Neuron, 8*(4), 811-9.

Jayaraman S, Joo NS, Reitz B, Wine JJ, & Verkman AS. (2001). Submucosal gland secretions in airways from cystic fibrosis patients have normal [na(+)] and pH but elevated viscosity. *Proceedings of the National Academy of Sciences of the United States of America, 98*(14), 8119-23.

Ji, H. L., Chalfant, M. L., Jovov, B., Lockhart, J. P., Parker, S. B., Fuller, C. M., *et al*. (2000). The cytosolic termini of the beta- and gamma-ENaC subunits are involved in the functional interactions between cystic fibrosis transmembrane conductance regulator and epithelial sodium channel. *The Journal of Biological Chemistry, 275*(36), 27947-27956.

Jia Y, Mathews CJ, & Hanrahan JW. (1997). Phosphorylation by protein kinase C is required for acute activation of cystic fibrosis transmembrane conductance regulator by protein kinase A. *The Journal of Biological Chemistry, 272*(8), 4978-84.

Jia, Y., Mathews, C. J., & Hanrahan, J. W. (1997). Phosphorylation by protein kinase C is required for acute activation of cystic fibrosis transmembrane conductance regulator by protein kinase A. *The Journal of Biological Chemistry, 272*(8), 4978-4984.

Joo NS, Irokawa T, Wu JV, Robbins RC, Whyte RI, & Wine JJ. (2002). Absent secretion to vasoactive intestinal peptide in cystic fibrosis airway glands. *The Journal of Biological Chemistry, 277*(52), 50710-5.

Joo, N. S., Cho, H. J., Khansaheb, M., & Wine, J. J. (2010). Hyposecretion of fluid from tracheal submucosal glands of CFTR-deficient pigs. *The Journal of Clinical Investigation, 120*(9), 3161-3166.

Kälin, N., Claaß, A., Sommer, M., Puchelle, E., & Tümmler, B. (1999). ΔF508 CFTR protein expression in tissues from patients with cystic fibrosis. *J.Clin.Invest.Journal of Clinical Investigation, 103*(10), 1379-1389.

Kartner N, Augustinas O, Jensen TJ, Naismith AL, & Riordan JR. (1992). Mislocalization of delta F508 CFTR in cystic fibrosis sweat gland. *Nature Genetics, 1*(5), 321-7.

Kennedy, M. B. (1995). Origin of PDZ (DHR, GLGF) domains. *Trends in Biochemical Sciences, 20*(9), 350.

Knight, D. A., & Holgate, S. T. (2003). The airway epithelium: Structural and functional properties in health and disease. *Respirology (Carlton, Vic.), 8*(4), 432-446.

Kondo, T., Takeuchi, K., Doi, Y., Yonemura, S., Nagata, S., & Tsukita, S. (1997). ERM (ezrin/radixin/moesin)-based molecular mechanism of microvillar breakdown at an early stage of apoptosis. *The Journal of Cell Biology, 139*(3), 749-758.

Koss, M., Pfeiffer, G. R.,2nd, Wang, Y., Thomas, S. T., Yerukhimovich, M., Gaarde, W. A., *et al*. (2006). Ezrin/radixin/moesin proteins are phosphorylated by TNF-alpha and modulate permeability increases in human pulmonary microvascular endothelial cells. *Journal of Immunology (Baltimore, Md.: 1950), 176*(2), 1218-1227.

Kreda, S. M., Gynn, M. C., Fenstermacher, D. A., Boucher, R. C., & Gabriel, S. E. (2001). Expression and localization of epithelial aquaporins in the adult human lung. *American Journal of Respiratory Cell and Molecular Biology, 24*(3), 224-234.

Kreimann, E. L., & Cabrini, R. L. (2013). Subcellular redistribution of NHERF1 in response to dehydroepiandrosterone (DHEA) administration in endometrial glands of wistar rats. *Reproductive Sciences (Thousand Oaks, Calif.), 20*(1), 103-111.

Kunzelmann, K., Kiser, G. L., Schreiber, R., & Riordan, J. R. (1997). Inhibition of epithelial na+ currents by intracellular domains of the cystic fibrosis transmembrane conductance regulator. *FEBS Letters, 400*(3), 341-344.

Kwon, S., Pollard, H., & Guggino, W. B. (2007). Knockdown of NHERF1 enhances degradation of temperature rescued ΔF508 CFTR from the cell surface of human airway cells. *Cellular Physiology and Biochemistry, 20*(6), 763-772.

Ladias, J. A. A. (2003). Structural insights into the CFTR-NHERF interaction. *The Journal of Membrane Biology., 192*(2), 79.

Laitinen, A., Partanen, M., Hervonen, A., Pelto-Huikko, M., & Laitinen, L. A. (1985). VIP like immunoreactive nerves in human respiratory tract. light and electron microscopic study. *Histochemistry, 82*(4), 313-319.

Lankes, W. T., & Furthmayr, H. (1991). Moesin: A member of the protein 4.1-talin-ezrin family of proteins. *Proceedings of the National Academy of Sciences of the United States of America, 88*(19), 8297-8301.

Larsson, C. (2006). Protein kinase C and the regulation of the actin cytoskeleton. *Cellular Signalling, 18*(3), 276-284.

Lee, H. J., & Zheng, J. J. (2010). PDZ domains and their binding partners: Structure, specificity, and modification. *Cell Communication and Signaling : CCS, 8*, 8-811X-8-8.

Lehrich RW, Aller SG, Webster P, Marino CR, & Forrest JN Jr. (1998). Vasoactive intestinal peptide, forskolin, and genistein increase apical CFTR trafficking in the rectal gland of the spiny dogfish, squalus acanthias. acute regulation of CFTR trafficking in an intact epithelium. *The Journal of Clinical Investigation, 101*(4), 737-45.

LeSimple, P., Liao, J., Robert, R., Gruenert, D. C., & Hanrahan, J. W. (2010). Cystic fibrosis transmembrane conductance regulator trafficking modulates the barrier function of airway epithelial cell monolayers. *The Journal of Physiology, 588*(Pt 8), 1195-1209.

Leto, D., & Saltiel, A. R. (2012). Regulation of glucose transport by insulin: Traffic control of GLUT4. *Nature Reviews.Molecular Cell Biology, 13*(6), 383-396.

Leuchte, H. H., Baezner, C., Baumgartner, R. A., Bevec, D., Bacher, G., Neurohr, C., *et al*. (2008). Inhalation of vasoactive intestinal peptide in pulmonary hypertension. *The European Respiratory Journal, 32*(5), 1289-1294.

Li C., & Naren A.P. (2010). CFTR chloride channel in the apical compartments: Spatiotemporal coupling to its interacting partners. *Integr.Biol.Integrative Biology, 2*(4), 161-177.

Li, C., & Naren, A. P. (2005). Macromolecular complexes of cystic fibrosis transmembrane conductance regulator and its interacting partners. *Pharmacology & Therapeutics., 108*(2), 208-223.

Li, J., Callaway, D. J. E., & Bu, Z. (2009). Ezrin induces long-range interdomain allostery in the scaffolding protein NHERF1. *Journal of Molecular Biology, 392*(1), 166-180.

Li, J., Dai, Z., Jana, D., Callaway, D. J., & Bu, Z. (2005). Ezrin controls the macromolecular complexes formed between an adapter protein Na+/H+ exchanger regulatory factor and the cystic fibrosis transmembrane conductance regulator. *The Journal of Biological Chemistry, 280*(45), 37634-37643.

Li, J., Poulikakos, P. I., Dai, Z., Testa, J. R., Callaway, D. J., & Bu, Z. (2007). Protein kinase C phosphorylation disrupts Na+/H+ exchanger regulatory factor 1 autoinhibition and promotes cystic fibrosis transmembrane conductance regulator macromolecular assembly. *The Journal of Biological Chemistry, 282*(37), 27086-27099.

Liedtke CM, & Wang X. (2006). The N-terminus of the WD5 repeat of human RACK1 binds to airway epithelial NHERF1. *Biochemistry, 45*(34), 10270-7.

Liedtke, C. M., Cody, D., & Cole, T. S. (2001). Differential regulation of cl- transport proteins by PKC in calu-3 cells. *American Journal of Physiology.Lung Cellular and Molecular Physiology, 280*(4), L739-47.

Liedtke, C. M., & Cole, T. S. (1998). Antisense oligonucleotide to PKC-epsilon alters cAMP-dependent stimulation of CFTR in calu-3 cells. *The American Journal of Physiology, 275*(5 Pt 1), C1357-64.

Liedtke, C. M., Raghuram, V., Yun, C. C., & Wang, X. (2004). Role of a PDZ1 domain of NHERF1 in the binding of airway epithelial RACK1 to NHERF1. *American Journal of Physiology., 286*(5), C1037-C1088.

Liedtke, C. M., Yun, C. H., Kyle, N., & Wang, D. (2002). Protein kinase C epsilon-dependent regulation of cystic fibrosis transmembrane regulator involves binding to a receptor for activated C kinase (RACK1) and RACK1 binding to Na+/H+ exchange regulatory factor. *The Journal of Biological Chemistry, 277*(25), 22925-22933.

Linden, A., Hansson, L., Andersson, A., Palmqvist, M., Arvidsson, P., Lofdahl, C. G., *et al*. (2003). Bronchodilation by an inhaled VPAC(2) receptor agonist in patients with stable asthma. *Thorax, 58*(3), 217-221.

Lincoln, T. M., Cornwell, T. L., & Taylor, A. E. (1990). cGMP-dependent protein kinase mediates the reduction of Ca2+ by cAMP in vascular smooth muscle cells. *The American Journal of Physiology, 258*(3 Pt 1), C399-407.

Loffing, J., Moyer, B. D., McCoy, D., & Stanton, B. A. (1998). Exocytosis is not involved in activation of cl- secretion via CFTR in calu-3 airway epithelial cells. *The American Journal of Physiology, 275*(4 Pt 1), C913-20.

Lopez, J. P., Turner, J. R., & Philipson, L. H. (2010). Glucose-induced ERM protein activation and translocation regulates insulin secretion. *American Journal of Physiology.Endocrinology and Metabolism, 299*(5), E772-85.

- . (2000). ERM proteins: From cellular architecture to cell signaling. *Biology of the Cell / Under the Auspices of the European Cell Biology Organization, 92*(5), 305-16.

Lukacs GL, Segal G, Kartner N, Grinstein S, & Zhang F. (1997). Constitutive internalization of cystic fibrosis transmembrane conductance regulator occurs via clathrin-dependent endocytosis and is regulated by protein phosphorylation. *The Biochemical Journal, 328*, 353-61.

Lukacs, G. L., & Verkman, A. S. (2012). CFTR: Folding, misfolding and correcting the DF508 conformational defect. *Trends in Molecular Medicine, 18*(2), 81-91.

Lundberg JM, Anggard A, Fahrenkrug J, Hokfelt T, & Mutt V. (1980). Vasoactive intestinal polypeptide in cholinergic neurons of exocrine glands: Functional significance of coexisting transmitters for vasodilation and secretion. *Proceedings of the National Academy of Sciences of the United States of America, 77*(3), 1651-5.

Lundberg, J. M. (1981). Evidence for coexistence of vasoactive intestinal polypeptide (VIP) and acetylcholine in neurons of cat exocrine glands. morphological, biochemical and functional studies. *Acta Physiologica Scandinavica.Supplementum, 496*, 1-57.

Mall, M., Grubb, B. R., Harkema, J. R., O'Neal, W. K., & Boucher, R. C. (2004). Increased airway epithelial na+ absorption produces cystic fibrosis-like lung disease in mice. *Nature Medicine, 10*(5), 487-493.

Mall, M., Wissner, A., Schreiber, R., Kuehr, J., Seydewitz, H. H., Brandis, M., *et al*. (2000). Role of K(V)LQT1 in cyclic adenosine monophosphate-mediated cl(-) secretion in human airway epithelia. *American Journal of Respiratory Cell and Molecular Biology, 23*(3), 283-289.

Mall, M. A. (2008). Role of cilia, mucus, and airway surface liquid in mucociliary dysfunction: Lessons from mouse models. *Journal of Aerosol Medicine and Pulmonary Drug Delivery, 21*(1), 13-24.

Mamonova T, Kurnikova M, & Friedman PA. (2012). Structural basis for NHERF1 PDZ domain binding. *Biochemistry, 51*(14), 3110-20.

Martin, S. C., & Shuttleworth, T. J. (1994). Vasoactive intestinal peptide stimulates a cAMP-mediated cl- current in avian salt gland cells. *Regulatory Peptides, 52*(3), 205-214.

Maudsley, S., Zamah, A. M., Rahman, N., Blitzer, J. T., Luttrell, L. M., Lefkowitz, R. J., *et al*. (2000). Platelet-derived growth factor receptor association with na(+)/H(+) exchanger regulatory factor potentiates receptor activity. *Molecular and Cellular Biology, 20*(22), 8352-8363.

Milewski, M. I., Mickle, J. E., Forrest, J. K., Stafford, D. M., Moyer, B. D., Cheng, J., *et al*. (2001). A PDZ-binding motif is essential but not sufficient to localize the C terminus of CFTR to the apical membrane. *Journal of Cell Science, 114*(Pt 4), 719-726.

Mohler, P. J., Kreda, S. M., Boucher, R. C., Sudol, M., Stutts, M. J., & Milgram, S. L. (1999). Yes-associated protein 65 localizes p62(c-yes) to the apical compartment of airway epithelia by association with EBP50. *The Journal of Cell Biology, 147*(4), 879-890.

Monterisi S., Favia M., Guerra L., Cardone R.A., Reshkin S.J., Casavola V., *et al*. (2012). CFTR regulation in human airway epithelial cells requires integrity of the actin cytoskeleton and compartmentalized cAMP and PKA activity. *J.Cell Sci.Journal of Cell Science, 125*(5), 1106-1117.

Morales FC, Takahashi Y, Momin S, Adams H, Chen X, & Georgescu MM. (2007). NHERF1/EBP50 head-to-tail intramolecular interaction masks association with PDZ domain ligands. *Molecular and Cellular Biology, 27*(7), 2527-37.

Morales, F. C., Takahashi, Y., Kreimann, E. L., & Georgescu, M. M. (2004). Ezrin-radixin-moesin (ERM)-binding phosphoprotein 50 organizes ERM proteins at the apical membrane of polarized epithelia. *Proceedings of the National Academy of Sciences of the United States of America, 101*(51), 17705-17710.

Moyer BD, Denton J, Karlson KH, Reynolds D, Wang S, Mickle JE, *et al*. (1999). A PDZ-interacting domain in CFTR is an apical membrane polarization signal. *The Journal of Clinical Investigation, 104*(10), 1353-61.

Moyer, B. D., Duhaime, M., Shaw, C., Denton, J., Reynolds, D., Karlson, K. H., *et al*. (2000). The PDZ-interacting domain of cystic fibrosis transmembrane conductance regulator is required for functional expression in the apical plasma membrane. *The Journal of Biological Chemistry, 275*(35), 27069-27074.

Mutt V, & Said SI. (1974). Structure of the porcine vasoactive intestinal octacosapeptide. the amino-acid sequence. use of kallikrein in its determination. *European Journal of Biochemistry / FEBS, 42*(2), 581-9.

Naren, A. P., Cobb, B., Li, C., Roy, K., Nelson, D., Heda, G. D., *et al*. (2003). A macromolecular complex of beta 2 adrenergic receptor, CFTR, and ezrin/radixin/moesin-binding phosphoprotein 50 is regulated by PKA. *Proceedings of the National Academy of Sciences of the United States of America, 100*(1), 342-346.

Neisch, A. L., & Fehon, R. G. (2011). Ezrin, radixin and moesin: Key regulators of membrane-cortex interactions and signaling. *Current Opinion in Cell Biology, 23*(4), 377-382.

Neudauer, C. L., Joberty, G., & Macara, I. G. (2001). PIST: A novel PDZ/coiled-coil domain binding partner for the rho-family GTPase TC10. *Biochemical and Biophysical Research Communications, 280*(2), 541-547.

Okiyoneda T., Barriere H., Bagdany M., Rabeh W.M., Du K., Lukacs G.L., *et al*. (2010). Peripheral protein quality control removes unfolded CFTR from the plasma membrane. *Science Science, 329*(5993), 805-810.

Okiyoneda T, Harada K, Yamahira K, Wada I, Hashimoto Y, Ueno K, *et al*. (2004). Characterization of the trafficking pathway of cystic fibrosis transmembrane conductance regulator in baby hamster kidney cells. *Journal of Pharmacological Sciences, 95*(4), 471-5.

Okiyoneda, T., & Lukacs, G. L. (2007). Cell surface dynamics of CFTR: The ins and outs. *Biochimica Et Biophysica Acta, 1773*(4), 476-479.

Orr Gandy, K. A., Adada, M., Canals, D., Carroll, B., Roddy, P., Hannun, Y. A., *et al*. (2013). Epidermal growth factor-induced cellular invasion requires sphingosine-1-phosphate/sphingosine-1-phosphate 2 receptor-mediated ezrin activation. *FASEB Journal : Official Publication of the Federation of American Societies for Experimental Biology,*

Ostedgaard, L. S., Randak, C., Rokhlina, T., Karp, P., Vermeer, D., Ashbourne Excoffon, K. J., *et al*. (2003). Effects of C-terminal deletions on cystic fibrosis transmembrane conductance regulator function in cystic fibrosis airway epithelia. *Proceedings of the National Academy of Sciences of the United States of America, 100*(4), 1937-1942.

Pearson, M. A., Reczek, D., Bretscher, A., & Karplus, P. A. (2000). Structure of the ERM protein moesin reveals the FERM domain fold masked by an extended actin binding tail domain. *Cell, 101*(3), 259-270.

Penque D, Mendes F, Beck S, Farinha C, Pacheco P, Nogueira P, *et al*. (2000). Cystic fibrosis F508del patients have apically localized CFTR in a reduced number of airway cells. *Laboratory Investigation; a Journal of Technical Methods and Pathology, 80*(6), 857-68.

Phillips, J. E., Hey, J. A., & Corboz, M. R. (2003). Tachykinin NK3 and NK1 receptor activation elicits secretion from porcine airway submucosal glands. *British Journal of Pharmacology, 138*(1), 254-260.

Piserchio, A., Fellows, A., Madden, D. R., & Mierke, D. F. (2005). Association of the cystic fibrosis transmembrane regulator with CAL: Structural features and molecular dynamics. *Biochemistry, 44*(49), 16158-16166.

Ponting, C. P. (1997). Evidence for PDZ domains in bacteria, yeast, and plants. *Protein Science : A Publication of the Protein Society, 6*(2), 464-468.

Prat AG, Cunningham CC, Jackson GR Jr, Borkan SC, Wang Y, Ausiello DA, *et al*. (1999). Actin filament organization is required for proper cAMP-dependent activation of CFTR. *The American Journal of Physiology, 277*(6), 1160-9.

Prasse, A., Zissel, G., Lutzen, N., Schupp, J., Schmiedlin, R., Gonzalez-Rey, E., *et al*. (2010). Inhaled vasoactive intestinal peptide exerts immunoregulatory effects in sarcoidosis. *American Journal of Respiratory and Critical Care Medicine, 182*(4), 540-548.

Prince, L. S., Tousson, A., & Marchase, R. B. (1993). Cell surface labeling of CFTR in T84 cells. *The American Journal of Physiology, 264*(2 Pt 1), C491-8.

Prince, L. S., Workman, R. B.,Jr, & Marchase, R. B. (1994). Rapid endocytosis of the cystic fibrosis transmembrane conductance regulator chloride channel. *Proceedings of the National Academy of Sciences of the United States of America, 91*(11), 5192-5196.

Qu, F., Liu, H. J., Xiang, Y., Tan, Y. R., Liu, C., Zhu, X. L., *et al*. (2011). Activation of CFTR trafficking and gating by vasoactive intestinal peptide in human bronchial epithelial cells. *Journal of Cellular Biochemistry, 112*(3), 902-908.

Quinton, P. M. (1979). Composition and control of secretions from tracheal bronchial submucosal glands. *Nature, 279*(5713), 551-552.

Quinton, P. M. (1983). Chloride impermeability in cystic fibrosis. *Nature, 301*(5899), 421-422.

Rab, A., Rowe, S. M., Raju, S. V., Bebok, Z., Matalon, S., & Collawn, J. F. (2013). Cigarette smoke and CFTR: Implications in the pathogenesis of COPD. *American Journal of Physiology.Lung Cellular and Molecular Physiology,*

Reczek, D., Berryman, M., & Bretscher, A. (1997). Identification of EBP50: A PDZ-containing phosphoprotein that associates with members of the ezrin-radixin-moesin family. *The Journal of Cell Biology, 139*(1), 169-179.

Reczek, D., & Bretscher, A. (1998). The carboxyl-terminal region of EBP50 binds to a site in the amino-terminal domain of ezrin that is masked in the dormant molecule. *The Journal of Biological Chemistry, 273*(29), 18452-18458.

Reddy, M. M., Light, M. J., & Quinton, P. M. (1999). Activation of the epithelial na+ channel (ENaC) requires CFTR cl- channel function. *Nature, 402*(6759), 301-304.

Ren, A., Zhang, W., Yarlagadda, S., Sinha, C., Arora, K., Moon, C. S., *et al*. (2013). MAST205 competes with cystic fibrosis transmembrane conductance regulator (CFTR)-associated ligand for binding to CFTR to regulate CFTR-mediated fluid transport. *The Journal of Biological Chemistry, 288*(17), 12325-12334.

Riordan, J. R., Rommens, J. M., Kerem, B., Alon, N., Rozmahel, R., Grzelczak, Z., *et al*. (1989). Identification of the cystic fibrosis gene: Cloning and characterization of complementary DNA. *Science (New York, N.Y.), 245*(4922), 1066-1073.

Rommens, J. M., Iannuzzi, M. C., Kerem, B., Drumm, M. L., Melmer, G., Dean, M., *et al*. (1989). Identification of the cystic fibrosis gene: Chromosome walking and jumping. *Science (New York, N.Y.), 245*(4922), 1059-1065.

Said SI. (1982). Vasoactive peptides in the lung, with special reference to vasoactive intestinal peptide. *Experimental Lung Research, 3*(3-4), 3-4.

Said SI. (1991). Vasoactive intestinal polypeptide: Biologic role in health and disease. *Trends in Endocrinology and Metabolism: TEM, 2*(3)

Said SI, & Mutt V. (1969). A peptide fraction from lung tissue with prolonged peripheral vasodilator activity. *Scandinavian Journal of Clinical and Laboratory Investigation.Supplementum, 107*, 51-6.

Said SI, & Mutt V. (1970). Polypeptide with broad biological activity: Isolation from small intestine. *Science (New York, N.Y.), 169*(3951), 1217-8.

Said, S. I. (1991). Vasoactive intestinal polypeptide (VIP) in asthma. *Annals of the New York Academy of Sciences, 629*, 305-318.

Said, S. I., & Faloona, G. R. (1975). Elevated plasma and tissue levels of vasoactive intestinal polypeptide in the watery-diarrhea syndrome due to pancreatic, bronchogenic and other tumors. *The New England Journal of Medicine, 293*(4), 155-160.

Said, S. I., Giachetti, A., & Nicosia, S. (1980). VIP: Possible functions as a neural peptide. *Advances in Biochemical Psychopharmacology, 22*, 75-82.

Said, S. I., & Vasoactive Intestinal Polypeptide and Pituitary Adenylate Cyclase-Activating Polypeptide. (2007). The discovery of VIP: Initially looked for in the lung, isolated from intestine, and identified as a neuropeptide. *Peptides, 28*(9), 1620-1621.

Salinas, D., Haggie, P. M., Thiagarajah, J. R., Song, Y., Rosbe, K., Finkbeiner, W. E., *et al*. (2005). Submucosal gland dysfunction as a primary defect in cystic fibrosis. *FASEB Journal : Official Publication of the Federation of American Societies for Experimental Biology, 19*(3), 431-433.

Santos, G. F., & Reenstra, W. W. (1994). Activation of the cystic fibrosis transmembrane regulator by cyclic AMP is not correlated with inhibition of endocytosis. *Biochimica Et Biophysica Acta, 1195*(1), 96-102.

Sato, N., Funayama, N., Nagafuchi, A., Yonemura, S., Tsukita, S., & Tsukita, S. (1992). A gene family consisting of ezrin, radixin and moesin. its specific localization at actin filament/plasma membrane association sites. *Journal of Cell Science, 103 (Pt 1)*(Pt 1), 131-143.

Savage, M. V., Brengelmann, G. L., Buchan, A. M., & Freund, P. R. (1990). Cystic fibrosis, vasoactive intestinal polypeptide, and active cutaneous vasodilation. *Journal of Applied Physiology (Bethesda, Md.: 1985), 69*(6), 2149-2154.

Seavilleklein, G., Amer, N., Evagelidis, A., Chappe, F., Irvine, T., Hanrahan, J. W., *et al*. (2008). PKC phosphorylation modulates PKA-dependent binding of the R domain to other domains of CFTR. *American Journal of Physiology.Cell Physiology, 295*(5), C1366-75.

Sharma,R.K.;Addis,B.J.;Jeffery,P.K.(1995).The distribution and density of airway vasoactive intestinal polypeptide (VIP) binding sites in cystic fibrosis and asthma, 8(2-3), 91-96.

Shibata, T., Chuma, M., Kokubu, A., Sakamoto, M., & Hirohashi, S. (2003). EBP50, a beta-catenin-associating protein, enhances wnt signaling and is over-expressed in hepatocellular carcinoma. *Hepatology (Baltimore, Md.), 38*(1), 178-186.

Short DB, Trotter KW, Reczek D, Kreda SM, Bretscher A, Boucher RC, *et al*. (1998). An apical PDZ protein anchors the cystic fibrosis transmembrane conductance regulator to the cytoskeleton. *The Journal of Biological Chemistry, 273*(31), 19797-801.

Simons, P. C., Pietromonaco, S. F., Reczek, D., Bretscher, A., & Elias, L. (1998). C-terminal threonine phosphorylation activates ERM proteins to link the cell's cortical lipid bilayer to the cytoskeleton. *Biochemical and Biophysical Research Communications, 253*(3), 561-565.

Smith, L., Litman, P., Kohli, E., Amick, J., Page, R. C., Misra, S., *et al*. (2013). RACK1 interacts with filamin-A to regulate plasma membrane levels of the cystic fibrosis transmembrane conductance regulator. *American Journal of Physiology.Cell Physiology, 305*(1), C111-20.

Songyang Z, Fanning AS, Fu C, Xu J, Marfatia SM, Chishti AH, *et al*. (1997). Recognition of unique carboxyl-terminal motifs by distinct PDZ domains. *Science (New York, N.Y.), 275*(5296), 73-7.

Steiger, J., Bray, M. A., & Subramanian, N. (1987). Platelet activating factor (PAF) is a potent stimulator of porcine tracheal fluid secretion in vitro. *European Journal of Pharmacology, 142*(3), 367-372.

Sun, T. X., Van Hoek, A., Huang, Y., Bouley, R., McLaughlin, M., & Brown, D. (2002). Aquaporin-2 localization in clathrin-coated pits: Inhibition of endocytosis by dominant-negative dynamin. *American Journal of Physiology.Renal Physiology, 282*(6), F998-1011.

Swiatecka-Urban, A., Duhaime, M., Coutermarsh, B., Karlson, K. H., Collawn, J., Milewski, M., et al. (2002). PDZ domain interaction controls the endocytic recycling of the cystic fibrosis transmembrane conductance regulator. *The Journal of Biological Chemistry, 277*(42), 40099-40105.

Takahashi, A., Watkins, S. C., Howard, M., & Frizzell, R. A. (1996). CFTR-dependent membrane insertion is linked to stimulation of the CFTR chloride conductance. *The American Journal of Physiology, 271*(6 Pt 1), C1887-94.

Tarran, R., Button, B., & Boucher, R. C. (2006). Regulation of normal and cystic fibrosis airway surface liquid volume by phasic shear stress. *Annual Review of Physiology, 68*, 543-561.

Tarran, R., Button, B., Picher, M., Paradiso, A. M., Ribeiro, C. M., Lazarowski, E. R., et al. (2005). Normal and cystic fibrosis airway surface liquid homeostasis. the effects of phasic shear stress and viral infections. *The Journal of Biological Chemistry, 280*(42), 35751-35759.

Trout, L., Corboz, M. R., & Ballard, S. T. (2001). Mechanism of substance P-induced liquid secretion across bronchial epithelium. *American Journal of Physiology.Lung Cellular and Molecular Physiology, 281*(3), L639-45.

Trout, L., King, M., Feng, W., Inglis, S. K., & Ballard, S. T. (1998). Inhibition of airway liquid secretion and its effect on the physical properties of airway mucus. *The American Journal of Physiology, 274*(2 Pt 1), L258-63.

Trout, L., Townsley, M. I., Bowden, A. L., & Ballard, S. T. (2003). Disruptive effects of anion secretion inhibitors on airway mucus morphology in isolated perfused pig lung. *The Journal of Physiology, 549*(Pt 3), 845-853.

Tsukita, S., Hieda, Y., & Tsukita, S. (1989). A new 82-kD barbed end-capping protein (radixin) localized in the cell-to-cell adherens junction: Purification and characterization. *The Journal of Cell Biology, 108*(6), 2369-2382.

Tsukita, S., Oishi, K., Sato, N., Sagara, J., Kawai, A., & Tsukita, S. (1994). ERM family members as molecular linkers between the cell surface glycoprotein CD44 and actin-based cytoskeletons. *The Journal of Cell Biology, 126*(2), 391-401.

Turcios, N. L. (2005). Cystic fibrosis: An overview. *Journal of Clinical Gastroenterology, 39*(4), 307-317.

Uddman, R., Alumets, J., Densert, O., Hakanson, R., & Sundler, F. (1978). Occurrence and distribution of VIP nerves in the nasal mucosa and tracheobronchial wall. *Acta Oto-Laryngologica, 86*(5-6), 443-448.

Ueki, I., German, V. F., & Nadel, J. A. (1980). Micropipette measurement of airway submucosal gland secretion. autonomic effects. *The American Review of Respiratory Disease, 121*(2), 351-357.

Valentine, C. D., Lukacs, G. L., Verkman, A. S., & Haggie, P. M. (2012). Reduced PDZ interactions of rescued DeltaF508CFTR increases its cell surface mobility. *The Journal of Biological Chemistry, 287*(52), 43630-43638.

Valerie Chappe and Sami I. Said. (2012). VIP as a corrector of CFTR trafficking and membrane stability, cystic fibrosis - renewed hopes through research, dr. dinesh sriramulu (ed.), ISBN: 978-953-51-0287-8.

Vouilleme, L., Cushing, P. R., Volkmer, R., Madden, D. R., & Boisguerin, P. (2010). Engineering peptide inhibitors to overcome PDZ binding promiscuity. *Angewandte Chemie (International Ed.in English), 49*(51), 9912-9916.

Wang, S., Raab, R. W., Schatz, P. J., Guggino, W. B., & Li, M. (1998). Peptide binding consensus of the NHE-RF-PDZ1 domain matches the C-terminal sequence of cystic fibrosis transmembrane conductance regulator (CFTR). *FEBS Letters, 427*(1), 103-108.

Wattchow, David A., Furness, John B., Gibbins, Ian L., Little, Ken E., Carter, Rodney F. (1988), Vasoactive intestinal peptide immunoreactive nerve fibres are deficient in intestinal and nasal mucosa affected by cystic fibrosis. J Gastroenterol Hepatol Journal of Gastroenterology and Hepatology, 3(6), 549-555.

Weinman, E. J., Steplock, D., Wang, Y., & Shenolikar, S. (1995). Characterization of a protein cofactor that mediates protein kinase A regulation of the renal brush border membrane na(+)-H+ exchanger. *The Journal of Clinical Investigation, 95*(5), 2143-2149.

Welsh, M. J., Denning, G. M., Ostedgaard, L. S., & Anderson, M. P. (1993). Dysfunction of CFTR bearing the delta F508 mutation. *Journal of Cell Science.Supplement, 17*, 235-239.

Widdicombe, J. G. (1966). Action potentials in parasympathetic and sympathetic efferent fibres to the trachea and lungs of dogs and cats. *The Journal of Physiology, 186*(1), 56-88.

Wine, J. J. (2007). Parasympathetic control of airway submucosal glands: Central reflexes and the airway intrinsic nervous system. *Autonomic Neuroscience : Basic & Clinical, 133*(1), 35-54.

Winpenny, J. P., McAlroy, H. L., Gray, M. A., & Argent, B. E. (1995). Protein kinase C regulates the magnitude and stability of CFTR currents in pancreatic duct cells. *The American Journal of Physiology, 268*(4 Pt 1), C823-8.

Wolde, M., Fellows, A., Cheng, J., Kivenson, A., Coutermarsh, B., Talebian, L., *et al*. (2007). Targeting CAL as a negative regulator of DeltaF508-CFTR cell-surface expression: An RNA interference and structure-based mutagenetic approach. *The Journal of Biological Chemistry, 282*(11), 8099-8109.

Wu, D., Lee, D., & Sung, Y. K. (2011). Prospect of vasoactive intestinal peptide therapy for COPD/PAH and asthma: A review. *Respiratory Research, 12*, 45-9921-12-45.

Yamaya, M., Sekizawa, K., Kakuta, Y., Ohrui, T., Sawai, T., & Sasaki, H. (1996). P2u-purinoceptor regulation of chloride secretion in cultured human tracheal submucosal glands. *The American Journal of Physiology, 270*(6 Pt 1), L979-84.

Yonemura, S., Tsukita, S., & Tsukita, S. (1999). Direct involvement of ezrin/radixin/moesin (ERM)-binding membrane proteins in the organization of microvilli in collaboration with activated ERM proteins. *The Journal of Cell Biology, 145*(7), 1497-1509.

Zhang, W., Fujii, N., & Naren, A. P. (2012). Recent advances and new perspectives in targeting CFTR for therapy of cystic fibrosis and enterotoxin-induced secretory diarrheas. *Future Medicinal Chemistry, 4*(3), 329-345.

Zuelzer, W. W., & Newton, W. A.,Jr. (1949). The pathogenesis of fibrocystic disease of the pancreas; a study of 36 cases with special reference to the pulmonary lesions. *Pediatrics, 4*(1), 53-69.